



Tectonics of the Strandja Massif, NW Turkey: History of a Long-Lived Arc at the Northern Margin of Palaeo-Tethys

BORIS A. NATAL'IN¹, GÜRSEL SUNAL¹, MUHARREM SATIR² & ERKAN TORAMAN³

¹ Istanbul Technical University, Department of Geological Engineering, TR–34469 İstanbul, Turkey
(E-mail: natalin@itu.edu.tr)

² Universität Tübingen, Institut für Geowissenschaften, Wilhelmstrasse 56, D-72074 Tübingen, Germany

³ Department of Geology and Geophysics, University of Minnesota, 310 Pillsbury Dr. SE, Minneapolis, MN, 55455, USA

Received 30 June 2010; revised typescripts received 11 October 2011 & 11 May 2011; accepted 09 June 2011

Abstract: The Strandja Massif, Thrace Peninsula, NW Turkey, forms an important link between the Balkan Zone of Bulgaria, which is usually correlated with Variscan orogen in Central Europe, and the Pontides, where Cimmerian structures are the most prominent. The massif is composed of a Palaeozoic basement and a Triassic metasedimentary cover. The basement is made of various granite gneisses, paragneisses, and schists that are intruded by large plutons of monzonitic metagranites. Detrital zircon studies have revealed Ordovician (433 and 446 Ma) and Carboniferous (305 Ma) ages of the metasedimentary rocks. The isotopic age of the granite gneisses is 308–315 Ma (Carboniferous, Bashkirian–Moscovian) as single zircon evaporation method and conventional U-Pb technique show. The Palaeozoic basement was deformed and metamorphosed before the emplacement of the large monzonitic metagranite plutons yielding zircon ages from 309±24 to 257 Ma (Moscovian–Permian). Geochemical features of the Carboniferous and Permian magmatic rocks indicate a subduction-related tectonic setting similar to coeval rocks exposed in the Balkan zone of Bulgaria.

The Triassic metasedimentary cover unconformably overlies the basement with basal conglomerate and arkosic sandstone that pass upward into a thick pile of lithic metasandstones and a metasandstone/pelitic schist alternation. Calcareous metasandstones and black slates appear at the highest structural levels. The Triassic succession reveals obvious orogenic features judged from its great thickness, sedimentary features indicating high-energy currents and the presence of intermediate pillow lavas. Both the basement and the cover units were affected by strong deformation and epidote-amphibolite to greenschist facies metamorphism during the Late Jurassic–Early Cretaceous. This event was terminated by the emplacement of a nappe of unmetamorphosed Jurassic limestones and dolomites occurring at the top of the structural column. Kinematic indicators in mylonites at the base of the nappe suggest its original location in the south.

The Strandja Massif shows remarkable similarity to the late Palaeozoic–early Mesozoic Silk Road arc that evolved at the southern margin of Eurasia due to the northward subduction of Palaeo-Tethys (Natal'in & Şengör 2005). The fragments of this arc are exposed in Caucasus, Iran, South Tien Shan, Pamir, and Kunlun. The Precambrian history of the Strandja Massif, as recorded by detrital and inherited zircon ages, reveals many common features with the Baltica-Timaniide collage including its fragments distributed in Central Asia. Various sets of data and correlations with surrounding tectonic units show that the Strandja Massif is a fragment of the long-lived, Ordovician to Triassic Silk Road magmatic arc, which evolved on the northern side of Palaeo-Tethys.

Key Words: tectonics, stratigraphy, geochronology, Palaeo-Tethys, tectonic evolution, Strandja Massif, Balkan, NW Turkey

Istranca Masifi'nin Tektoniği, KB Türkiye: Paleo-Tetis'in Kuzey Kenarında Yer Alan Uzun Süreli Bir Yayın Evrimi

Özet: Istranca Masifi, Trakya Yarımadası, KB Türkiye, Bulgaristan'da yer alan Balkan Zonu ile önemli bir bağlantı oluşturur ve genellikle de Orta Avrupa'daki Variscan orojeni ve Kimmeriyen yapılarının en çok göze çarptığı Pontidlerle denestirilmektedir. Masif, Paleozoyik bir temel ile Triyas yaşlı bir metasedimenter örtüden oluşur. Temel geniş monzonitik metagranitlerin sokulduğu çeşitli granit gnayslar, paragneyslar ve şistlerden meydana gelir. Taşıma zirkon yaşları göstermiştir ki metasedimenter kayaların yaşları Ordovisyen (443 ve 446 My) ve Karbonifer'dir (305 My). Granit gnaysların izotopik yaşları tekil zirkon buharlaşma ve geleneksel U-Pb yöntemlerinin gösterdiği üzere 308–315 My'dir (Karbonifer, Başkiran–Moskoviye). Paleozoyik temel 309±24 ila 257 My (Moskoviye–Permiyen)

zirkon yaşlarında olan geniş monzonitik metagranitlerin yerleşiminden önce deforme olmuş ve metamorfizmaya uğramışlardır. Karbonifer ve Permian magmatik kayalarına ait jeokimyasal özellikler, Bulgaristan'ın Balkan Zonu'nda yüzeyleyen eş yaşlı kayalarla benzer olarak dalma-batma ile ilintili bir tektonik ortamı işaret etmektedir.

Triyas yaşlı metasedimenter örtü, temeli bir taban konglomerası ve üste doğru kalın metakumtaşı ve metakumtaşı/pelitlik şist ardalınmasına geçen arkozik kumtaşlarıyla aşısız uyumsuz olarak üzerler. Karbonatlı metakumtaşı ve siyah sleytler daha üst yapısal seviyelerde görülür. Triyas istifi önemli kalınlığı, yüksek enerji akıntılarını gösteren sedimentler yapıları ve ara yastık lavların varlığı ile açık orojenik özellikler sunar. Hem temel hem de örtü birimleri Geç Jura-Erken Kretase döneminde güçlü bir deformasyon ve epidote-amfibolitten yeşil şist fasiyesine varan bir metamorfizma geçirmişlerdir. Bu olay yapısal kolonun en üstünde yer alan, metamorfizmaya uğramamış Jura yaşlı kireçtaşı ve dolomit napının yerleşmesiyle sona ermiştir. Napın tabanında yer alan milonitlerdeki kinematik göstergeler, orijinal konumunun güneyde olduğunu önermektedir.

Istranca Masifi Paleo-Tetis'in kuzey yönlü dalma-batması sonucunda Avrasya'nın güney kenarında gelişmiş olan Geç Paleozoyik-Erken Mesozoyik yaşlı İpek Yolu yayıyla (*Silk Road arc*) dikkate değer benzerlikler sunmaktadır (Natal'in & Şengör 2005). Bu yaya ait parçalar Kafkaslar, İran, Güney Tien Şan, Pamir ve Kunlun'da yüzeylemektedir. Istranca Masifi'nin taşıma zirkon yaşları tarafından kayıt edilen Prekambriyen evrimi, Baltika-Timmanid kolajı ve onun Orta Asya'da dağılmış olan parçalarıyla bir çok ortak özellik sunmaktadır. Çeşitli veri setleri ve çevre tektonik birimlerle yapılan karşılaştırmalar göstermektedir ki Istranca Masifi Paleo-Tetis'in kuzey kenarında, Ordovisyen'den Triyas'a kadar gelişmiş olan uzun dönemli İpek Yolu (*Silk Road*) yayının bir parçasını oluşturmaktadır.

Anahtar Sözcükler: tektonik, stratigrafi, jeokronoloji, Paleo-Tetis, tektonik evrim, Istranca Masifi, Balkanlar, KB Türkiye

Introduction

The Strandja Massif forms an important link between the Pontides that are exposed along the Black Sea coast of Turkey and the Balkan Zone in Bulgaria. The Pontides are traditionally interpreted as a product of the Cimmerian orogeny with oceanic subduction continuing until the Late Triassic to Early Jurassic (Şengör 1984; Şengör & Yılmaz 1981; Şengör *et al.* 1984) as in regions located farther east in Iran (Alavi 1991). In the Pontides and in Iran, the record of the Palaeozoic history is fragmentary, more so in the Pontides than in Iran (Natal'in & Şengör 2005; A.I. Okay *et al.* 2006). In contrast, Hercynian events are well documented in the Balkan Zone (Haydoutov 1989; Haydoutov & Yanev 1997; Yanev 2000) whereas the Palaeo-Tethyan history is poorly documented (Chatalov 1991).

The Strandja Massif, exposed in NW Turkey (Figure 1), consists of greenschist to epidote-amphibolite facies metamorphic rocks that are subdivided into a Palaeozoic basement and a Triassic-Jurassic sedimentary cover (Ayhan *et al.* 1972; Aydın 1982; Çağlayan & Yurtsever 1998; A.I. Okay *et al.* 2001). There are three principal ideas on the tectonic nature of these rocks, each of which implies significantly different scenarios for understanding the tectonic evolution of both the massif itself and the Palaeozoic and early Mesozoic

correlative tectonic processes in the Palaeo-Tethyan domain: (1) the tectonic correlation within the Pontides; (2) connection of the Strandja Massif and Balkan and the Rhodope zones; (3) continuity of the European tectonic units into Asia.

The earliest interpretation considers the Strandja Massif as a part of the Rhodope-Pontide continental fragments originating from Gondwanaland (Şengör & Yılmaz 1981; Şengör 1984; Şengör *et al.* 1984). After Permian rifting, these fragments drifted toward Eurasia, being framed in the north by a south-dipping subduction zone. They collided with Eurasia in the Triassic-Early Jurassic (Cimmerian orogeny) and formed the Palaeo-Tethyan suture. This suture was shown as crosscutting the Balkan/Strandja units (Figure 1) approximately following the Turkish/Bulgarian state border (Şengör 1984; Şengör *et al.* 1984). This interpretation was accepted by other researchers (Chatalov 1988, 1991; Yılmaz *et al.* 1997).

Ustaömer & Robertson (1993, 1997) suggested that prior to the late Palaeozoic (early to middle Palaeozoic history is not discussed) the Rhodope-Pontide fragments belonged to Eurasia. The northward subduction of Palaeo-Tethys caused the late Palaeozoic-Triassic opening of the Küre back-arc basin that moved the fragments to the south. The Cimmerian closure of the back-arc basin moved them back to Eurasia. The Strandja Massif is interpreted as

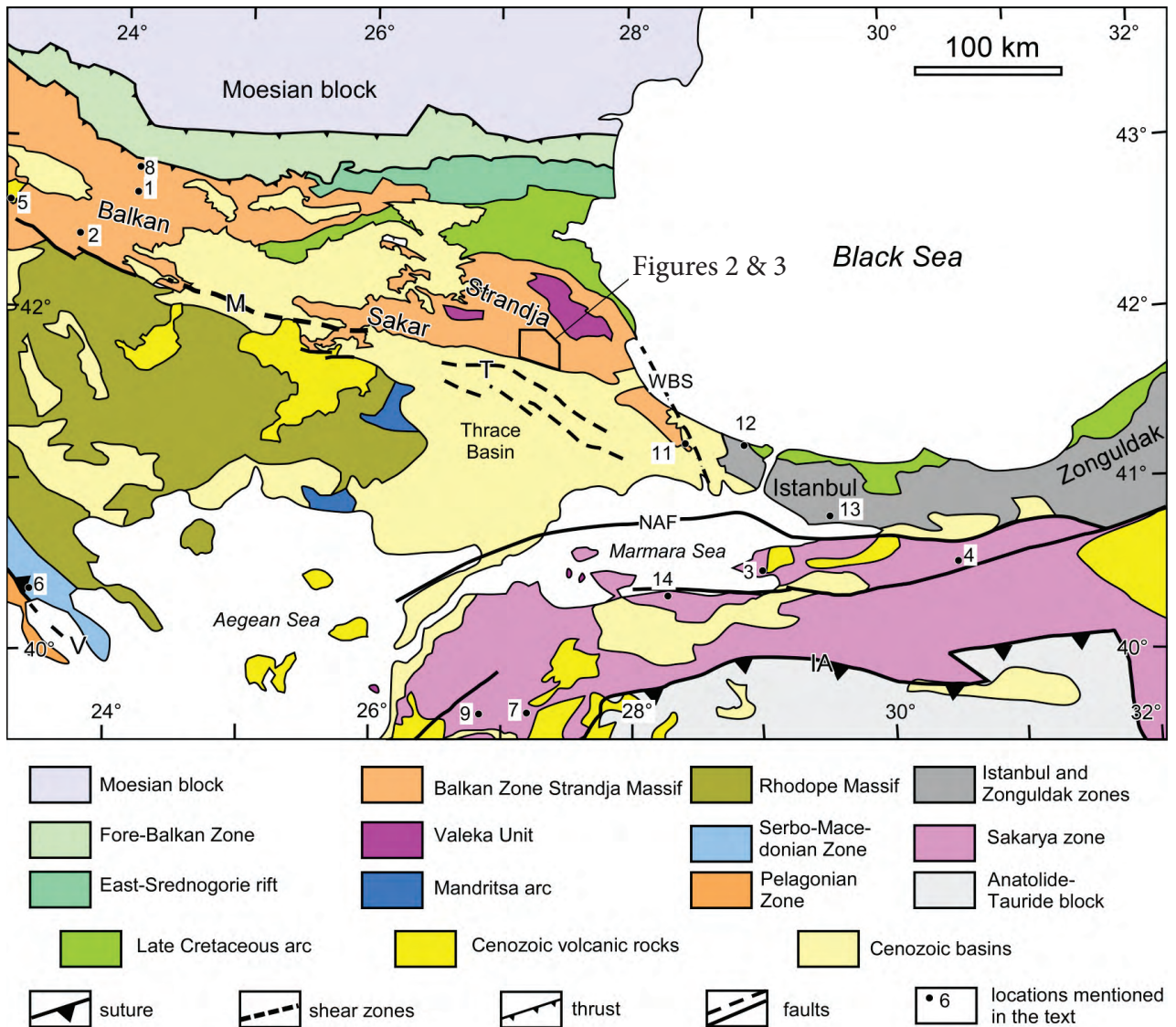


Figure 1. Tectonic map of north-western Turkey and surrounding regions (compiled using data obtained in this study as well as information in published sources: Şengör & Yılmaz 1981; Şengör *et al.* 1984; Şengör 1984; Yılmaz *et al.* 1997; A.I. Okay *et al.* 2001; Ricou *et al.* 1998; Okay & Tüysüz 1999; Yanev 2000; Gerdjikov 2005). Box indicates the studied area. The Balkan tectonic unit corresponds to the Balkan and Thracian ‘terrane’ (Yanev 2000) or Balkan Terrane (Yanev *et al.* 2006) or the Balkan and Srednogorie zones of Hsü *et al.* (1977). Keys to abbreviations: IA – İzmir-Ankara suture, M – Maritsa Fault, NAF – the North Anatolian fault, V – Vardar suture, WBS – the West Black Sea Fault.

containing remnants of this back-arc basin. This idea was also supported by several researchers (Nikishin *et al.* 2001; Stampfli *et al.* 2001a, b; Kazmin & Tikhonova 2006). These two initial models implied that the magmatic activity of the Strandja Massif during the late Palaeozoic–Triassic was in an arc and back-arc tectonic setting.

The third model (A.I. Okay *et al.* 1996, 2001) viewed the Strandja Massif as a part of the European

Variscan orogen, in which Triassic–Jurassic rocks were formed in epicontinental basins making the transition to a passive continental margin developed on the northern side of Palaeo-Tethys. In terms of Palaeozoic history, A.I. Okay *et al.* (1996, 2001) considered the Strandja Massif to be the eastern continuation of the Central European Variscan belt, in which the orogeny happened not in the mid-Carboniferous as in Europe and Bulgaria but later,

in the early Permian. This orogeny resulted in the metamorphism and emplacement of widespread early Permian granites.

According to most popular opinion, the Variscan orogeny in the Balkans is related to the late Carboniferous collision of the Balkan and Moesia continental blocks (Yanev 2000), both originating from Gondwanaland (Haydoutov & Yanev 1997; Yanev 2000; Yanev *et al.* 2006). The position of the Strandja Massif at the Eurasian margin in the late Palaeozoic and the Gondwanan nature of the early–middle Palaeozoic basement are popular ideas among researchers (Golonka 2000, 2004; Stampfli 2000; Stampfli & Borel 2002, 2004; Sunal *et al.* 2008). However, the Gondwanan origin of the Strandja Massif is difficult to prove because of its Late Jurassic to Early Cretaceous metamorphism (A.I. Okay *et al.* 2001; Lilov *et al.* 2004; Sunal *et al.* 2011) so these ideas are based on the position of the Balkan and İstanbul zones. It should be noted that Yanev *et al.* (2006) considered the stratigraphic similarity and the Gondwanan nature of these zones during the early–middle Palaeozoic and ascribed their juxtaposition with Laurasia to the Variscan collision during the Carboniferous. A.I. Okay *et al.* (2006) inferred that the İstanbul Zone had amalgamated with Eurasia in the late Ordovician.

The aim of this paper is to provide new data on the stratigraphy and structure of the central part of the Strandja Massif, elucidating several important episodes of the Palaeozoic history, including the late Carboniferous magmatism and deformation, and emplacement of the Permian granites. Unlike other researchers, we also hold that the accumulation of Triassic rocks occurred in an orogenic setting rather than quiet environments of epicontinental basins. Finally, we present data allowing the correlation of the Precambrian, Palaeozoic, and early Mesozoic tectonic events in the Strandja Massif with those occurring in the neighbouring regions and along the southern margin of Asia.

Tectonostratigraphic Units of the Strandja Massif

The Terzili (Turgut & Eseller 2000) or Thrace fault zone (Sakinç *et al.* 1999), cutting the Eocene–Miocene rocks of the Thrace Basin, defines the southern

boundary of the Strandja Massif (T in Figure 1). It evolved as a dextral strike-slip fault in the Cenozoic (Perinçek 1991; Coşkun 1997), but perhaps these motions were localised along older faults with main displacements in the Late Jurassic–Early Cretaceous (Natal'in *et al.* 2005a). The western termination of the Strandja Massif is determined by the West-Black Sea fault zone (A.I. Okay *et al.* 1994).

Strong Late Jurassic to Early Cretaceous deformations and related greenschist facies metamorphism (A.I. Okay *et al.* 1996, 2001; Natal'in *et al.* 2005a, b, 2009) hinder the study of the Palaeozoic and early Mesozoic rocks. These deformations produced a penetrative S_2 foliation and wide zones of mylonites showing an early top-to-the-NW sense of shear and a top-to-the-NE sense of shear during the later stage of the same deformation (Natalin *et al.* 2005a, b). These two sub-phases of deformation almost completely reworked previously formed structures and original relations between the lithostratigraphic units. Due to high strain, all studied depositional contacts are always suspect and sedimentary structures indicating younging directions are rarely preserved. The history and nature of the Late Jurassic–Early Cretaceous deformation will be described in a companion paper.

Five tectonostratigraphic units (Figures 2–4) have been recognized: (1) the Palaeozoic metasedimentary complex, (2) the late Palaeozoic–Triassic metasedimentary complex (the Koruköy Complex), (3) the Kuzulu Complex of unknown age, (4) the Triassic metasedimentary complex, and (5) the Jurassic carbonate complex. All are treated as lithodemic stratigraphic units (Nomenclature, 2005). In previous studies, the first unit, together with large early Permian granitic plutons, was assigned to the basement of the Strandja Massif with others forming its sedimentary cover (Ayhan *et al.* 1972; Aydın 1982; Çağlayan & Yurtsever 1998; A.I. Okay *et al.* 2001). Our studies have shown that the Palaeozoic metasedimentary rocks are intruded by late Carboniferous granitoids that are now represented by various granite gneisses. Both of them are cut by the large early Permian Kırklareli granite plutons.

Several units occupying rather large areas (Figure 3) are difficult to assign to a certain unit because they are represented by fault rocks (mylonites and

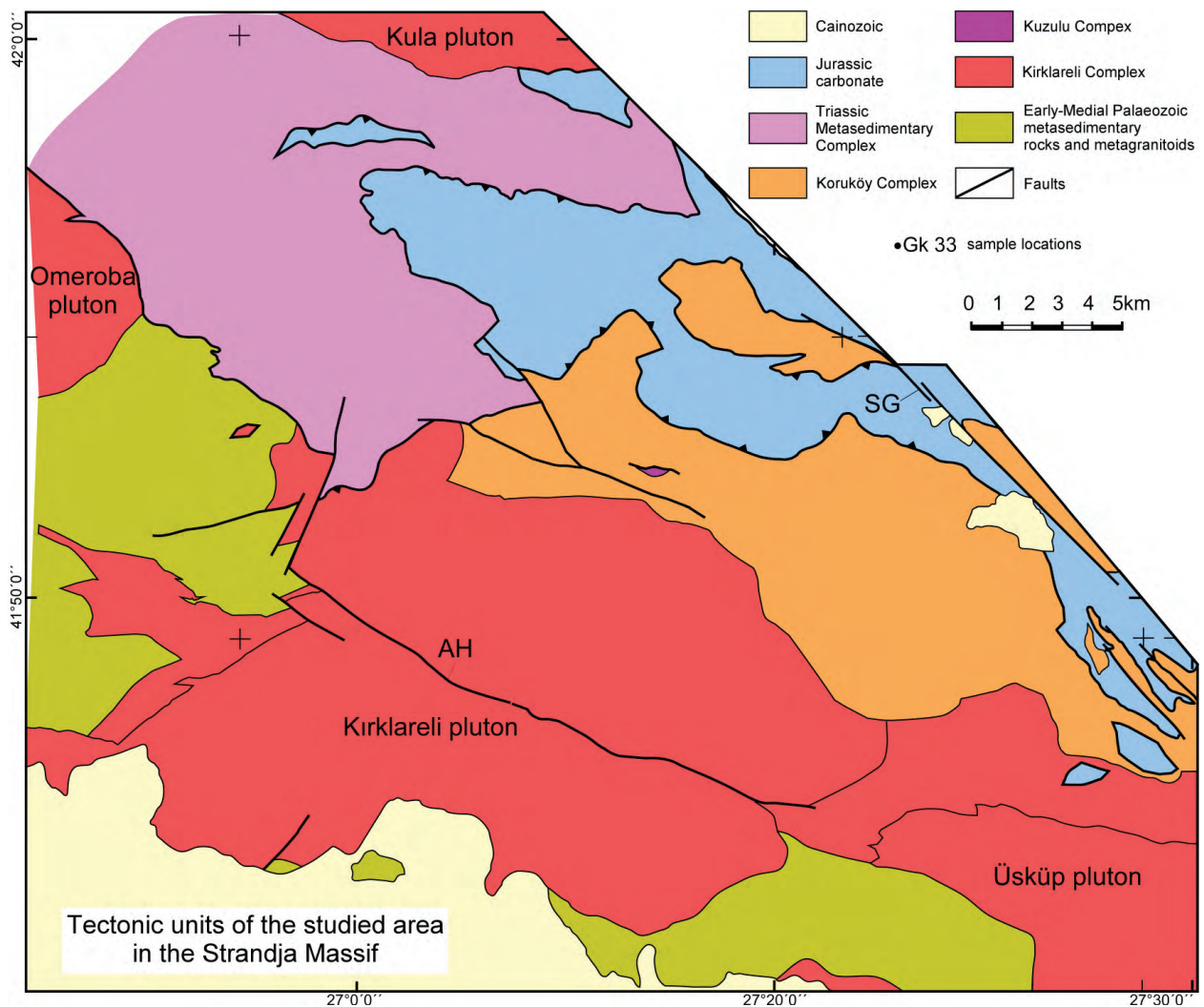


Figure 2. Tectonostratigraphic units of the studied area (see Figure 1 for the geographic location of this map). Black and open circles indicate locations of samples for geochronological studies of magmatic rocks and detrital zircons respectively. Keys to abbreviations: AH– the Ahmetce Fault, SG – the Sergen Fault.

blastomylonites, Figure 3) and their protoliths show mixing of different lithologies.

North of the studied area, Chatalov (1990, 1991) described Triassic volcanic and sedimentary rocks and assigned them to the Zubernovo nappe marking the Palaeo-Tethyan suture and occupying the highest structural position in the Strandja Massif. This interpretation was shared by other authors who studied the Turkish segment of this unit (Şengör *et al.* 1984) and named it as the Strandja allochthon (A.I. Okay *et al.* 2001). Later studies have established the Palaeozoic age of the unit and shown that its

allochthonous position requires additional kinematic and structural studies (Gerdjikov 2005). We support this conclusion and to evade confusion accept Gerdjikov’s name of this unit – the Valeka Unit (Figure 1).

Palaeozoic Basement

Palaeozoic Metasedimentary Complex

In previous studies (Çağlayan & Yurtsever 1998; A.I. Okay *et al.* 2001), all Palaeozoic metamorphosed rocks in the studied area were assigned to the

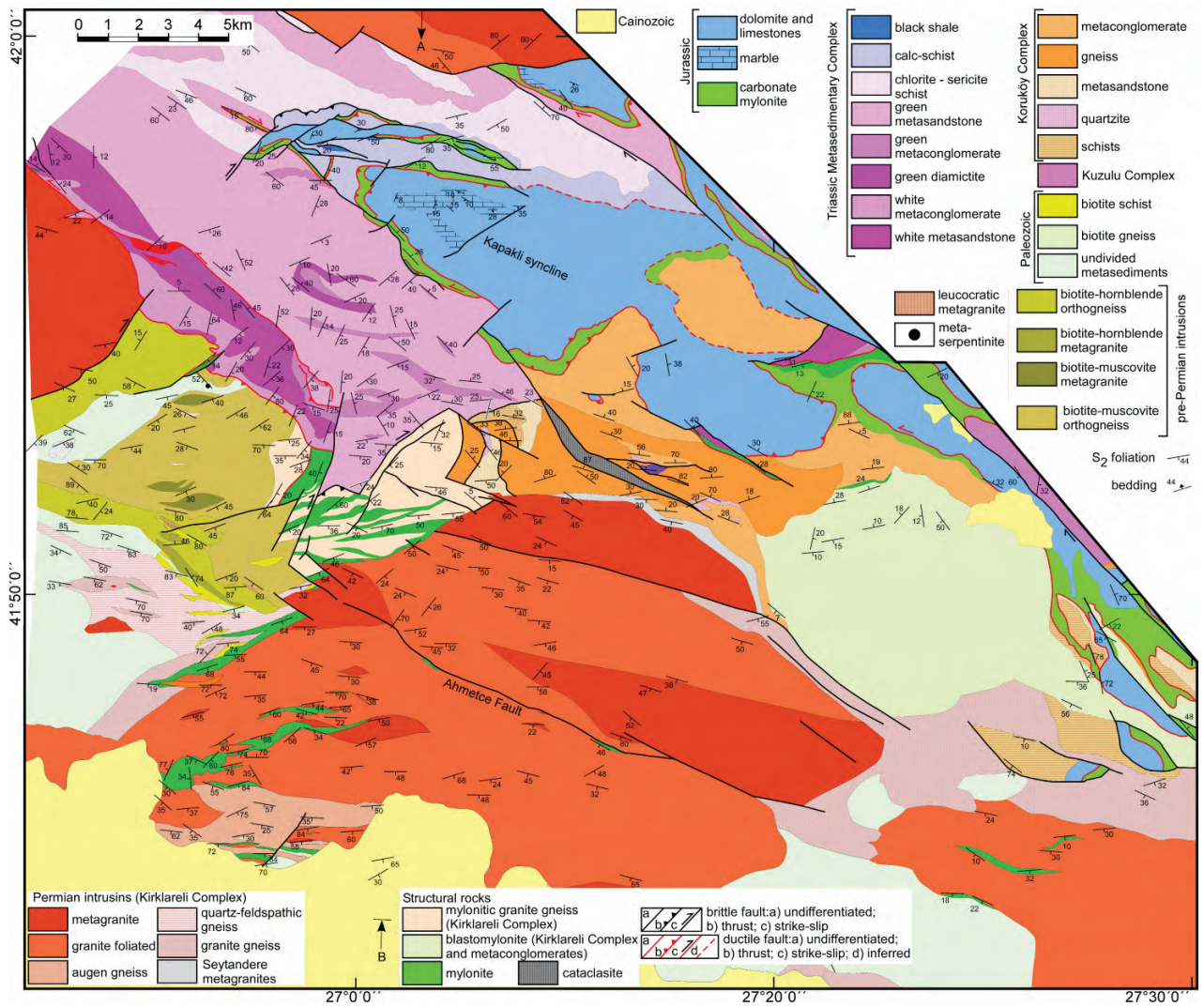


Figure 3. Geological map of the Kırklareli-Kofcaz region. A and B indicate the cross section shown in the Figure 4. Ductile faults marked in red were formed during the Late Jurassic–Early Cretaceous. Their kinematics are based on a stretching lineation sense of shear. Note that the S_2 foliation is generally highly oblique to lithologic boundaries. The map is compiled using the Universal Transverse Mercator projection UTM Zone 35N and European Datum 1950.

Tekedere Group. Çağlayan & Yurtsever (1998) stated that this group includes a wide range of metamorphic and igneous rocks such as biotite gneisses, alkali granites, orthogneisses, amphibolites, biotite-hornblende granite, blastomylonites, muscovite-quartz schists, biotite-quartz-epidote schists, quartz-muscovite-sericite schists, amphibolite schists, garnet-biotite schists, quartz-plagioclase-biotite gneisses and granite gneisses. Our studies show that the Tekedere Group contains diachronous rocks of various origins and granite gneisses compositionally

similar to the Kırklareli metagranites. In the studied area, Carboniferous granite gneisses form the bulk of the Palaeozoic metasedimentary complex. True metasedimentary rocks constitute narrow (800–250 m) NW–SE-striking strips surrounded by orthogneisses. They include biotite and biotite-muscovite schists and gneisses preserving relicts of sedimentary structures (Figure 5). In places, they contain layers of amphibolite consisting of hornblende and actinolite, minor plagioclase and garnet. Euhedral relicts of plagioclase suggest their

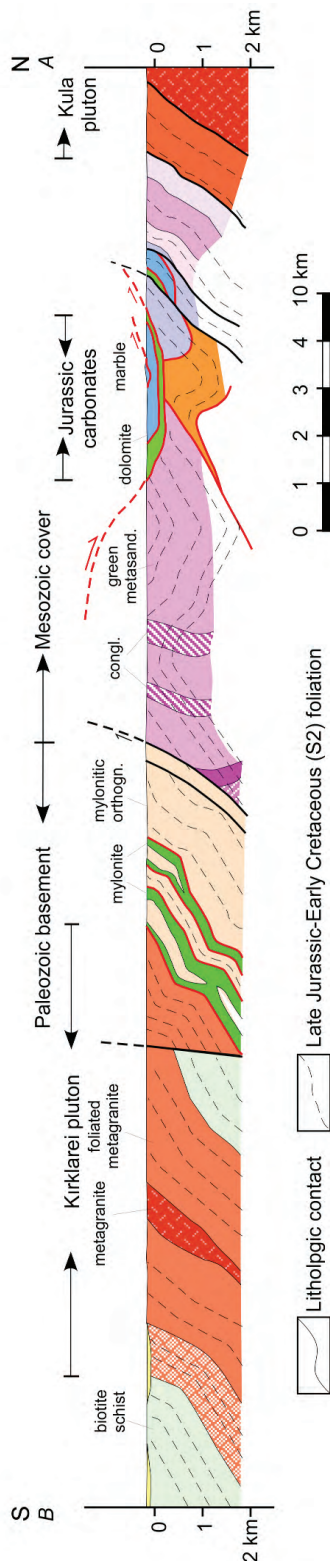


Figure 4. N-S geological cross-section showing contact relations and structures of the studied area. See Figure 3 for location.



Figure 5. Metasedimentary rocks of the Palaeozoic basement. (A) Compositional layering. The layer at the top consists of medium-grained biotite gneiss. The layer in the centre has a similar composition. Biotite schists with thin compositional layering are at the bottom of the photo. The vertical size is about 30 cm. (B) Compositional layering in thin alternation of biotite schists (darker) and biotite gneisses (lighter). Note sharp and diffuse boundaries of a layer at the top of the hammer that may represent original graded bedding.

magmatic origin and the range of amphibole-plagioclase ratios indicates a range of primary rock compositions. Only one (Figures 3 & 4, 13; E27°6'29.078"E, N41°53'48.7"N) tectonic lens (10x20 m) of massive antigorite rock suggesting the presence of serpentinites, was found. Together with the amphibolites, this finding shows the remarkable lithologic difference from the Palaeozoic rocks of the İstanbul Zone.

The age of the metasedimentary rocks in the Palaeozoic basement of the Strandja Massif was viewed differently in previous studies. Çağlayan & Yurtsever (1998) suggested a Palaeozoic age for their Tekedere Group; A.I. Okay *et al.* (2001) inferred that country rocks of the Kirklareli pluton are late

Variscan in age; and, finally, Türkecan & Yurtsever (2002) interpreted their age as the Precambrian. In an attempt to resolve this problem we performed detrital zircon studies both to establish some age constraints and to evaluate possible source areas (Figure 6). Detailed analytical procedures of zircon isotopic dating used here are described in Sunal *et al.* (2008). Petrographic features of the metasediments used for zircon dating are as follows.

The biotite schist (sample Gk 33, see Figure 2 for location) consists of quartz (20–25%), K-feldspar (20–25%), plagioclase (10–15%), biotite (10–15%), muscovite (5–10%), epidote (2–5%), calcite (3–5%), minor zircon, and opaque minerals. In total, 21 grains of rounded and semi-rounded zircons with magmatic zoning have been dated in 29 evaporation-heating steps. The prominent age group (31%) lies between 484.2 ± 4.6 Ma and 433.6 ± 4.8 (Figure 6). These ages have been obtained in all heating steps, including the last one (at 1440°C). It indicates the depositional age of rocks is younger than Early Silurian.

Sample Gk 206 (see Figure 2 for location) is medium- to fine-grained, greenish grey biotite schist that was intruded by late Carboniferous biotite-muscovite granite gneiss (see below). It consists of quartz (5–10%), plagioclase (35–40%), K-feldspar (10–15%), biotite (15–20%), epidote (20–25%), garnet (2–5%), titanite (1–3%), and minor zircon and opaque minerals. The ages of 24 magmatic zircons were obtained in 35 heating steps. The cluster between 495 and 446 Ma (Figure 5) reflects sedimentary reworking of early Palaeozoic magmatic rocks and three dates around 446 constrain the late Ordovician depositional age of the schists. The difference of age spectra older than early Palaeozoic (from 1700 Ma to 434 Ma for sample Gk 33 and from 2700 Ma to 446 Ma for sample Gk 206; Figure 5) allows us to speculate that clastic rocks of more or less similar ages were derived from different sources, which in turn suggests an active tectonic setting.

Sample Gk 200 was collected from the southern part of the basement near the contact with the

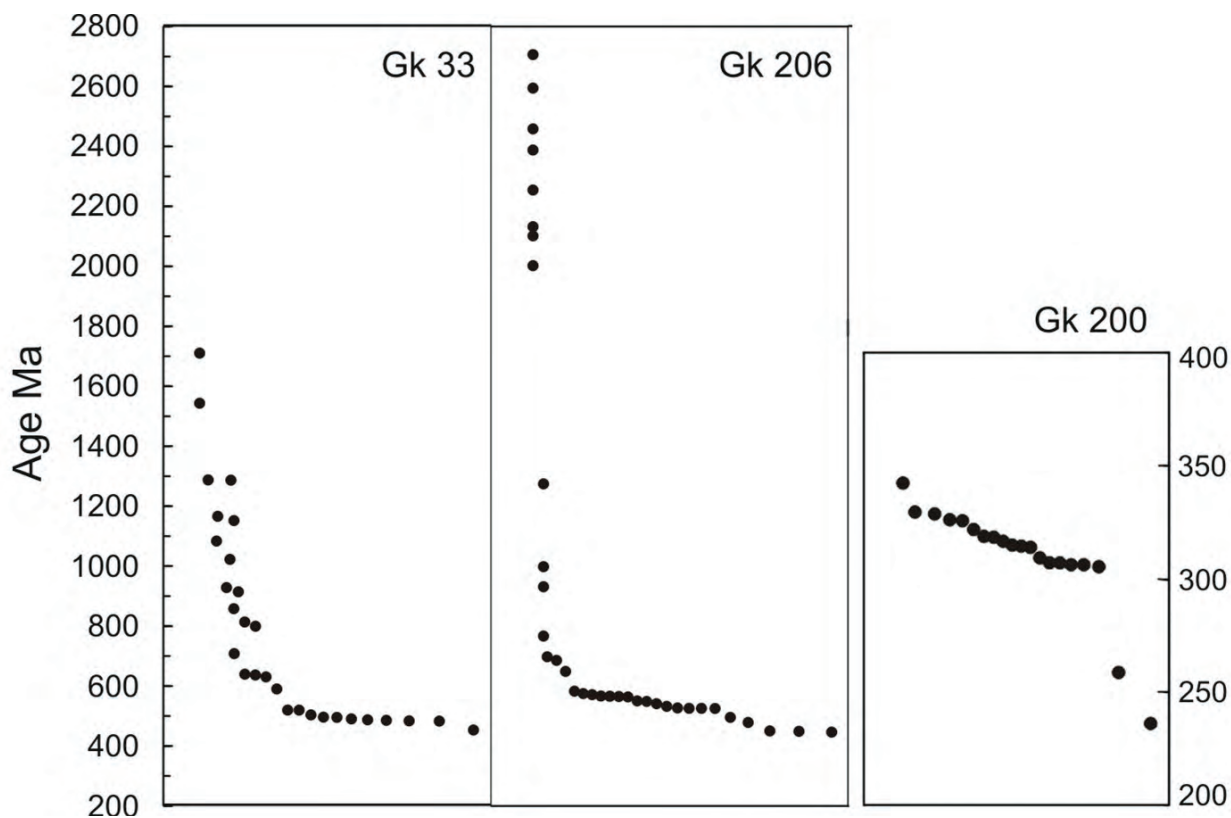


Figure 6. Ages of detrital zircons extracted from the metasedimentary rocks of the Palaeozoic basement of the Strandja Massif (Sunal *et al.* 2008).

Permian Kirklareli metagranite from two-mica schists alternating with amphibolites (Figure 2). The rock consists of quartz (10–15%), plagioclase (25–30%), K-feldspar (15–20%), biotite (15–20%), muscovite (5–10%), garnet (3–8%), epidote (3–5%), chlorite (3–5%), amphibole (3–5%), as well as minor zircon, titanite, and opaque minerals. Ten magmatic zircons were dated in 20 heating steps. We interpret the cluster between 328 and 305 Ma (Carboniferous) as a possible lower limit of deposition age. The young 236 Ma age is unreliable because of a 314 Ma age obtained during the second evaporation step. The 258 Ma date was obtained by one-step measurement at 1400° and has a large 29% error (Sunal *et al.* 2008).

Carboniferous Granite Gneisses and Metagranites

Carboniferous granitic rocks are represented by biotite-hornblende granite gneisses, biotite-muscovite granite gneisses and leucocratic granite gneisses and metagranites. They usually reveal the strong S_2 foliation and L_2 lineation, but in places, where strain is lower, their magmatic fabrics are preserved despite the presence of metamorphic minerals.

The biotite-hornblende granite gneisses are medium-grained, greenish grey to grey and consist of quartz, albite-oligoclase, biotite, hornblende-actinolite, zoisite, chlorite, and muscovite. Green to brown biotite forms intergrowths with muscovite. Relicts of altered plagioclase form porphyroclasts. Sometimes microcline twins are preserved. Thin mafic dykes, xenoliths of biotite schists, and schlieren of amphibolites are common features of these granite gneisses (Figure 7A, B). The schlieren vary in shape from equidimensional to strongly elongated. The elongated schlieren in weakly foliated rocks (Figure 7B) suggest that they formed because of magma flow (Wiebe & Collins 1998; Paterson *et al.* 2004).

The biotite-muscovite granite gneisses are medium grained, greenish-grey to grey. The composition of weakly deformed rocks is very homogeneous. Foliated rocks sometimes reveal a vague compositional layering. Green biotite, muscovite, quartz, albite, and chlorite are the main rock-forming minerals. In contrast to the biotite-hornblende granite gneisses, schlieren and biotite xenoliths are absent.

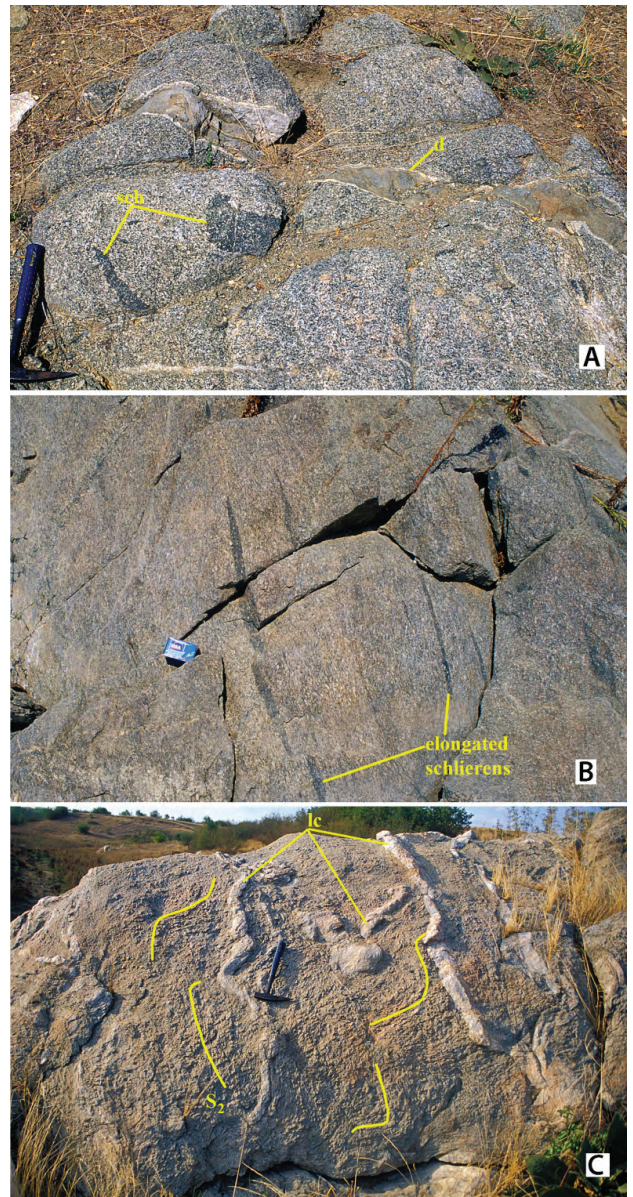


Figure 7. Carboniferous metagranites and granite gneisses of the Palaeozoic basement. (A) Mafic enclaves (sch) and mafic dyke (d) in the biotite-hornblende metagranites indicate magma mingling. Note chilled contacts of the dyke. (B) Strongly elongated schlieren in the biotite-hornblende granite gneisses. (C) Thin leucocratic dykes (lc) in biotite-muscovite granite gneisses. Note folding of leucocratic dykes and the S_2 foliation.

The biotite-hornblende and biotite-muscovite granite gneisses are cut by sheet-like bodies of leucocratic granite gneisses and granites (Figure 7C), the thickness of which varies from several centimetres to tens of metres. The leucocratic granitic rocks have

sharp contacts and tabular shapes suggesting that originally they formed dykes.

The biotite-hornblende granite gneisses contain about 50–60 wt% SiO_2 and 14–19 wt% Al_2O_3 (Sunal *et al.* 2006). Their modal compositions correspond to the tonalite and quartz monzodiorite fields (Figure 8A, B). XMgO [$\text{MgO}/(\text{Fe}_2\text{O}_3 \text{ tot} * 0.9 + \text{MgO})$] values vary between 0.51 and 0.68 and the aluminium saturation index [ASI= molecular

$\text{Al}_2\text{O}_3/(\text{CaO} + \text{Na}_2\text{O} + \text{K}_2\text{O})$] ranges from 0.63 to 0.91 (Figure 8D). Patterns of incompatible elements in the hornblende-biotite gneisses on the spider diagrams (normalized to primitive mantle according to values presented in Sun & McDonough 1989) shows a regular decrease of the enrichment factor with the increasing compatibility of the elements. They are also characterized by slight negative anomalies of Th, Nb, Sr, and Ti (Figure 9).

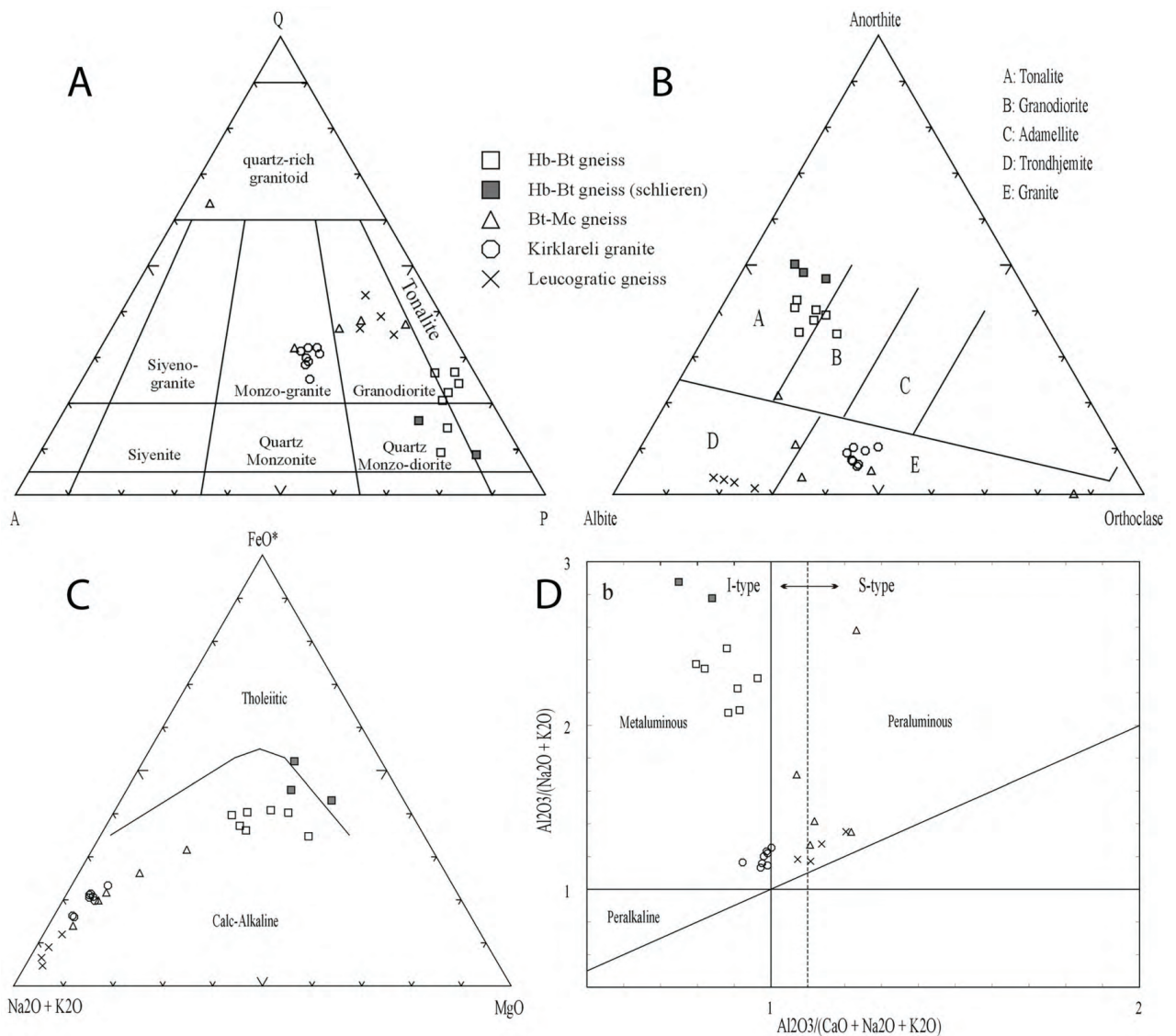


Figure 8. Geochemical features of the Palaeozoic magmatic rocks. (A, B) Normative compositions as (A) Quartz-Alkali Feldspar-Plagioclase (Q-A-P) diagram (Le Maitre 1989) and (B) Anorthite-Albite-Orthoclase diagram (O'Connor 1965) diagrams show. (C) AFM diagram (Irvine & Baragar 1971) indicates that all magmatic complexes follow the same calc-alkaline trend. (D) Shand's index (Maniar & Piccoli 1989; Shand 1927) shows that the magmatic complexes of the studied area have different features, being mainly in the field of I-type granitoids.

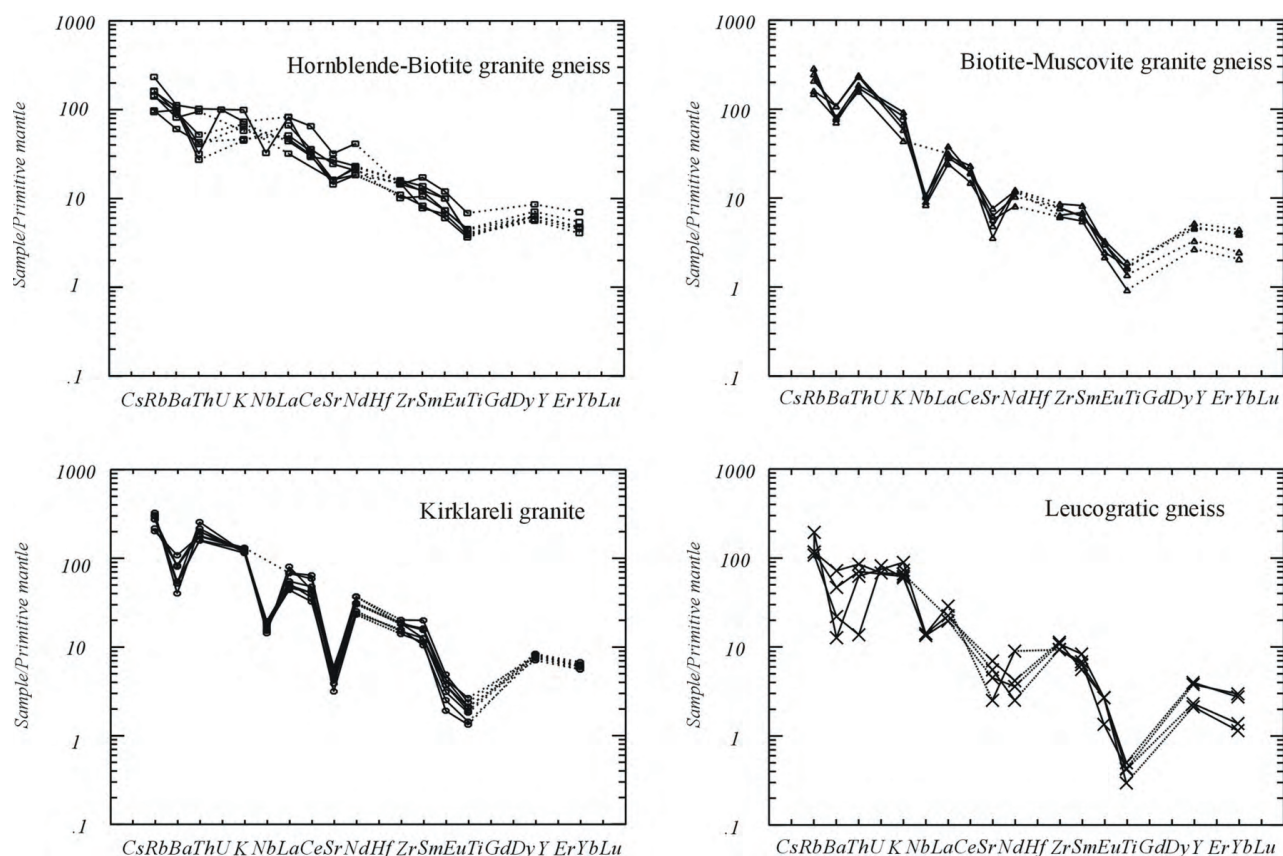


Figure 9. Trace and REE elements normalized to primitive mantle according to values presented in Sun & McDonough (1989). Note Nb anomalies in all analyzed magmatic complexes.

The biotite-muscovite orthogneisses are more felsic in composition. Their SiO_2 contents range between 66–76 wt% and they have relatively low Al_2O_3 contents of 14–15 wt%. Their modal compositions are scattered in the granite, trondjemite, and granodiorite fields (Figure 8A, B). XMgO values vary between 0.39 and 0.51 and aluminium saturation index ranges from 1.07 to 2.26. The patterns of incompatible elements show similar behaviour to the biotite-hornblende granite gneisses, but slopes more steeply towards the high field strength elements.

All Carboniferous orthogneisses follow a single trend on the AFM diagram, being within the calc-alkaline field (Figure 8C). Using geochemical data to determine tectonic setting is constrained by the mobility of major elements and the low strength incompatible elements (Rollinson 1994). Nevertheless, more or less compact distribution of compositions of various rock types on diagrams and

their fitness to compositions of the standards gives us a chance. The biotite-hornblende gneisses exhibit calc-alkaline affinity and metaluminous I-type character that is very similar to Andean-type magmatic rocks (Figure 8). The biotite-muscovite gneisses are intermediate between I- and S-type granites and have peraluminous character (Figure 8). In general, these features are compatible with the Andean-type magmatic setting. Spider diagrams of trace and REE elements reveal a negative Nb anomaly that, together with Ta, is known as the subduction zone component (Condie 1989) and is especially important for this conclusion (Figure 9).

Geochronology of Carboniferous Orthogneisses

Two biotite-hornblende gneiss samples (Gk115 and Gk35) have been dated using the single-zircon $^{207}\text{Pb}/^{206}\text{Pb}$ stepwise-evaporation method (Sunal

et al. 2006) (see Figure 2 for location of samples). All zircons in these samples are idiomorphic and prismatic. They are classified into two groups: (1) colourless or light brown, transparent and translucent and (2) dark brown, semi-transparent, euhedral prismatic. Cathodoluminescence images (see Sunal *et al.* 2006) show that both zircon populations exhibit oscillatory magmatic zoning. Some zircons contain rounded cores that also reveal magmatic zoning. All the grains exhibit low CL outer rims representing a metamorphic overprint.

Six grains in the hornblende-biotite orthogneiss (sample Gk115) belonging to the first group yield ages between 309 and 316 Ma in all evaporation steps. Four grains of the same morphological group (2 in the sample Gk115 and 2 in Gk35) reveal increasing ages with the increase of the evaporation temperature. These old ages may indicate either inherited cores or mixed ages of these cores and young magmatic overgrowth. Zircons of the second group (3 grains in sample Gk115 and 2 grains in sample Gk35) yielded ages older than 340 Ma at all heating steps. These zircons probably represent xenocrysts incorporated by granitic magma from older intrusions.

Figure 10b shows a histogram of $^{206}\text{Pb}/^{207}\text{Pb}$ ratios obtained from both samples and plotted on the same diagram. Note that peaks of samples Gk 115 and Gk 35 fit each other giving an age of 312.3 ± 1.7 Ma (weighted mean of 13 grains, 20 heating steps). We interpret this date as the magmatic age of the hornblende-biotite orthogneisses.

The application of the conventional U-Pb method also shows mixing of zircon ages (Figure 10d). Five fractions consisting of four to seven zircons of the same morphological features have been analysed. The fractions 1–3, and 5 represent the first group and fraction 4 belongs to the second one (see above). The fractions 1, 3, and 5 plot near the concordia. The fraction 1 reveals U loss and gives U-Pb ages of 308 and 315 Ma which fit the magmatic ages obtained by $^{207}\text{Pb}/^{206}\text{Pb}$. Fractions 3 and 5 yield U-Pb ages of 330–334 and 390–399 Ma, respectively. These ages are more concordant than the ages of the previous fraction. The age of fraction 5 may have a geological meaning because some of the evaporated zircons have similar ages of 330–355 Ma. All these ages may reflect a protracted magmatic activity preceding the

hornblende-biotite granite formation. We interpret the age of fractions 3 (399 Ma), 2 (the first group zircon population) and 4 (the second group) as the age of inherited zircons or as a mixed age of cores and later magmatic overgrowth. Following Chen *et al.* (2003) we calculate a forced regression through 308 Ma to evaluate a possible age range of inherited zircons (Figure 10d). This gives a range between 650 and 1300 Ma, which is in accordance with the inherited zircon ages obtained by the single zircon evaporation method.

As in the previous magmatic complex all zircons extracted from sample Gk117 representing biotite-muscovite granite gneisses (see Figure 2 for location) have a prismatic partly corroded shape and their cathodoluminescence images show magmatic oscillatory zoning (Sunal *et al.* 2006). All the grains exhibit low CL outer rims representing a metamorphic overprint (Nemchin & Pidgeon 1997). Three distinct populations have been recognized: (1) dark brown, semi-transparent; (2) colourless to light brown, transparent; and (3) greenish, semi-transparent. The single grain from the first population yielded 460 and 472 Ma ages. The second population has mixed ages varying from 318 to 460 Ma, increasing with the increase of the evaporation temperature. Greenish and semi-transparent crystals yielded ages of 306 and 319 Ma and we interpret these consistent ages as the magmatic age of the biotite-muscovite orthogneisses – a weighted average mean is 314.7 ± 2.6 Ma (Figure 10a). The older ages of the first two groups represent either mixed or inherited ages of individual zircons.

The age of the leucocratic gneisses (sample GK39) is poorly constrained because of the scarcity of zircons (Sunal *et al.* 2006). Two extracted grains show a scatter of ages similar to the biotite-hornblende and biotite-muscovite orthogneisses. One grain yielded 313.3 ± 10 Ma in the first heating step and older (~350 Ma) ages at higher evaporation temperatures. The second grain yielded only old ages exceeding 650 Ma. Taking the geological relationships into account (Figure 7C) we infer that 313 ± 10 Ma is the magmatic age of the leucocratic orthogneisses.

Late Palaeozoic Metamorphism and Deformations

In the late Palaeozoic, the early Palaeozoic and Carboniferous metasediments and the upper

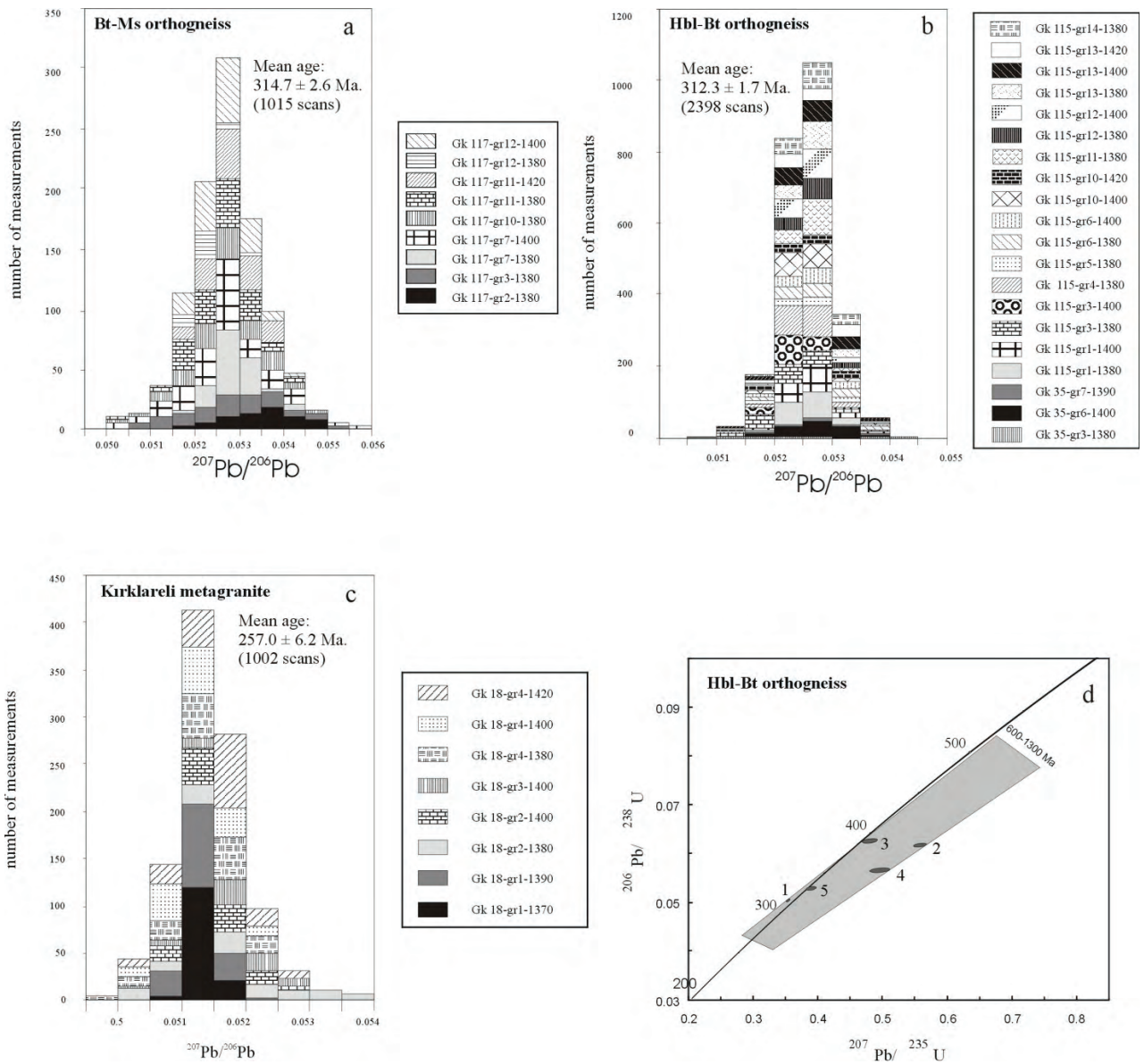


Figure 10. Ages of the Palaeozoic granitoids of the Strandja Massif (Sunal *et al.* 2006). Histograms show the frequency distributions of radiogenic $^{207}\text{Pb}/^{206}\text{Pb}$ ratios obtained by evaporation of single zircon grains extracted from: (a) Carboniferous biotite-muscovite orthogneiss, (b) Carboniferous hornblende-biotite orthogneiss, (c) Permian Kırklareli metagranites, (d) U-Pb concordia plots for zircon of the hornblende-biotite orthogneiss (Gk 35). Ellipses indicate 2σ errors. The upper intercept ages are calculated from zircon fractions taking a forced regression (Chen *et al.* 2003) through 310 Ma. The data were calculated with ISOPLOT program (Ludwig 2003).

Carboniferous granite gneisses were deformed and metamorphosed under greenschist to amphibolite facies conditions (Çağlayan & Yurtsever 1998; A.I. Okay *et al.* 2001; Natal'in *et al.* 2005a, b, 2009; Sunal *et al.* 2006, 2008), but the exact timing of this event

is disputed. A.I. Okay *et al.* (2001) suggested an early Permian age synchronous to the emplacement of the Kırklareli granites, because there are: (1) unconformable relations between the Palaeozoic basement and the Triassic metasedimentary rocks,

and (2) southerly foliation dips in the Palaeozoic basement, but northeasterly dips in the cover allegedly indicate their contrasting structure.

Natalin *et al.* (2005a, b, 2009) and Sunal *et al.* (2006, 2008) inferred that the late Palaeozoic deformation and metamorphism predated the granite emplacement. The most obvious evidence for this inference is the crosscutting relationships of the Permian Kırklareli metagranites and country rocks (Figure 3). This figure also shows that the Middle Jurassic–Early Cretaceous foliation, S_2 , which yielded $^{40}\text{Ar}/^{39}\text{Ar}$ ages varying between 165 and 157 Ma (Natalin *et al.* 2005a, b) and Rb-Sr (whole rock and mica) ages of 141–162 Ma (Sunal *et al.* 2011), cuts lithostratigraphic boundaries and cannot be used as an age constraint for the late Palaeozoic deformation. Unfortunately, the Mesozoic deformation and metamorphism almost completely reworked the previous fabric and metamorphic assemblages. However, in places, the Carboniferous granite gneisses and Palaeozoic metasediments reveal two foliations and two mineral lineations, the geometric relations of which imply two deformation episodes. The Kırklareli metagranites do not have these fabrics. The youngest detrital zircons, dated between 328 and 305 Ma, from the metasedimentary rocks impose a lower limit on the age of the late Palaeozoic deformation and metamorphism. Poor preservation of the earliest fabric does not allow the vergence of structures to be determined.

Late Palaeozoic Magmatism (Kırklareli Complex)

Çağlayan & Yurtsever (1998) assigned the upper Palaeozoic intrusive rocks of the Strandja Massif to the Kırklareli Group. The term group is used to name lithostratigraphic units (Salvador 1994), so we have changed this name into the Kırklareli Complex. During field mapping this complex was subdivided into several rock types (Figures 3 & 4), each of them indicating different degree of strain (Figure 11). Three plutons of the Kırklareli intrusive complex are exposed in the studied area: the Kırklareli, Üsküp and Ömeroba plutons (Figure 2). Similar granites are widespread in both NW Turkey and Bulgaria (A.I. Okay *et al.* 2001; Gerdjikov 2005).

Rocks of the Kırklareli and Üsküp plutons are typical monzonitic granites. Their characteristic

feature is the presence of large (up to 5 cm) phenocrysts of pink K-feldspar and an almost ubiquitous porphyritic texture (Figure 11A, B), especially characteristic of the Kırklareli pluton. In places, rocks are converted to augen gneisses (Figure 11C). Rocks of the Üsküp pluton usually have a smaller grain size. However, this intrusion is more deformed than the Kırklareli pluton and grain size reduction may be explained by higher strain. The Ömeroba granites are less deformed and metamorphosed. They are often equigranular, with grain size varying from 0.5 to 1–1.5 cm. They are more typical of normal granites.

The Kırklareli pluton, 25 km long and 14 km wide, is elongated east–west, parallel with the strike of the S_2 foliation (Figure 3). Strong foliation and contact relationships with country rocks where the S_2 foliation is parallel with the lithological boundaries suggests that the pluton is a sheet-like body dipping moderately south.

Çağlayan & Yurtsever (1998) described the following mineral content for the Kırklareli pluton: quartz ~30%, K-feldspar (about 80% of total feldspar), plagioclase (oligoclase replaced by albite constituting the remaining 20%). The content of dark minerals (biotite, metamorphic muscovite, and epidote) varies from 10 to 20%. In thin sections, quartz reveals undulose extinction and dynamic recrystallization into a fine-grained aggregate. K-feldspar is often characterized by microcline twinning and marginal replacement by myrmekites directing their lobes toward K-feldspar grains. Its crystals reveal both cataclastic and crystal-plastic deformations. The latter was responsible for formation of the augen gneisses (Figure 11C), which are widespread in the Üsküp pluton. Together with myrmekite, the crystal-plastic deformation of K-feldspar suggests local increase of metamorphic temperature above 600°C (Vernon 2004; Passchier & Trouw 2005). Biotite is brown to dark green. Kinking and bending of its crystals, grains shredding along cleavage planes, displaced cleavage fragments of former grains forming wedge-shaped terminations are very common. Sometimes biotite forms typical folia wrapping around K-feldspar. All these features indicate solid-state deformation (Vernon 2004) of the Kırklareli granites. Rb-Sr dating of biotite (see below) always gives more

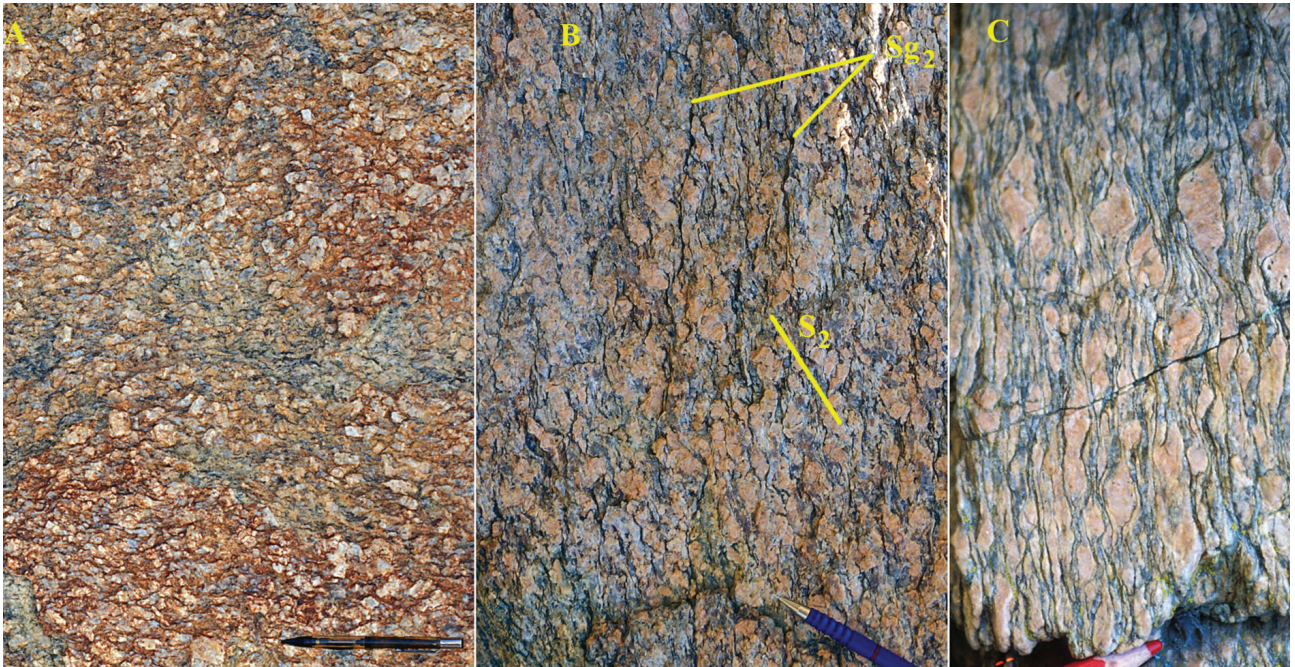


Figure 11. The Kirklareli type granites show porphyritic fabric regardless of strain. (A) Weakly-deformed granites in which K-feldspar shows cataclastic deformation. (B) Foliated metagranites showing two foliations: rough anastomosing S_{g2} cleavage (dark streaks) and metamorphic foliation S_2 . (C) Transition of metamorphic foliation into augen gneiss.

or less consistent young Mesozoic ages remarkably different from the early Permian ages of magmatic zircons. Together with structural observations, this suggests that biotites of the Kirklareli granites have a metamorphic origin. However, A.I. Okay *et al.* (2001) described magmatic muscovite in these rocks. In our thin sections, muscovite always appears as a mineral that replaces biotite.

The pluton is affected by the late Mesozoic deformations; the S_2 foliation and mineral L_2 lineation are well developed, and in places, are penetrative. The degree of this deformation varies across the pluton. Less deformed rocks are exposed along the northern boundary of the pluton (Figures 3 & 4). In the west, these weakly deformed granites have a sharp contact with white mylonitic granitic gneisses (Figures 3 & 4), which originally were part of the Kirklareli Complex. The sharpness of the contact implies the presence of a later brittle fault that eliminated part of the structural section, which were formed at a transition between the low-strained granites and white mylonitic granite gneisses. Another explanation of the sharpness of the contact is a low-temperature deformation that makes strain gradient stronger.

In the eastern segment of the northern contact, Çağlayan & Yurtsever (1998) mapped the Şeytandere metagranites and pegmatites that define the margin of the Kirklareli intrusion (Figures 3 & 4). These equigranular granites have a transitional contact with the porphyritic granites. Unlike at the southern margin, migmatites are absent, and we interpret this contact as the overturned upper contact of the intrusion.

The central part of the Kirklareli intrusion consists of foliated metagranites containing lenses (2.5 km wide) of weakly deformed granite. These rocks are very homogeneous in composition. As in the northern part of the intrusion, xenoliths of country rocks are absent except for a zone along the Ahmetce Fault (Figures 2–4) where xenoliths of biotite schists ten metres across appear in the walls of the fault. Within the same zone, a few tectonic lenses of dark biotite schist occur in fault contact with mylonites or strongly foliated Kirklareli granites. These schists are slightly migmatized, suggesting proximity to the pluton contact. Their position right in the middle of a large intrusion suggests the pluton has a sheet-like shape. In the south, the Kirklareli pluton consists of

strongly foliated granite gneisses, augen gneisses, and mylonites. In many places, contacts with country rocks are mylonitic. In contrast to the northern and central regions, xenoliths of biotite schists and paragneisses, mafic schlieren, and mafic dykes are common. Country rocks show migmatization – banded rocks with diffuse contacts between layers of leucogranite (neosome) and biotite schist (palaeosome). Magmatic granite contacts, where preserved, are characterized by thin (tens centimetres) zones enriched in biotite (melanosome?). These suggest a greater original depth of this part of the Kırklareli pluton where the temperature contrast between granitic magma and country rocks allowed anatexis. Thus, we infer that the sheet-like body of the Kırklareli granites has its root zone in the south.

In the southern and western part of the Kırklareli pluton, there are bodies of quartzo-feldspathic gneisses containing relicts of large crystals of K-feldspar (Figure 3). We infer that they also belong to the Kırklareli magmatic complex. In the north, a strip of white and light grey mylonites and mylonitic granite gneisses are exposed between the weakly deformed Kırklareli granites and the Triassic metasedimentary complex (Figure 3). These rocks often contain relicts of Kırklareli-type granites. Therefore, they probably represent a highly deformed part of the pluton. In places, the same rocks reveal relicts of clastic fabric indicating the heterogeneous nature of the protolith of the mylonites and mylonitic gneisses. Relicts of sedimentary clastic rocks become more frequent in the east in a wide strip of blastomylonites exposed between the Üsküp pluton and the Koruköy complex (Figures 2–4).

The Kırklareli metagranites cluster within the monzogranite field (QFP diagram, Figure 8A) while they are in the granite field on the AAO diagram (Figure 8B). Compared to the Carboniferous orthogneisses, the Kırklareli metagranites have a more restricted content of SiO₂ (70–74 wt%) and Al₂O₃ (13–15 wt%). Their XMgO values vary between 0.28 and 0.36 and ASI values are 0.9–1.0 (Figure 8D). Like the Carboniferous orthogneisses the K-feldspar metagranites show a calc-alkaline affinity, occurring on the same trend (Figure 8C).

Patterns of incompatible element (normalized to primitive mantle) show a decrease of the enrichment factor with increasing compatibility of the elements

(Figure 9), and are characterized by distinct negative anomalies of Ba, Nb, Sr, Eu and Ti (Figure 9). The Nb negative anomaly, together with the calc-alkaline affinities of the rocks and the cluster of their contents within the volcanic arc field on some diagrams (Sunal *et al.* 2006), suggests that the Permian magmatic rocks of the Strandja Massif are subduction-related.

Geochronology of the Kırklareli Metagranites

The Kırklareli metagranites have already been dated by Aydın (1982) and A.I. Okay *et al.* (2001) as 245 Ma and ~271 Ma, respectively. In this study, we have obtained an additional age determination from sample Gk18 (see Figure 2 for location) using the single zircon evaporation method.

Sample Gk18 is an augen gneiss consisting of quartz, porphyroblasts of strongly altered and in places completely recrystallized K-feldspar, altered plagioclase, brown muscovite, epidote, titanite, and rutile. Zircons from this sample form a uniform population represented by brown, semi-transparent, and euhedral, prismatic crystals. Clear oscillatory magmatic zoning is characteristic in all selected grains.

All evaporated grains yielded ages between 253.8 and 276.1 Ma, which give a weighted average mean of 257±6.2 Ma (Figure 10C) (Sunal *et al.* 2006), similar to results from A.I. Okay *et al.* (2001). Neither A.I. Okay *et al.* (2001) nor our studies, which used the same zircon evaporation technique, have revealed a large scatter of ages typically indicating the presence of inherited zircon cores.

Our 16 Rb-Sr age determinations of white mylonitic granite gneisses and quartz-feldspathic gneisses, containing relicts of the Kırklareli-type granites, vary between 136 and 162 Ma (Sunal *et al.* 2011). These ages are derived from isochron calculations using whole rock ages and the age of biotite and/or muscovite. Compared to zircon ages from the Kırklareli pluton, they are too young and reflect the Late Jurassic–Early Cretaceous metamorphism and deformation. Vonderschmidt (unpublished MSc Thesis, Tübingen, 2004) reported an additional four dates from the same rocks ranging between 148 and 162 Ma. At the same time two of his samples (WMG1 and WMG2, see Figure 2 for

locations) yielded Rb-Sr isochron ages of 279 and 295 Ma, respectively. These ages are 8–18 Ma older than ages obtained by the single zircon evaporation method from the Kırklareli granites. An 'old' zircon age of 309 Ma has also been reported from the Üsküp granite (A.I. Okay *et al.* 2001). It was obtained by using the evaporation method applied to a single grain with low numbers of scans (42). It also has a high error (± 24 Ma). Such ages are suspicious, but the absence of inherited or mixed ages in zircons of the Kırklareli granites allows us to consider this date to have some significance. All of the dates mentioned above may reflect prolonged magmatic activity that produced the Kırklareli-type granites.

Upper Palaeozoic–Triassic Metasedimentary Complex (Koruköy Complex)

The Koruköy Complex, with north-dipping S_2 foliation, forms a rock package in the central part of the studied area north of the Kırklareli pluton (Figures 3 & 4). In the western part of the complex, the S_2 foliation crosscut lithological boundaries at almost right angles, which we interpret as evidence of rotation that may predate or be synchronous with the earliest stage of the Late Jurassic to Early Cretaceous deformation.

The Koruköy Complex was mapped (A.I. Okay *et al.* 2001) as the Triassic sedimentary cover of the Strandja Massif, but its lithological features are quite different from those of the Triassic rocks (see below). The Koruköy Complex, bounded by faults and shear zones (Figures 3 & 4), consists of several lithostratigraphic units showing more or less consistent lithological content and structural style: the rocks of the complex never reveal two foliations. These units are metaconglomerates, metaquartzites, schists, metasandstones, and mylonitic gneisses (Figure 12), but their stratigraphic succession is not clear.

The metaconglomerates, with an exposed structural thickness of about 1600 m, are structurally overlain by a nappe of Jurassic carbonates (Figures 3 & 4). Their original thickness may have been much greater (perhaps 2–3 km) because the pebbles show strong flattening and their upper contact is

not exposed. The metaconglomerates are usually matrix-supported, unsorted or poorly sorted, and in places, reveal a transition to diamictite (nongenetic term!). Pebble sizes vary from 1–2 cm to 10 cm. The matrix is represented by medium-grained lithic metasandstone. These rocks are foliated; muscovite, chlorite, and rare biotite coat the S_2 foliation planes. Pebbles, commonly stretched and flattened, consist of granite gneisses, aplite, quartzites, milky quartz, biotite schists, and biotite gneisses bearing their own foliation. The granite gneiss and aplite pebbles are similar to Carboniferous orthogneisses. Porphyritic granites of the Kırklareli type have never been observed as clasts in the Koruköy metaconglomerates. The roundness of pebbles is generally good while the sorting is poor. In places, the angular shape of clasts and variety in sizes make the rock similar to a metamorphosed olisthostrome. There, some clasts are reddish laminated microquartzites, which may be interpreted as metacherts.

Metaquartzites are exposed as lensoid bodies 50–300 m thick. They often reveal a compositional layering (2–5 cm) formed by changes of mica content. The lack of feldspar suggests the possibility of two types of protolith: pure quartzites or cherts. Schists and metasandstones consist of quartz, albite, muscovite, epidote, chlorite, and rare biotite. Much of the Koruköy Complex consists of light grey and grey thinly-laminated gneisses with mylonitic foliation. Relicts of igneous and clastic rocks suggest the heterogeneity of the protoliths but they definitely include magmatic rocks because of the homogeneity of bodies with magmatic fabric relicts.

Small (0.5–1 m) lenses of pegmatites with crystals of pink K-feldspar cut the gneisses and metaconglomerates. They are similar to the pegmatite of the Şeytandere metagranites (marginal facies of the Kırklareli granites). Thus, the gneisses and the metaconglomerate both already existed during the emplacement of the Permian Kırklareli type granites. The absence of the Kırklareli granites in the conglomerate clasts indicate that the Kırklareli pluton was not then exhumed at the surface. At the same time, the structural style of the Koruköy Complex is identical with the style of the Triassic metasedimentary rocks, namely no relicts of pre-Mesozoic foliation have been identified in

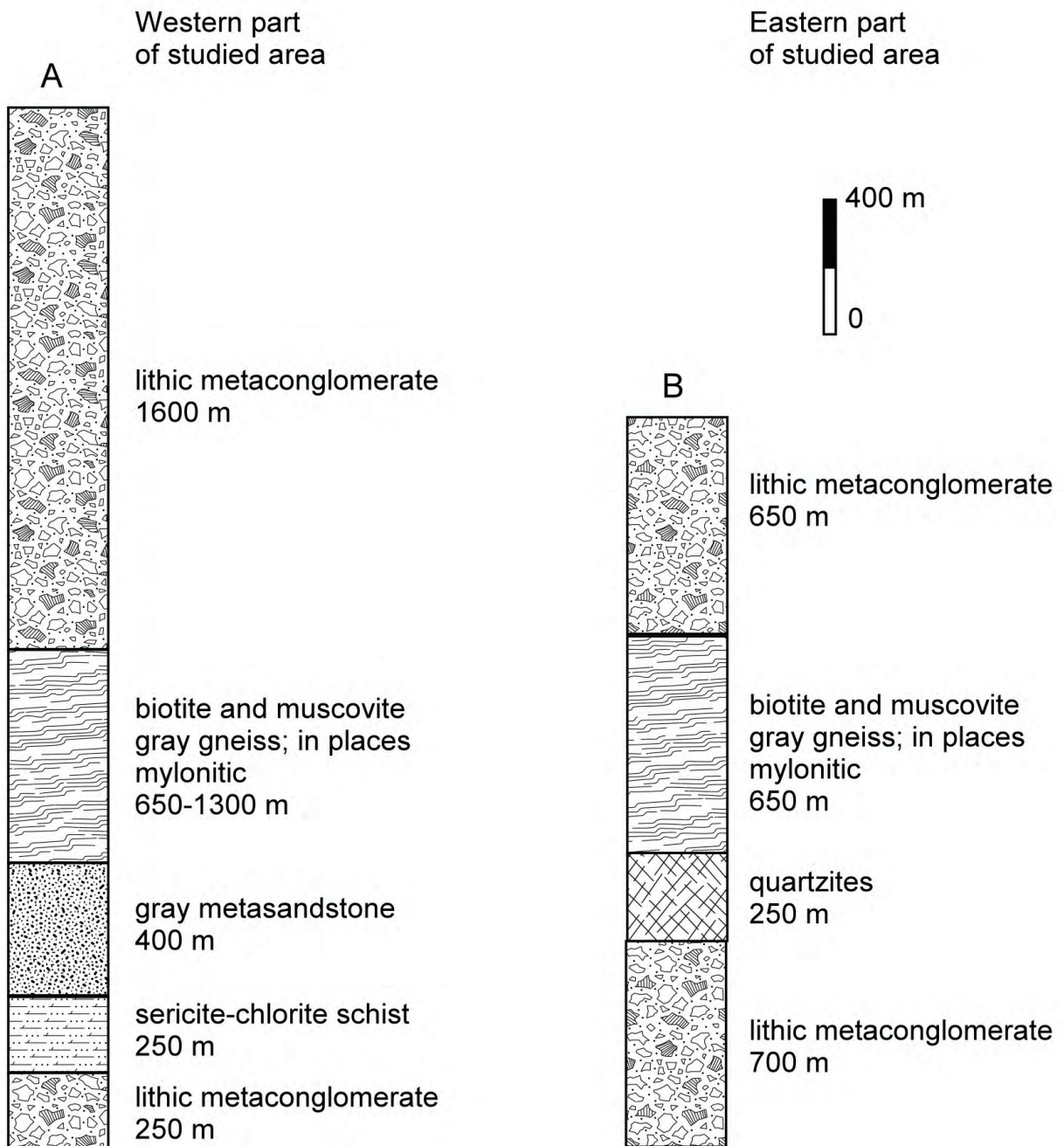


Figure 12. Structural successions of lithostratigraphic units in the Koruköy complex (see locations in Figure 2).

these rocks. In addition, the Koruköy schists and metasandstones are lithologically similar to the Triassic metasedimentary rocks (see below). All of these constrain the age of the Koruköy Complex as Permian to Triassic, as originally inferred by Çağlayan & Yurtsever (1998).

Kuzulu Complex

The Kuzulu Complex is exposed in the central part of the Koruköy Complex (Figures 3 & 4) as a tectonic slice 1 km long and 0.3 km wide (the coordinate of the best section is 523,693; 4,635,522). We infer that ductile shear zones parallel to the S_2 foliation form

the original contacts of this unit, although strong crenulation cleavage overprints the S_2 foliation along the northern boundary of the complex and late faulting with cataclasites was observed along the southern boundary (Figure 13).

The Kuzulu Complex consists of metavolcanic rocks, metacherts, schists, and meta-gabbroic rocks (Figure 13). The metavolcanic rocks are dark green fine-grained rocks, in which all primary minerals are replaced by metamorphic dark green biotite, green chlorite, and epidote. In spite of well-developed S_2 foliation, the rocks are massive. In places, relicts of pillows can be observed. The metagabbro is a medium-grained, dark greenish rock, in which primary minerals are also replaced by epidote, chlorite, and epidote. The metacherts are fine-grained reddish rocks. Lamination is common, defined by the presence of thin (0.3–1.0 cm) laminae of dark grey or reddish grey pelitic schists. The reddish colour of the metacherts makes these rocks distinct from the light grey to white quartzites of the Koruköy Complex.

Pelitic schists and phyllites form a large body in the southern part of the Kuzulu Complex. Their characteristic feature is a reddish colour produced by thin laminae or lenses of fine-grained metacherts or quartz-rich schists. We suggest that these quartz-rich

rocks were formed from siliceous shales. In places, dark grey pelitic schists and reddish cherty rocks show a strong transposition along foliation planes. We infer that this fabric may indicate the presence of an original *mélange* that was reworked by Mesozoic deformation.

The Kuzulu rock assemblage is similar to the upper parts of the ophiolitic succession. We interpret the laminated metacherts and quartz-rich schists as pelagic and hemipelagic rocks accordingly. If true, they contrast greatly with the depositional environments of the surrounding units, further indicating the great magnitude of displacements along shear zones bounding the Kuzulu Complex.

Triassic Metasedimentary Complex

The Triassic metasedimentary complex was interpreted as the cover of the Strandja Massif, deposited in rather quiet tectonic environments after the late Palaeozoic orogeny, and assigned to the Istranca Group (Çağlayan & Yurtsever 1998; A.I. Okay *et al.* 2001). Indeed, Triassic metaconglomerates contain clasts of various granite gneisses, metagranites, schists, quartzites, and paragneisses that often reveal a pre- S_2 foliation. These clasts indicate that Triassic rocks

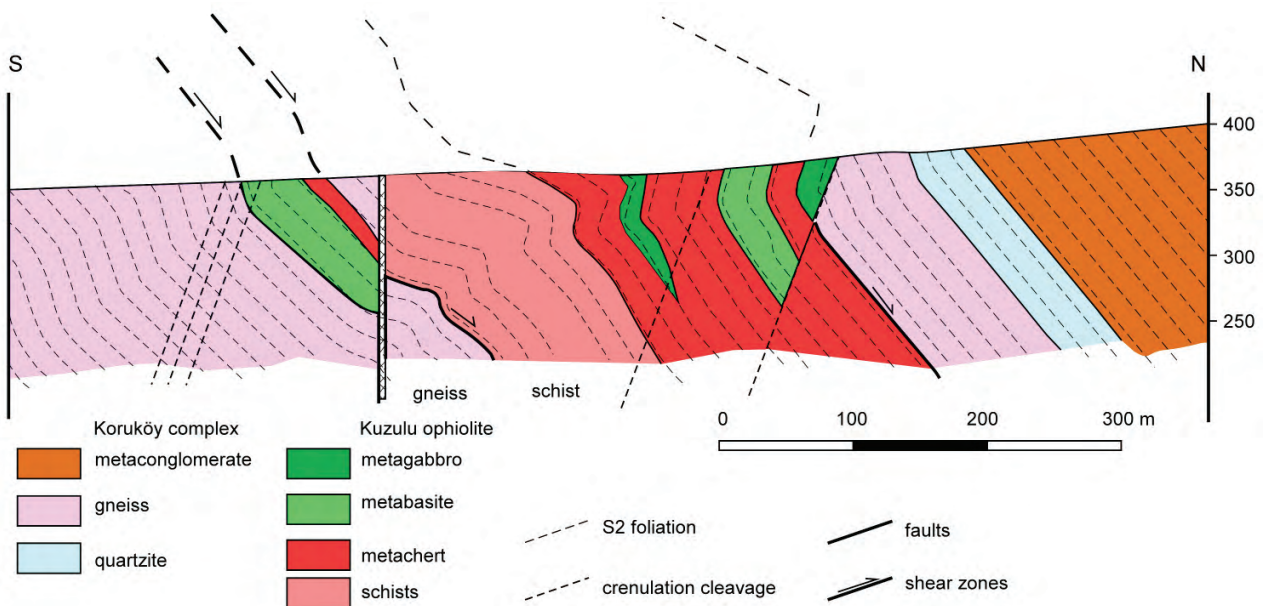


Figure 13. Cross section of the Kuzulu ophiolites (see geographic location in Figure 2).

were deposited after the late Palaeozoic deformation and metamorphism. However, we disagree with A.I. Okay *et al.* (2001, their figure 7) who interpreted the Triassic metasedimentary rocks as a simply deformed and gently dipping sedimentary cover. In fact, the contact with the Palaeozoic metamorphic rocks is overturned to the north and bedding of the Triassic rocks dips to the south at 60–90° (Figures 4 & 14). Crosscutting relationships of bedding and S_2 foliation imply that the Triassic metasedimentary rocks form the core of a large synform that is overturned to the north (Figure 4). This structure further implies that at least part of the Palaeozoic metamorphic column in the southern limb is overturned.

The Triassic lithostratigraphic units fine up to the north and reveal the following succession: metaconglomerates with quartzitic matrix, quartzose metasandstones, diamictites (non-genetic term used for poorly sorted conglomerate with abundant matrix) and conglomerates with lithic matrix, lithic green metasandstones (see Figure 14 for this part of the succession), metaconglomerates with lithic sandstone matrix, diamictites with lithic sandstone matrix, chlorite-sericite schists, calcareous schists and metasandstones, and black graphitic phyllites and shales (Figure 3). We infer that this is the original stratigraphic succession although additional studies are necessary. The total structural thickness of the Triassic rocks is about 8 km. Despite the penetrative S_2 foliation, outcrop-scale isoclinal folding was not detected. Therefore, evaluations of original thickness must account for some flattening during the Mesozoic deformations.

White metaconglomerates and diamictites exposed in the south (Figures 3, 4 & 14) consist of poorly sorted but well-rounded pebbles 0.5 to 15 cm across of granitic gneisses, paragneisses, quartz, biotite and muscovite schists, and quartzites. Pebbles of ortho- and para-gneisses and mica schists are similar to those in the Palaeozoic basement. Pebbles of quartzites could have been derived from the Koruköy Complex. The white matrix consists of quartz-feldspathic medium- to coarse-grained metasandstone. White coarse- to medium-grained metasandstones are exposed farther northeast and are most likely have a depositional contact with the conglomerate.

In the western part of the studied area, white quartzo-feldspathic metasandstone contains a lens (10x40 m) of andesitic pillow lava (Figures 3 & 4). The rocks are strongly altered with development of chlorite and epidote. Pillows vary from 20 to 50 cm across. Rare dykes of intermediate to mafic composition have been reported in the neighbouring region of Bulgaria (Nikolov *et al.* 1999).

To the north quartzo-feldspathic metasandstone passes into diamictites and metaconglomerates with a lithic matrix, and then to green and greenish grey metasandstone containing metaconglomerates lenses of various sizes, which may represent distributary channels. The structural thickness of the green sandstones is 3–4 km. They have a uniform composition. In the lower part, near the underlying metaconglomerates, relicts of graded bedding have been observed. Besides the clasts of the Palaeozoic basement, pebbles of volcanic rocks and metacherts are also found. Quartz, albite-oligoclase, chlorite, phengite, and epidote are principal minerals, indicating greenschist facies metamorphism (Sunal *et al.* 2011).

The green metasandstones pass into chlorite-sericite schists (1.5–3 km), which formed from a thin alternation of shale and fine-grained sandstones. The S_2 foliation in this unit dips to the southwest (Figure 3) indicating its lower structural position. This relationship can be explained by the strong tectonic movements to the northeast during the late stage of the Late Jurassic–Early Cretaceous deformation. However, the asymmetry of rock-type distribution, from the metaconglomerate in the south to the chlorite-sericite schists in the north (Figure 3), may be also interpreted as facies changes as originally suggested by A.I. Okay *et al.* (2001).

Calcareous schists, calcareous metasandstones, and black phyllites belong to the uppermost lithostratigraphic units of the Triassic metasedimentary complex. They are exposed along the northern limb of the Kapaklı syncline, and their structure does not fit with the underlying metasandstones and chlorite-sericite schists (Figure 3). These units probably represent a tectonic slice lying above all previously-described units of the Triassic metasedimentary complex. Unlike the structurally overlying Jurassic carbonates, the calcareous rocks and black phyllites reveal the same structural style

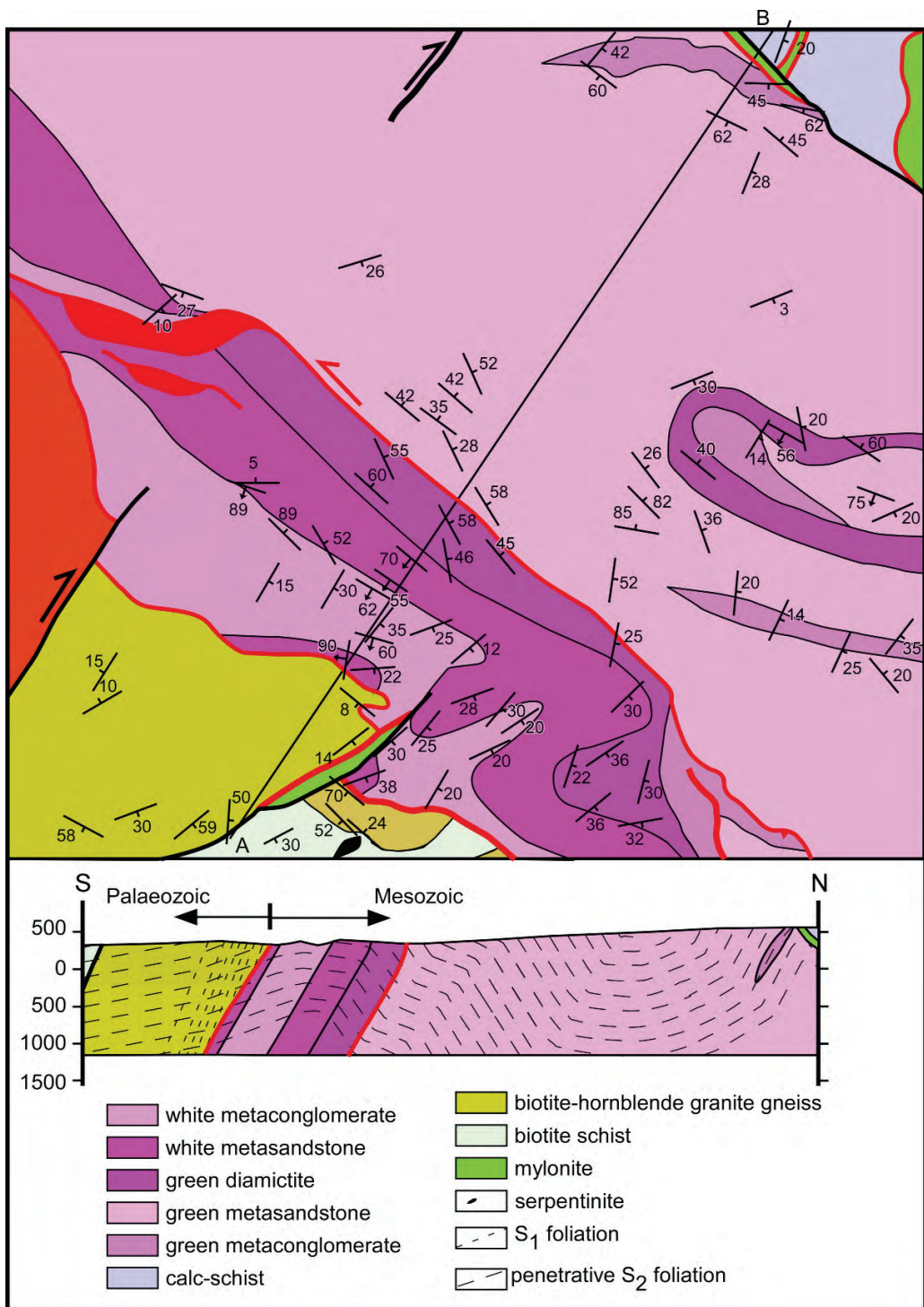


Figure 14. Geological map (A) and cross section (B) showing the relationships between the Palaeozoic basement and Triassic metasedimentary cover of the Strandja Massif (see Figure 2 for location). Note regional crosscutting relationships between the folded Late Jurassic–Early Cretaceous S_2 foliation and lithological boundaries. Dip angles of the S_2 foliation are moderate, while bedding is steep. The bedding should be overturned. Absence of sedimentary structures did not allow this inference to be checked.

as the underlying rocks. Therefore, we place them within the Triassic metasedimentary complex.

The Triassic calcareous schists and metasediments contain horizons (2–7 m thick) of calcitic marbles and in places show a thin alternation with them, as in calc-turbidites. Observing that the metaconglomerates contain clasts of carbonates, mafic volcanics, and cherts Hagdorn & Göncüoğlu (2007) inferred an unconformity at the base of the calcareous rocks. We place these conglomerates as a small channel deposit (Figures 3 & 4) within the lower green metasediment. This alleged 'basal conglomerate' has not been observed elsewhere. The black graphite-bearing phyllites and slates structurally overlie the calcareous schists and metasediments in all observed localities (Figures 3 & 4) but their stratigraphic relationships remain uncertain because of later deformation.

With respect to sedimentary facies, Çağlayan & Yurtsever (1998) and A.I. Okay *et al.* (2001) claimed that the Triassic metasedimentary complex represents alluvial fans, braided river valleys, and large sandy beaches. Indeed, thick homogeneous metaconglomerates, monotonous green metasediments, rare thinly-laminated rocks, and conglomeratic lenses in the green lithic metasediments do indicate deposition in high-energy environments. However, the almost complete absence of sedimentary structures does not allow us to corroborate this facies interpretation. For instance, in high-strain rocks, flaser bedding and cross stratification can be easily mixed with transposition via folding oblique to bedding and foliation. However, we agree with the previous researchers that the Triassic metasedimentary complex reveals a transgressive nature in its lowest part. In the upper parts, we infer shallow-marine to deep-marine environments of deposition. Relicts of graded bedding and thin alternations of metasediment and chlorite-sericite schists with the perfect parallelism of lithologic boundaries may also suggest that most of the Triassic complex is turbiditic. Çağlayan & Yurtsever (1998) suggested a Permo–Triassic age, while Chatalov (1990, 1991) and A.I. Okay *et al.* (2001) proposed a Triassic age for this metasedimentary complex. We accept the latter interpretation here. This assessment is based on long-distance correlation with Bulgaria, where similar rocks contain fossils (Chatalov 1990,

1991). Recently, Hagdorn & Göncüoğlu (2007) confirmed this correlation by finding Early–Middle Triassic crinoids in limestones alternating with calcareous schists. Despite the inferred unconformity at the base, they extended this age determination for the entire Istranca Group of Çağlayan & Yurtsever (1998). We have mentioned that the calcareous rocks and black phyllites may represent an independent tectonic slice, so it is reasonable to clarify why the correlation with the Bulgarian Triassic is justifiable, as well as pointing out some differences in correlation.

In Bulgaria, Triassic rocks have been classified as the Balkanide, Sakar, and Strandzha types (Chatalov 1991). The first two types characterize rocks deposited on the northern (Europe) and southern (Balkan) continents accordingly. The Strandzha type (Valeka Unit in Figure 1) represents an oceanic domain between them. Chatalov (1991) correlated the Turkish Triassic metasedimentary complex with his Sakar type; Gerdjikov (2005) with the Strandzha type, and A.I. Okay *et al.* (2001) and Hagdorn & Göncüoğlu (2007) saw more similarities with the 'European' Balkanide facies.

The Balkanide Triassic rocks are unmetamorphosed, and consist of Lower Triassic (~300 m thick) fluvial redbeds and minor andesites passing into shale, marls, and dolomites deposited in lagoons, overlain by Middle–Upper Triassic carbonate rocks (~2000 m thick) (Chatalov 1990, 1991). We think that this succession alone does not support the correlation between the Triassic metasedimentary complex and the Balkanide type. The structural thickness of siliciclastic rocks south of the Kapaklı syncline is about 8 km (Figure 14). The red colour of the rocks indicating an oxidizing depositional environment is typical for the Balkanide Triassic. There are no redbeds in the Triassic metasedimentary complex. The rocks are green, white or grey, and often contain pyrite crystals suggesting rather anoxic depositional environments.

The Sakar type of the Triassic is subdivided into two parts (Chatalov 1990, 1991). The lower part starts with metaconglomerates and mica schists (400 m), grading up into an alternation of the quartz-carbonate schists, meta-arkoses and metaquartzites, marbles, and amphibole schists (2000 m thick). Small bodies of quartz porphyry were also observed. Early Triassic

bivalves were found in amphibole schists, marbles, and metaquartzites. The rocks were deposited in shallow-water environments. The upper part of the Sakar type consists of Middle Triassic calcic and dolomitic marbles (1000 m thick). Thus, the Triassic metasedimentary rocks of the studied area may be correlated with the Lower Triassic part of the Sakar-type Triassic rocks in Bulgaria. The only problem with this correlation is the absence of thick marbles in the Strandja Massif. However, marbles are present among calcareous rocks appearing in the upper part of the succession. The Triassic metasedimentary complex may also correspond to the Strandzha type of Triassic rocks in Bulgaria as Gerdjikov (2005) suggested. This suggestion is more plausible for us.

Black shales at the top of our Triassic metasedimentary succession are not mentioned in Chatalov's (1990, 1991) descriptions of the Sakar type of the Triassic. Anoxic environments, in which such rocks are deposited, are very distinctive in the geological history, and helpful in correlation. In the Valeka Unit (Figure 1), Chatalov (1990) defined the Graphitic Formation as a facies of the lower part of the Carnian–Norian Lipachka flysch but its age has not been confirmed by fossils. Another stratigraphic level of black shales (confirmed by fossils) is Middle Jurassic. It is known in the Kotel Belt, located near the boundary between the Moesian Platform and the Balkan Zone (Figure 1), where black shales are associated with flysch and olisthostrome, and near the Valeka Unit (Georgiev *et al.* 2001; Tchoumatchenco *et al.* 2004; Sapunov & Metodiev 2007). These two levels may be coeval with the black shales in the studied area. If so, the Triassic metasedimentary succession may include the whole of the Triassic, and calcareous schists of this succession may be a facies equivalent of the Middle Triassic carbonates known in Bulgaria.

Jurassic Carbonates

Çağlayan & Yurtsever (1998) assigned large bodies of carbonate rocks to the Jurassic Dolapdere Formation (Figures 3 & 4) based on the discovery of the Early Jurassic *Pentacrinus cf. laevisutus* Pompeckj. A.I. Okay *et al.* (2001) and Hagdorn & Göncüoğlu (2007), assuming conformable relationships with underlying Triassic siliciclastic rocks, correlated these carbonates with the Middle Triassic carbonates in Bulgaria.

The Jurassic age of these rocks was accepted in the recent 1:500,000 scale Geological Map of Turkey (Türkecan & Yurtsever 2002). We follow here this age assignment. Both Çağlayan & Yurtsever (1998) and A.I. Okay *et al.* (2001) suggested that the carbonate rocks constitute the core of a large Kapaklı syncline. Our observations corroborate this conclusion; although this syncline is discordant with respect to the structures in the underlying rocks (Figures 3 & 4). Firstly, the syncline rests on different complexes – the Triassic metasedimentary complex in the west and north and the Koruköy Complex in the southeast. Secondly, the Triassic complex also forms a large synform made by the S_2 foliation but its axis does not coincide with the axis of the Kapaklı syncline (Figures 3 & 4). Thirdly, strikes of the S_2 foliation in the Triassic metasedimentary rocks are generally oblique to the contacts of the Jurassic carbonates (Figure 3).

The Jurassic carbonate complex consists of white to grey dolomite, limestone, dolomite and calcitic marble, and rare carbonate breccia. Unlike all other Palaeozoic and Triassic rocks, large volumes of these carbonates reveal very low-strain. These rocks preserve well-defined bedding, which varies from thin to thick with usually parallel bedding planes. Massive rocks have also been observed. The carbonates are fine-grained and perhaps recrystallized (especially dolomites), but metamorphic mica does not appear, even along the bedding planes, where the concentration of clay minerals should be higher. Despite intense fracturing, calcite veins are very rare (Figure 15A), which is in great contrast to the underlying calcareous schists and metasandstones where quartz, calcite, quartz-*adularia*-sulphide veins are abundant.

The high-strain carbonates are found at the base of the Dolapdere Formation and in several higher structural levels. They are well foliated and lineated. Metamorphic mica coats the foliation planes; calcite veins are common. The lineation orientation is similar to the underlying Palaeozoic and Triassic rocks, which implies that these ductile structures are coeval with the Late Jurassic to Early Cretaceous regional deformation. Compared to the underlying rocks the foliation in the carbonates is gentler dipping and parallel to the bedding planes. In many

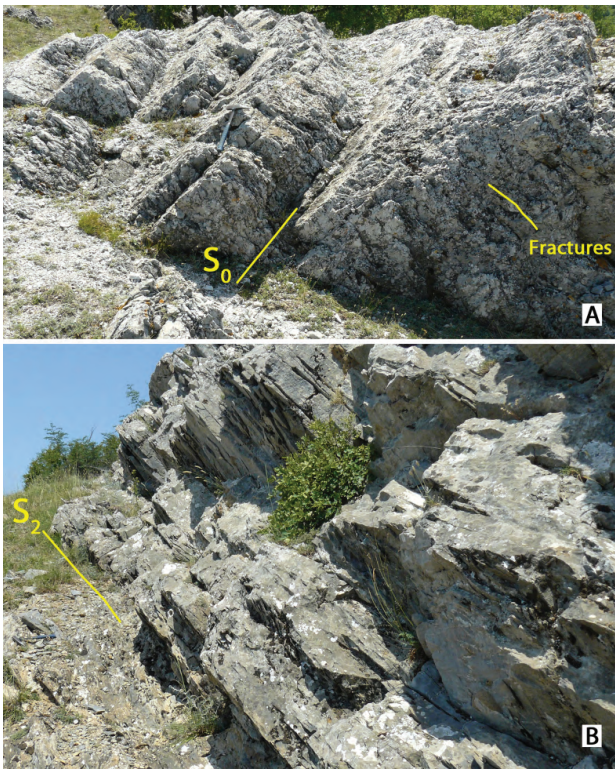


Figure 15. (A) Jurassic limestones on the southern limb of the Kapaklı syncline. Foliation is absent. Bedding (S_0) is moderately dipping while it has a gentle or subhorizontal attitude in the central part of the syncline (Figure 3). (B) Strongly foliated limestones passing down to limestone mylonites at the contact between the Dolapdere Formation and underlying Triassic siliciclastic rocks.

places, the contacts of the Jurassic carbonates and underlying Palaeozoic and Triassic rocks are marked by carbonate mylonites (Figures 3 & 15B). When these mylonites are absent, the contacts are defined by high-angle brittle faults.

All these features suggest that the Jurassic carbonates form a nappe. This nappe overlies different tectonostratigraphic units (Figures 3 & 4) suggesting its emplacement from the south during the Late Jurassic–Early Cretaceous deformation (Natal'in *et al.* 2005a, b, 2009). Chatalov (1990) and Gerdjikov (2005) also described klippen of unmetamorphosed Jurassic sandstones, limestones, and shales thrust over the Strandja Massif in Bulgaria. It has a younger-over-older relationship with its underlying units, but this is the result of out-of-sequence thrusting during a multi-phase deformation that will be discussed in a

separate paper, where we shall deal with the structure in detail.

Tectonic History

The reconstruction of the tectonic history of the Strandja Massif is a difficult task because the Late Jurassic–Early Cretaceous greenschist to epidote-amphibolite facies metamorphism and deformation have destroyed and defaced so much of the older history. This high strain deformation produced numerous ductile shear zones with a complicated kinematic history (Natal'in *et al.* 2005a), and created large volumes of mylonites and blastomylonites (Figure 3). Under these circumstances, correlations with surrounding regions can be useful where the relevant rocks are less metamorphosed or better dated. However, interpretations of tectonic processes in these regions are extremely controversial. Most researchers hold that the Strandja Massif, together with the İstanbul and Balkan zones, belongs to the European Variscan orogen (e.g., Haydoutov 1989; A.I. Okay *et al.* 1996, 2006; Yanev *et al.* 2006), Precambrian continental blocks of which derived from Gondwanaland. After their alleged Early Ordovician separation these blocks supposedly travelled toward the Russian Craton and collided with it around the Ordovician/Silurian boundary and/or in the Carboniferous (Stampfli *et al.* 20001a, b; Cocks & Torsvik 2005). Natal'in *et al.* (2005a, b) and Natal'in (2006) noted the similarity of the Ordovician–Triassic geological history of the Strandja Massif with the history of the late Palaeozoic–early Mesozoic Silk Road arc, which evolved on the northern boundary of the Palaeo-Tethyan Ocean (Natal'in & Şengör 2005). This interpretation implies an Asiatic origin for at least the Palaeozoic tectonic units. Sunal *et al.* (2008) showed that the age spectrum of the detrital and inherited zircons of the İstanbul Zone is similar to both the Avalonian units and Baltica (Russian Craton). Thus, to reconstruct the tectonic history of the Strandja Massif, we should discuss not only the tectonic units near the Strandja Massif but those across a wider region.

Precambrian–Early Palaeozoic History

Precambrian rocks are not exposed in the Strandja Massif but the inherited zircon cores in the

Carboniferous metagranites (Figure 16B) show their likely presence at deeper structural levels. Rocks of this age are exposed in the İstanbul Zone where they consist of paragneisses and migmatites, metaphtolites, felsic and intermediate metavolcanic rocks, and crosscutting granite yielding zircon ages of 565, 576, and 590 Ma. These rocks are metamorphosed under amphibolite and greenschist facies conditions and have been considered as relicts of the Pan-African structures (P.A. Ustaömer 1999; Chen *et al.* 2002, Yiğitbaş *et al.* 2004; P.A. Ustaömer *et al.* 2005). Similar structures are known in the Balkan zone (Haydoutov 1989; Haydoutov & Yanev 1997) as well as in many places of Europe where they are discriminated into Avalonian and Cadomian (Armorican) types (Matte 2001; Stampfli *et al.* 2002; von Raumer *et al.* 2002; Murphy *et al.* 2006). Tectonic units of the Avalonian type were accreted to Baltica at the end of the Ordovician. The Cadomian units, in places having a heterogeneous Precambrian basement, collided with each other and Baltica in the early Carboniferous (e.g., Cocks & Torsvik 2005). The correlation of the European units and those exposed in Turkey is hotly debated, in which the age of the basement, detrital zircons, stratigraphic record of the Palaeozoic rocks, time of accretion, and Palaeozoic palaeobiogeography are all considered.

Age spectra of Precambrian detrital and inherited zircons of the Strandja Massif (Figure 16A) and the İstanbul Zone have been correlated with the Saxothuringian Zone of Europe (Armorican type) and the Avalonian type, respectively (Sunal *et al.* 2008). Recent detrital zircon studies have also led to claims of the presence of Avalonian-type basement in the İstanbul Zone (P.A. Ustaömer *et al.* 2009; N. Okay *et al.* 2011) but the Palaeozoic stratigraphic record, tectonic history, and palaeobiogeography do not unequivocally corroborate this interpretation. Using various criteria the İstanbul Zone has been correlated with the Cadomian (cf. Murphy *et al.* 2006) tectonic units (Yiğitbaş *et al.* 2004; P.A. Ustaömer *et al.* 2005; P.A. Ustaömer 1999; Yanev *et al.* 2005) or, more specifically, with the Saxothuringian (Yanev *et al.* 2006) or Rhenohercynian zones (Kalvoda *et al.* 2002). In contrast to these authors, Stampfli *et al.* (2002), von Raumer *et al.* (2002), A.I. Okay *et al.* (2006, 2008), Bozkurt *et al.* (2008), and N. Okay *et al.* (2011) defended the Avalonian type of geologic

evolution. In the course of this discussion, some authors (e.g., Yanev *et al.* 2006) noted that the lower Palaeozoic stratigraphic record of the İstanbul and related Zonguldak zones is similar to Avalonian units, while the Middle Palaeozoic fits the Cadomian units. In order to reconcile Precambrian features of the basement and overlying Palaeozoic rocks two models have been suggested. The first implies Neoproterozoic dextral faulting that placed the Avalonian basement of the İstanbul Zone, originating near the Amazonian block in Southern America, eastward to North Africa where Cadomian units with the Pan-African basement were located (P.A. Ustaömer *et al.* 2009). Another solution suggests splitting of the Avalonian units after the Silurian collision with the Bruno-Silesian promontory, which has been created earlier on the Baltica margin. After this collision, the eastern segment of Avalonian units moved sinistrally, and collided with Baltica in the Carboniferous similar with the Cadomian units (Winchester *et al.* 2006; Bozkurt *et al.* 2008; N. Okay *et al.* 2011). We should mention that structural evidence for Neoproterozoic dextral or early Palaeozoic sinistral shearing has never been provided along the İstanbul Zone boundaries.

Following Şengör & Yılmaz (1981) and Okay & Tüysüz (1999), we accept here that the İstanbul and Zonguldak zones are facies variations of a single tectonic unit (Figure 1). The pre-Early Devonian disconformity in the Zonguldak Zone (Kozur & Göncüoğlu 2000) is frequently used to defend the Caledonian collision with Baltica that is typical for the Avalonian unit (A.I. Okay *et al.* 2006, 2008; Winchester *et al.* 2006; Bozkurt *et al.* 2008; P.A. Ustaömer *et al.* 2009). However, Kozlu *et al.* (2002) and Yalçın & Yılmaz (2010) have shown that Silurian and Devonian successions are continuous and include (Sachanski *et al.* 2010) originally missed Ludlovian–Pridolian rocks (Kozur & Göncüoğlu 2000; Sachanski *et al.* 2007). Moreover, palaeobiogeographic studies of early and mid-Palaeozoic fossils of the İstanbul and Zonguldak zones are not decisive to assign them to Gondwanaland or Baltica (e.g., Kozur & Göncüoğlu 2000; Kalvoda & Bábek 2010).

Palaeotectonic reconstruction (Cocks & Torsvik 2005) shows that Baltica and Siberia were close to Gondwanaland 550 Ma ago (Figure 17). Searching for detrital zircon provinces, some authors (e.g.,

A.I. Okay *et al.* 2008; P.A. Ustaömer *et al.* 2009) equated Baltica with the basement of the Russian Craton (Bogdanova *et al.* 2008) and disregarded it as a possible zircon source for the İstanbul zone (see Figure 18A but compare it with Figure 16C & 18B–F). These authors did not account for that at 550 Ma, hence before the separation of the Avalonia-type units from Gondwana, the Russian Craton was overgrown by the pre-Uralides (e.g., Şengör & Natal'in 1996) or Timanides (Zonenshain *et al.* 1990; Gee 2006). These structures continued farther to the east (Figure 17) and are known as the Baykalides at the periphery of the Siberian Craton. The Timanides and Baykalides are largely covered by younger deposits, but where they are exposed, they show a long evolution through the Neoproterozoic and Cambrian.

In the Timanides, volcanic and sedimentary rocks, granitoids, ultramafic rocks, and blueschist were accreted to the Russian Craton in latest Ediacaran to earliest Cambrian time (Zonenshain *et al.* 1990; Olovyanishnikov 1998; Gee *et al.* 2006). The accreted units are interpreted as a Neoproterozoic arc that was attached to a continental block – the Kara block (Metelkin *et al.* 2005) or the Arctida Continent (Zonenshain *et al.* 1990; Kuznetsov *et al.* 2010). The Timanide orogeny occurred between 500–550 Ma and caused intrusions of 550–560 Ma (Roberts & Olovyanishnikov 2004) and younger 510 Ma granites (Kuznetsov *et al.* 2010). Upper Cambrian but mainly Ordovician sandstones, quartzites, and other clastic rocks (similar to the İstanbul Zone) unconformably cover the accreted Neoproterozoic arc.

After the Timanide collision, two rifting events affected the orogen and obliquely cut Timanide structures. The earlier one, Ediacaran–Early Cambrian (Figure 17), separated the Kipchak arc (Şengör & Natal'in 1996). Fragments of this ribbon continent are now scattered in Kazakhstan and the Tien Shan where they form basements of the Kipchak Palaeozoic arc massifs. The Cambro–Ordovician rifting opened the Uralian Ocean (Zonenshain *et al.* 1990; Puchkov 2009). As the position of continents 550 Ma ago (Figure 17) and the brief outline of the Timanide history show, Gondwanaland may be not the sole source of Precambrian blocks in the Western Pontides.

In the Polar Urals, detrital zircons from the uppermost Cambrian–Ordovician clastic rocks covering the accreted arc have an age span from 550 to 750 Ma (Figure 18B) and do not reveal older Precambrian ages (Kuznesov *et al.* 2010). The older ages (0.9 to 2.7 Ga) are recorded by inherited zircons in granites cutting the Timanide arc. Across the suture, on the margin of the Russian Craton, detrital zircons cluster at 1.18–1.34, 1.5–2.1, and 2.35–2.8 Ga (Figure 18B). Similar age distributions of detrital zircon ages are reported from Novaya Zemlya (Figure 18C, D) located on the northern continuation of the Timanides (Pease & Scott 2009). The Precambrian history of Baltica and the Timanides, we can see in distributions of detrital zircon ages of modern sediments collected in the Volga delta (Figure 16A). The Volga drainage area covers the Russian craton and part of the Timanides. Note the presence of the Neoproterozoic and Grenvillian ages, the wide cluster around 1.5 Ga reflecting intrusions of rapakivi granites and the Danopolonian orogeny (Bogdanova *et al.* 2008), and minima between 2.1 and 2.3 Ga. Rino *et al.* (2008) and Safonova *et al.* (2010) reported the same distribution of detrital zircon ages for the Volga basin (Figure 18E, F). The pick around 1.5 Ga is considered as the characteristic feature of the Avalonian units (Murphy *et al.* 2006; Winchester *et al.* 2006) showing the proximity to the Rondonian orogeny in Amazonia, but the cited data show that it also exists in a Baltica source (Sunal *et al.* 2008).

The age spectra of the Strandja detrital zircons (Figure 16A & B, Sunal *et al.* 2008) and the İstanbul Zone (Figure 17A; P.A. Ustaömer *et al.* 2009) are similar to the spectra reported for the Baltica–Timanides collage. With a few exceptions, the Precambrian inherited zircons from the Strandja Massif (Figure 16B), which probably represent the ages of the vertical structural column, fit the ages reported (Kuznetsov *et al.* 2010; Pease & Scott 2009) for the Timanian arc (Figure 18B–D). These zircons have the Mesoproterozoic gap (Sunal *et al.* 2008), and alternatively may be compared with the Cadomian–Armorican type. Cambro–Proterozoic detrital zircons (640 to 520 Ma) extracted from the Carboniferous turbidites of the İstanbul Zone (N. Okay *et al.* 2011) have no Mesoproterozoic zircons, and therefore are similar to both Cadomian-type and the Timanide arcs. Fourteen Precambrian zircons

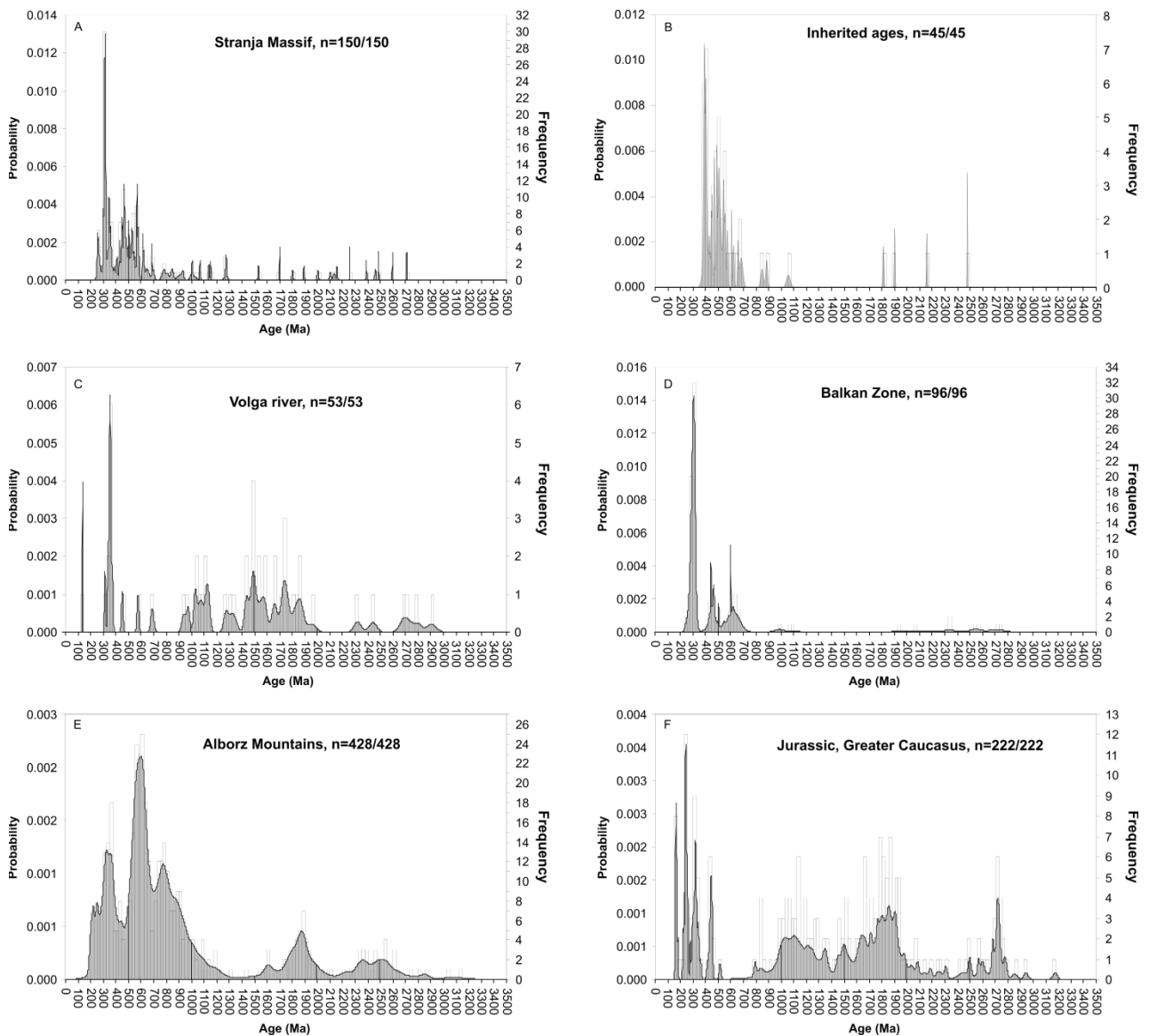


Figure 16. Detrital zircons from the Strandja Massif, Balkan Zone, Caucasus, and Iran. (A) Ages of detrital and inherited zircons of the Strandja Massif; (B) Ages of inherited zircons of the Strandja massif; (C) Zircon ages of recent sediments at the mouth of the Volga River (Allen *et al.* 2006); (D) Balkan Zone (Sunal *et al.* 2008); (E) The Alborz Mountains, Iran, the Shemshak Formation (Horton *et al.* 2008); (F) Bajocian sandstones from the eastern Greater Caucasus (Allen *et al.* 2006).

from the Carboniferous turbidites vary between 1701 and 2734 Ma. They can hardly be used for the province determination however, as they do not perfectly fit the Avalonian type because of the presence of two zircons of ~ 2.2 Ga (N. Okay *et al.* 2011) that are atypical of Avalonia (Murphy *et al.* 2006), but occur in Baltica (Figure 18B, E & F). The absence of the Mesoproterozoic zircons in the

Carboniferous turbidites but their presence in the Strandja Massif (Figure 16A) can be explained by the onset of deformation, which created dissected topography and localized areas subjected to erosion. It is clearly documented by the varieties of zircon age spectra in different samples collected from the Carboniferous turbidites in the İstanbul Zone (N. Okay *et al.* 2011, their figure 11).

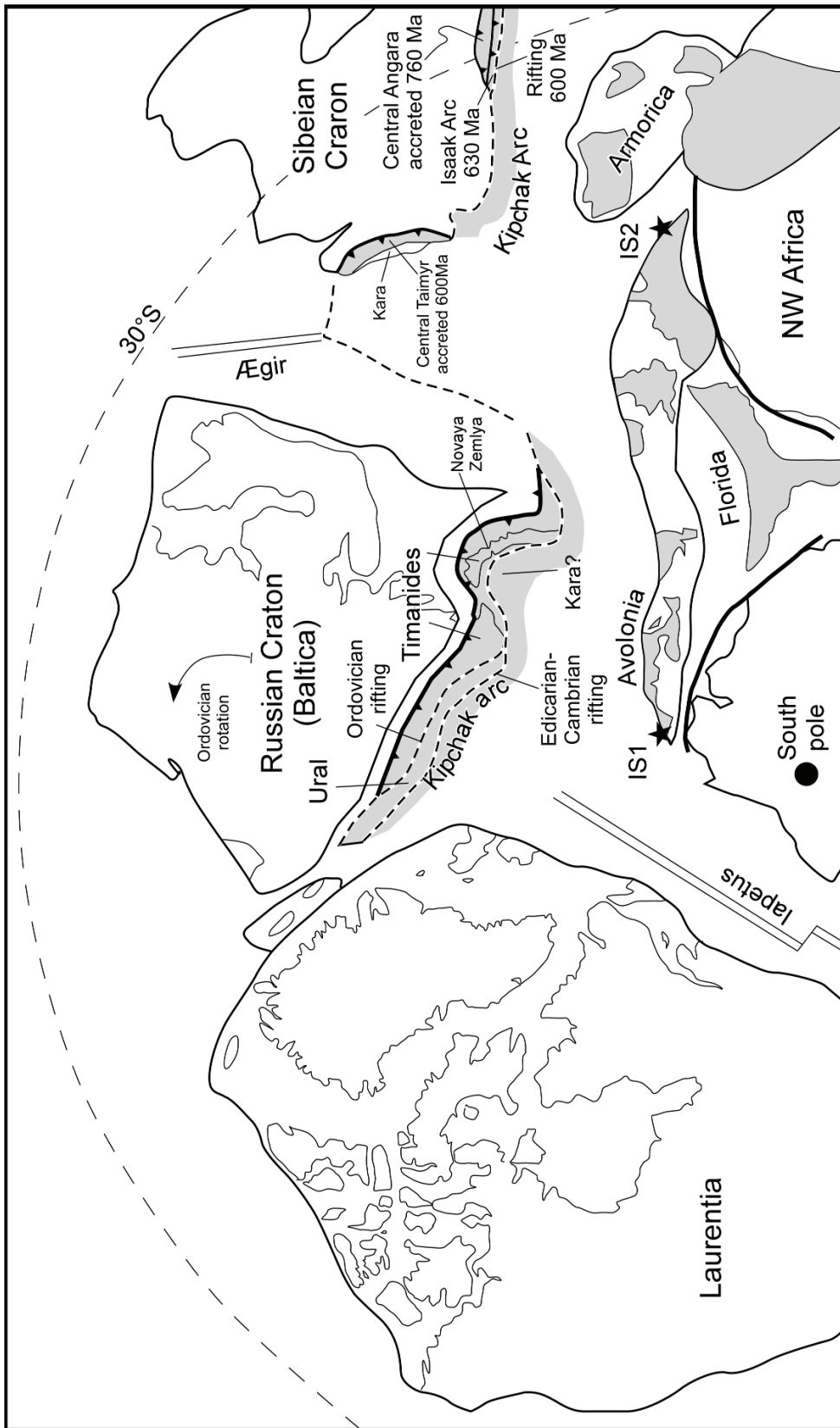


Figure 17. Reconstruction for ~550 Ma. Position of main continents and oceans is after Cocks & Torsvik (2005). The Timanides, as a part of the pre-Uralide-Baykalkide orogenic belt, were accreted to the Russian Craton in the latest Ediacarian-earliest Cambrian. Tectonic events in the Baykalkides are summarised after Metelkin *et al.* (2005) and Vernikhovskiy *et al.* (2009). Dashed lines indicate the positions of the Ediacarian-Early Cambrian rifting responsible for the Kipchak arc formation (Şengör & Natal'in 1996), and Ordovician rifting that opened the Uralian Ocean (Zonenshain *et al.* 1990). IS1 and IS2 are positions of the Istanbul zone after P.A. Ustaömer *et al.* (2009) and Bozkurt *et al.* (2008), respectively. The large uncertainty of these positions and data presented in this paper show the Istanbul Zone and neighbouring Strandja Massif can be derived from the Timanides or Baykalkides, fragments of which make the basement of the Kipchak arc massifs.

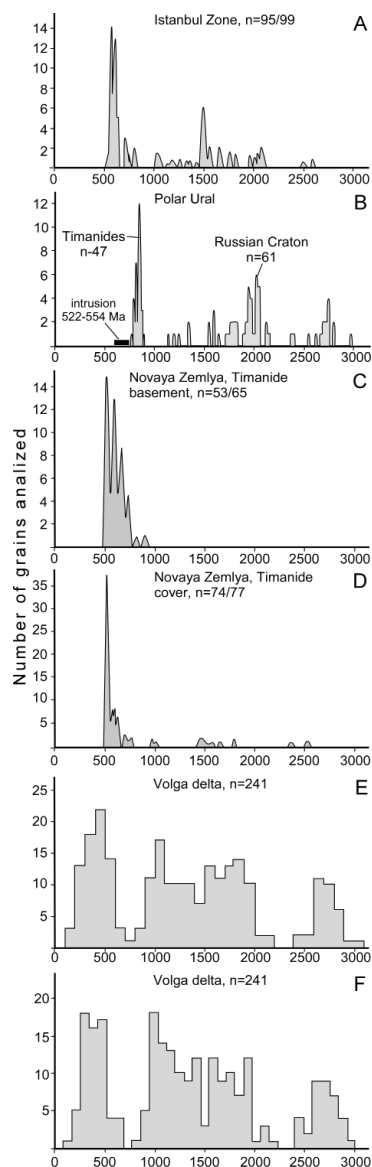


Figure 18. Detrital zircon ages of the İstanbul zone and Timanides and Russian craton indicate a possibility for correlation. (A) Ordovician quartzite of the İstanbul Zone (P.A. Ustaömer *et al.* 2009). (B) Zircon age spectra of the Timanides (left) and Russian Craton (right) exposed in the Polar Urals (Kuznetsov *et al.* 2010). The Timanide sample was collected from the unconformable Ordovician cover; basement is cut by 522–555 Ma intrusions that have no record in detrital zircons. Neoproterozoic sandstones in the right part of the figure show source ages of the Russian Craton. (C, D) Timanide age spectra from Novaya Zemlya (Pease & Scott 2009) below the Ordovician unconformity (C) and above it (D). (E) Recent sediments of Volga delta (Rino *et al.* 2008). (F) Recent sediments of the Volga delta (Safonova *et al.* 2010).

The above discussion shows that a Baltica-Timanide origin of the Strandja Massif and the İstanbul Zone is possible, if one considers the ages of detrital and inherited zircons. Geological considerations further support and elaborate this conclusion. For instance, as in the Timanides the Palaeozoic of the İstanbul and Zonguldak zones starts with the Ordovician but not with Cambrian as is characteristic for northern Gondwana (e.g., Dean *et al.* 2000) or the Avalonian units in Europe (e.g., Oczlon 2006). Another important issue is the palaeobiogeography of Ordovician fossils because the Early Ordovician is when the Avalonian blocks separated from Gondwana (Fortey & Cocks 2003; Cocks & Torsvik 2005; Winchester *et al.* 2006). In the Zonguldak Zone, Tremadocian–Arenigian acritarchs and conodonts, despite their high mobility, indicate a Baltic province but not Gondwanan. This is similar to the Caradocian (before the Avalonian unit collided around the Ordovician–Silurian boundary) ostracods and brachiopods that have low dispersion potential (Kalvoda & Bábek 2010). With Ediacaran and Ordovician rifting the Precambrian Baltic-Timanide fragments could be present in Kazakhstan and the Tien Shan. Two Early Ordovician trilobites (*Cyclopyge* and *Dionide*) out of five found in the Zonguldak Zone and comparable with the Anglo-Welsh successions (Dean *et al.* 2000) are known in Southern Tien Shan (Tulyaganov *et al.* 1972). Also, the Palaeozoic stratigraphic succession of the İstanbul Zone perfectly fits the succession of the Alay microcontinent as described by Tulyaganov *et al.* (1972), Biske (1996), and Brookfield (2000).

We have emphasized the possibility of Precambrian–early Palaeozoic ties of the Strandja, İstanbul, and Zonguldak zones with Baltican, Timanide, and Asiatic domains but this inference needs further support by more comprehensive and multidisciplinary geological studies.

Ordovician–Devonian History

The data set on the early Palaeozoic history of the Strandja Massif is limited. From detrital zircons studies, we know of the presence of the Ordovician and Silurian schists and paragneisses containing lenses of amphibolites. Other dates (328 and 305 Ma, Carboniferous) have been obtained from similar

lithologies. Field observations and thin-section studies show the compositional unity of all country rocks around the Carboniferous and Permian metagranites.

Palaeozoic rocks of the İstanbul Zone represent the continuous Ordovician to Devonian succession of a south-facing passive continental margin. The Late Silurian and Devonian neritic limestones signify the creation of a carbonate platform that experienced sudden drowning in the latest Devonian that was followed by deposition of pelagic cherts passing upward into the Lower Carboniferous turbidites (Şengör & Yılmaz 1981; Görür *et al.* 1997; Yılmaz *et al.* 1997; Yiğitbaş *et al.* 2004). The absence of magmatic rocks in this sequence and its early Carboniferous deformation make unlikely the correlation of this unit with the Strandja Massif.

In the Balkan Zone, the Lower–Middle Palaeozoic rocks are of two types: (1) those that are unmetamorphosed, and (2) those metamorphosed under greenschist to amphibolite facies conditions (Yanev *et al.* 2006; Carrigan *et al.* 2005, 2006). Their distribution is difficult to understand and especially to make a distinction between the regions affected by only Carboniferous (Carrigan *et al.* 2006) and/or Late Jurassic–Early Cretaceous metamorphism (Lilov *et al.* 2004; Gerdjikov 2005). The unmetamorphosed Lower to Middle Palaeozoic rocks are mainly distributed along the northern and southern boundaries of the zone (Figure 1; Boncheva *et al.* 2010) while the metamorphosed ones constitute its central part (Carrigan *et al.* 2006). In the northern zone, Ordovician to Devonian shales, sandstones and cherts rest on the Cambrian volcanic arc and its ophiolitic basement (563 Ma) (Haydoutov 1989; Haydoutov & Yanev 1997). This arc is interpreted as a typical Cadomian or Pan-African arc obducted onto the Moesian Platform in the Early Ordovician (e.g., Yanev *et al.* 2006). Other studies dispute this interpretation. Yanev (2000) showed that the Arenigian deformations were weak, and von Quadt *et al.* (2005) obtained U–Pb zircon age of 443 ± 1.5 Ma for the Berkovitsa Group described by Haydoutov (1989) as a Cambrian arc. In any case, the Arenigian obduction is difficult to reconcile with the synchronous opening of the Rheic Ocean, the history of which is essential for the evolution

of the Bulgarian tectonic units as the part of the European Variscan belt, as many authors think. The Ordovician–Devonian rocks in the northern and southern parts of the Balkan Zone are mainly deep marine facies (black and graptolitic shale, cherts) interpreted as a passive continental margin (Yanev *et al.* 2006; Boncheva *et al.* 2010). They are overlain by the Upper Devonian (Yanev 2000) or the Upper Devonian–Lower Carboniferous flysch (Yanev *et al.* 2006). These rocks are correlated with the İstanbul Zone (Yanev *et al.* 2006) but it is not clear whether or not they also represent a south-facing continental margin because Ordovician–Lower Carboniferous carbonate facies are exposed to the southwest (Boncheva *et al.* 2010). The facies and the absence of volcanic rocks make unlikely the correlation of the unmetamorphosed rocks of the Balkan Zone with the Strandja Massif.

The tectonic history of the metamorphosed Lower and Middle Palaeozoic rocks in Bulgaria remains uncertain. However, these units reveal more similarities with the Strandja Massif because of the presence of amphibolites. Some aspects of the tectonic history are better constrained in Bulgaria. Relicts of the Neoproterozoic basement (location 1 in Figure 1) are proved by U–Pb zircon dating of orthogneisses that yield 616.9 ± 9.5 and 595 ± 23 Ma ages (Carrigan *et al.* 2006). Tectonically juxtaposed with them are metapelites, paragneisses, garnet amphibolites, lenses of peridotites, and eclogites (location 2 in Figure 1) (Machev *et al.* 2006). The eclogites reveal an amphibolite facies overprint that occurred at 393 Ma (Ar–Ar age) and their geochemistry shows a MORB–subalkaline basalt transition (Gaggero *et al.* 2009). The eclogites are considered to be rift related (Gaggero *et al.* 2009), but we can accept this interpretation because the rock association is typical for a subduction setting, as documented in many regions of the world (Miyashiro 1973; Ernst 2010).

Another eclogite occurrence has been reported very close to the Bulgarian–Turkish state border on the direct continuation of the Strandja Massif (Gerdjikov 2005), but no information on rock types and relations were provided. The single occurrence of metamorphosed serpentinites in the Strandja Massif (Figure 14), with eclogites and peridotites in Bulgaria, suggests that at least part of the Lower–Middle

Palaeozoic rocks could represent a subduction-accretionary complex.

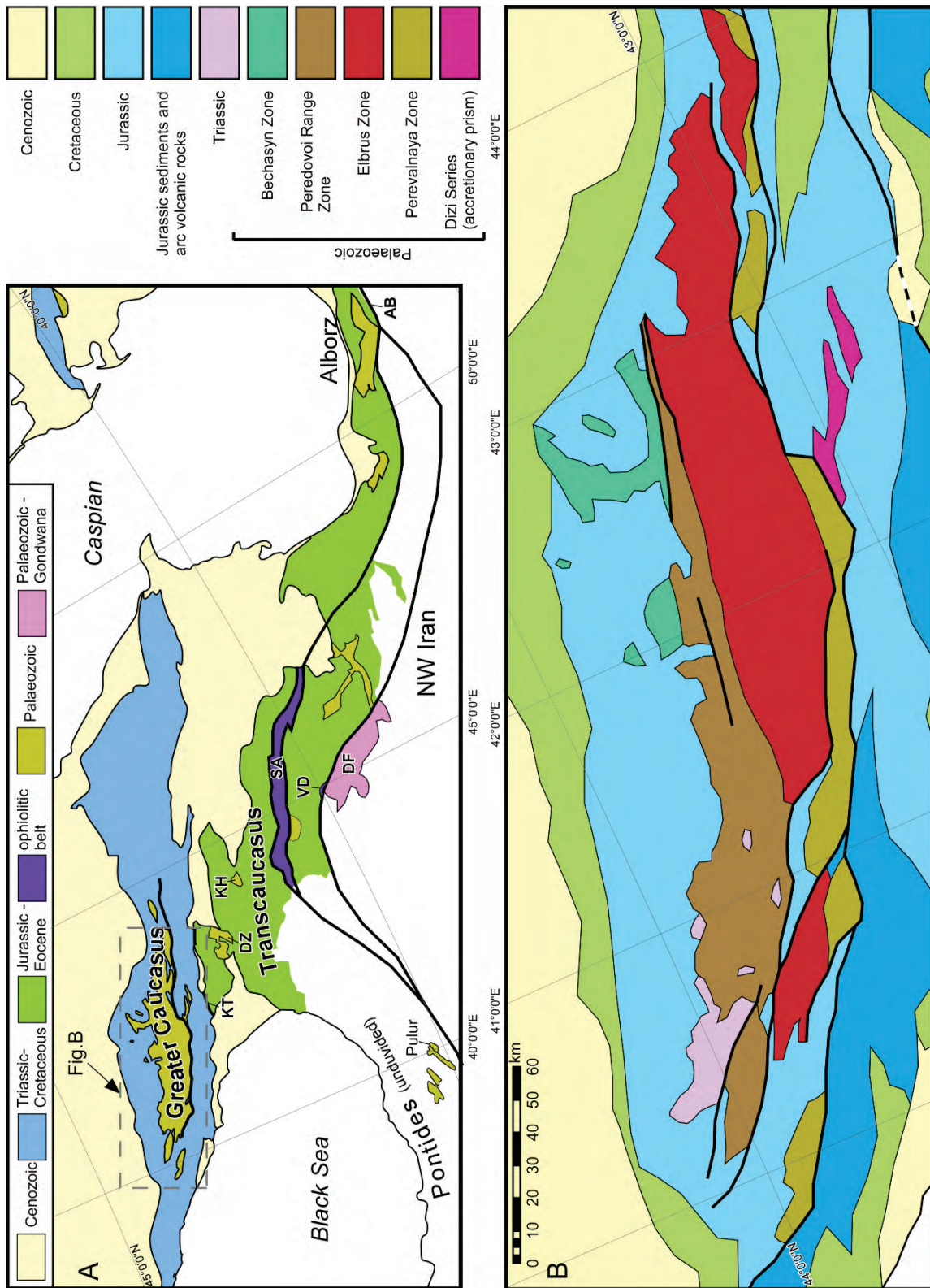
In the Strandja Massif, dates from detrital and inherited zircons show several maxima between 410 and 600 Ma (Figure 16A, B), which indicate persistent magmatic activity in the source areas. The Neoproterozoic–Cambrian zircon ages have already been discussed in the previous section. The youngest magmatic zircon from the Lower Ordovician quartzites of the İstanbul Zone yields an age of 526 Ma (P.A. Ustaömer *et al.* 2009). Zircons from the Lower Carboniferous rocks show similar Cambrian ages but only a few Ordovician–Silurian ages (N. Okay *et al.* 2011). Late Ordovician (457–464 Ma) metagranites, locally orthogneisses, have been established near the southern boundary of the İstanbul Zone in the Armutlu Peninsula and farther to the east (locations 3 and 4 in Figure 1; A.I. Okay *et al.* 2008). All contain inherited Cambrian zircons and cut gneisses, amphibolites, and meta-peridotites. There are no proven Ordovician to Silurian magmatic rocks in the Balkan Zone. At the same time Carrigan *et al.* (2006) reported detrital zircons with ages between 410 and 550 Ma (Figure 16D) extracted from the migmatite leucosome (location 1 in Figure 1). Ordovician–Silurian magmatic zircons could be derived from synchronous magmatic zones located along the southern and southwestern boundaries of the Rhodope Massif (Serbo-Macedonian Zone). There, Boncheva *et al.* (2010) reported an Ordovician–Devonian volcano-sedimentary complex in the Serbo-Macedonian zone (30 km to the west of location 5 in Figure 1), but provided no further details on the tectonic setting. At the southeastern end of the Serbo-Macedonian Zone, Himmerkus *et al.* (2006) described Silurian orthogneisses (428 and 433 Ma zircons Pb-Pb ages) with an arc-related geochemical signature (location 6 in Figure 1). These orthogneisses are tectonically mixed with orthogneisses having Pan-African ages, and wide mélangé zones with meta-ophiolite are exposed nearby. This tectonic mixing occurred because of closure of the Late Jurassic Vardar ocean (Himmerkus *et al.* 2006). Despite the age difference, we infer that the Serbo-Macedonian arc can be correlated with the Ordovician metagranites of the Armutlu Peninsula. The general structure of these zones is similar. Both have relicts of the Pan-African basement, mélangé structure, meta-

ophiolites and were strongly reworked by the late Mesozoic deformation. Another possible fragment of the same arc is exposed in the Biga Peninsula within the Sakarya Zone (location 7 in Figure 1), where the Early Devonian (397 Ma Pb-Pb zircon age) Çamlık granodiorites form a thrust sheet in an Alpine thrust stack (A.I. Okay *et al.* 2006). Like the Strandja Massif they are unconformably overlain by Triassic arkosic sandstones – the facies that are remarkably different from the Triassic accretionary prism lithologies of the Sakarya Zone.

We consider all the above-mentioned occurrences of Ordovician to Early Devonian magmatism in Bulgaria and Turkey as possible sources of the early Palaeozoic Strandja zircons. The geochemical signature of the Ordovician and Early Devonian granitoids exposed in Turkey is not reported in sources available to us. A.I. Okay *et al.* (2008) interpreted the Ordovician metagranites as rift-related, but we prefer the interpretation of Himmerkus *et al.* (2006) who suggested an arc-related setting. It better fits the wide Cambrian–Devonian age range of the Strandja zircons if our inference about their sources is correct. We further infer that the early Palaeozoic zircons inherited in the Carboniferous orthogneisses of the Strandja Massif suggest that a fragment of this arc may exist at depth. These fragments may also exist in the Balkan Zone if one considers its complicated structure, high to lower grade range of metamorphism, and reported ages (von Quadt *et al.* 2005) of 443 Ma for calc-alkaline diabbases, 502 Ma for orthogneisses (location 8 in Figure 1) and inherited zircon ages from 440 to 460 Ma enclosed in Cretaceous magmatic rocks.

In Turkey and Bulgaria, the early Palaeozoic arc fragments are much narrower than modern magmatic arcs (>50 km; e.g., Jarrard 1986). Obviously, to find related fragments or a fully developed arc we should search to the north of the Palaeo-Tethyan and Neo-Tethyan İzmir-Ankara sutures because the expected rocks are not exposed south of them (Şengör *et al.* 1991).

The Greater Caucasus is a segment of the Alpine belt, in which the pre-Alpine Palaeozoic basement (Figure 19A) is involved in a series of nappes with considerable magnitudes of displacement (Belov 1981; Khain 1984; Gamkrelidze 1991).



Their metamorphosed and unmetamorphosed Precambrian and Palaeozoic rocks have different compositions and tectonic nature. In the Bechasyn Zone (Figure 19B), calc-alkaline metavolcanic rocks are cut by orthogneisses yielding a U-Pb zircon age of 530 ± 8 Ma (Somin 2007). They are unconformably overlain by red and greenish arkosic sandstones and siltstone (1500 m) containing lenses of conglomerates and exotic blocks of limestone with Middle Cambrian trilobites of Siberian affinity, brachiopods, and algae, which are found in Siberia and Baltica (Andruschuk *et al.* 1968). Sedimentary structures indicate that source areas were to the north. According to Ruban (2007), the age of algal remnants in siltstones is Early–Middle Ordovician but other authors consider it to be Cambrian (Potapenko 2004). The sandstones are overlain by Silurian–Middle Devonian dark grey shales, slates, and limestones (mainly Upper Silurian–Lower Devonian) containing rich fossil remains (Andruschuk *et al.* 1968; Potapenko 2004). A thick sheet of ultramafic rocks is thrust over the metamorphic basement and cover and thus the top of the Silurian–Devonian succession is not known. The ages and facies of this succession are similar to those in the İstanbul and Zonguldak zones. Probably, the units exposed in the north of the Peredovoi Range also represent the Cadomian/Timanide basement and overlying it, south-facing passive continental margin.

Farther south in the Peredovoi Range Zone is exposed a thrust-bound collage of lower–middle Palaeozoic ophiolites, accretionary prisms, and magmatic arc rocks. The lowest tectonic unit consists of orthogneisses, amphibolite, kyanite-garnet schists, serpentinites, and eclogite (Blyb Complex). The Sm-Nd isochron age of this complex is 400 and 460 Ma (Potapenko *et al.* 1999) and U-Pb zircons date orthogneisses at between 400 and 354 Ma (Somin 2007). Detrital zircons extracted from metapelites and quartzites give ages of 2471–1513, 653–499, and 387–373 Ma (Somin 2007). The first two groups suggest Cadomian/Timanide and Baltican sources. Structurally higher, there is a fault-bounded unit of Silurian–Viséan arc volcanics that is tectonically overlain by ophiolites (Khain 1984) containing gabbro yielding a 416 Ma zircon age (Somin 2007).

The Elbrus Zone consists of amphibolite facies migmatitic gneisses and overlying epidote-

amphibolite facies schists, gneisses and amphibolites of the Makera complex. Orthogneisses of the granite-migmatite complex were formed in a magmatic arc tectonic setting and metamorphosed around 310–280 Ma (Gamkrelidze *et al.* 2002). They yield U-Pb zircon ages of 400 and 386 Ma (Somin 2007) and 432, 447, and 459 Ma (Gerasimov *et al.* 2010). The overlying and less metamorphosed Makera Complex also includes arc-related magmatic rocks (Gamkrelidze *et al.* 2002) but their U-Pb zircon ages are approximately the same age: 425–470 Ma (Somin 2007). The Ordovician–Devonian Elbrus Zone is 50 km wide, comparable with modern arcs.

The Perevalnaya Zone (Figure 19) is interpreted as an ensimatic arc (Somin 2007) that consists of schists, gneisses, amphibolites and marble of the Laba Series, and amphibolite, metasedimentary rocks and orthogneisses of the Bulgen Complex (Gamkrelidze *et al.* 2002; Potapenko 2004; Somin 2007). Stratigraphic relationships between these stratigraphic units are not clear. Epidote-amphibolite facies amphibolites originated from mafic and intermediate volcanic rocks. The U-Pb age of the orthogneisses is middle Devonian (381 Ma) to Carboniferous (312 Ma). Detrital zircons show four groups of ages 2394–1929 Ma, 669–483 Ma, 455–405 Ma, and 355–325 Ma (Somin 2007).

Finally, detrital zircons from Middle Jurassic sandstones in the eastern part of the Greater Caucasus have revealed a group of ages between 440 and 460 Ma, as well as older ages between 910 and 2565 Ma (Figure 16F) (Allen *et al.* 2006). A Neoproterozoic gap can be explained by the availability of suitable rocks to erode in the Middle Jurassic because these zircons are found in Palaeozoic sediments. They are present in recent sediments at the mouth of the Volga River (Figures 16C & 18E, F).

The magmatic history of the Greater Caucasus and especially the Elbrus Zone outlined above match some geological features established in the Strandja Massif, mainly its record of magmatic activity in source areas and the vertical structural column, as shown by ages of detrital and inherited zircons (Figure 16B).

Tectonic units of the Caucasus belong to the strike-slip bounded fragments of the Silk Road arc

that evolved along the southern margin of Eurasia in the late Palaeozoic–early Mesozoic (Natal'in & Şengör 2005) because of the northward subduction of Palaeo-Tethys. In many places, this arc was constructed on top of older Ordovician to early Carboniferous magmatic arcs (Natal'in 2006) as seen in the South Tien Shan (Volkova & Budanov 1999), Northern Pamir (Schwab *et al.* 2004), and Kunlun (Jiang *et al.* 2002; Şengör & Okuroğulları 1991; Xiao *et al.* 2005). In all these regions, the Cimmeride closure of the Palaeo-Tethyan Ocean is commonly accepted. At the same time, the Cimmerian blocks (Şengör 1984) south of the suture do not have records of Palaeozoic magmatic arc activities (Schwab *et al.* 2004; Horton *et al.* 2008), while in Iran detrital zircons to the north of the Palaeo-Tethyan suture show well-defined peaks in Palaeozoic–Triassic times (Figure 16E) (Horton *et al.* 2008).

Carboniferous History

The Carboniferous granite gneisses of the Strandja Massif were metamorphosed together with country rocks before the emplacement of the early Permian Kırklareli granites. They signify another important tectonic episode, allowing correlations with both the European Palaeozoic structures and structures that evolved along the southern margin of Eurasia in the Caucasus and Central Asia. The Carboniferous orthogneisses contain inherited magmatic zircons that are 320–360 Ma old. Detrital zircons of the same age have been found in the Lower Carboniferous turbidites in the İstanbul Zone (N. Okay *et al.* 2011). Intrusive rocks of this age have not yet been found in the Strandja Massif but they are known in Balkan Zone (location 8 in Figure 1; Malinov *et al.* 2004; Peytcheva *et al.* 2006) where they partly co-magmatic with Devonian–Carboniferous volcanic rocks of the Valeka Unit (Nikolov *et al.* 1999; Petrunova *et al.* 2010).

In the Strandja Massif, geochemical features of the upper Carboniferous orthogneisses suggest that they evolved as a continental arc. We further suggest that the Carboniferous arc magmatism migrated onto its earlier-formed accretionary wedge, as it is evident from the discovery of metaserpentinites in the studied area and HP rocks right across the Turkish/Bulgarian border area (Gerdjikov 2005). The same migration can be inferred in the Balkan Zone where

metamorphosed peridotite and eclogite are cut by the Carboniferous granites (Machev *et al.* 2006; Carrigan *et al.* 2005).

Carboniferous granitoids (310–285 Ma) in the Balkan Zone are divided into two groups (Carrigan *et al.* 2005): (1) calc-alkaline granite associated with gabbro and diorites that are commonly found in magmatic arcs and (2) peraluminous two-mica leucogranites carrying inherited zircon cores of various ages and characteristic of crustal melting. The emplacement ages of these groups overlap each other and therefore Carrigan *et al.* (2004) interpreted them as subduction-related in terms of the nature of the original melt and heat supply, which was accompanied by anatexis melting depending on local environments. The ages of these granitoids fit the ages of the Carboniferous metagranite and granite gneisses of the Strandja Massif, for which we infer the same tectonic setting. Moreover, the granitoids form a single belt (Carrigan *et al.* 2006) which we interpret as the Late Devonian–Carboniferous magmatic arc of the southern polarity. Unlike in the Strandja Massif, many granitic intrusions of this age in Bulgaria are not metamorphosed and cut the metamorphic fabric of country rocks. There, the age of the regional metamorphism is constrained to be 336 Ma, but in Strandja it postdated the emplacements of metagranite that are 312 Ma old. This difference in ages is difficult to reconcile with the Variscan collision common to the European Hercynides. It matches better a subduction setting affected by intra-arc deformation caused by oblique subduction (Beck 1991; Cembrano *et al.* 2000; Natal'in & Şengör 2005), or possible subduction of spreading centres (DeLong *et al.* 1979).

A slice of this arc may be exposed in the Sakarya Zone (location 9 in Figure 1) as the Kazdağ amphibolite to granulite facies metamorphic complex tectonically surrounded by the Triassic accretionary prism (A.I. Okay *et al.* 2006). There, orthogneisses yield a zircon Pb–Pb evaporation age of 308 Ma. A.I. Okay *et al.* (2006) suggested a Serpukhovian age of high-grade metamorphism, but it should be younger than the orthogneiss magmatic age and thus similar to the first metamorphism of the Strandja Massif. Despite the high-grade metamorphism, the Devonian granodiorites exposed nearby are not metamorphosed. Once again, it signifies the intra-arc nature of metamorphism and deformation and

later juxtaposition of arc segment with different local history due to arc-shaving strike-slip faults (Natal'in & Şengör 2005).

The Palaeozoic tectonics of the Caucasus is poorly understood because of high-grade metamorphism and a strong overprint of Mesozoic and Cenozoic deformations. We have already discussed the Silurian–Devonian arc in the Peredovoi Zone, that is overlain by the ophiolitic nappe containing fragments of its subduction-accretion complex. In general, the Greater Caucasus is considered to be a Palaeozoic arc operating until the early Carboniferous (Adamia *et al.* 1981; Gamkrelidze 1986), although recent isotopic dating (Somin 2007) extends the arc activity at least until the late Carboniferous (280 Ma). In the north (Elbrus Zone), the geochemical features of the Devonian orthogneisses indicate the ensialic origin of the arc, while in the south younger arc additions are ensimatic (Adamia *et al.* 1981; Somin 2007). We interpret these changes as the southward migration of the magmatic front of the long-lived magmatic arc onto its early-formed accretionary wedge. This inference is based on the discovery of ophiolites that occur sporadically among the arc orthogneisses. A thick continuous sequence of strongly deformed clastic rocks containing lenses of cherts, limestones and rare volcanic rocks (the Dizi Series) is exposed along the southern side of the Greater Caucasus arc (Adamia 1984; Somin 2007). These rocks contain marine fossils varying in age from middle Devonian to late Triassic. The Dizi Series was interpreted as a deep trough of unspecified nature (Adamia 1984; Somin 2007). Natal'in & Şengör (2005) interpreted these rocks as a subduction-accretion complex that was paired with the Greater Caucasus magmatic arc. The reason for this interpretation was the tectonic mixture of lithologies indicating different sedimentological environments – shallow-marine limestones with coral remnants, pelagic cherts with conodonts and radiolarians, and clastic continental slope facies in places with admixed arc volcanoclastics. The first two rock types occur as lenses and belong to different chronostratigraphic levels. All lithologies fit those of subduction-accretionary complexes (e.g., Isozaki 1990). We discuss this issue because in the Greater Caucasus the disposition of accretionary prism and the magmatic arc clearly indicate the southern polarity of the Devonian–Carboniferous arc. The same polarity is inferred for the Carboniferous

magmatic arc of the Balkan Zone (Carrigan *et al.* 2005) and we assume it was so for the Strandja Massif.

Natal'in & Şengör (2005) inferred that the Dizi Series marks the Palaeo-Tethyan suture. Here we follow an earlier suggestion (Gamkrelidze 1986) that the Palaeo-Tethyan suture or its amalgamation with the Neo-Tethyan suture runs south of the Transcaucasus Palaeozoic massifs (Dzurila, Krami; Figure 19), where Carboniferous arc volcanics and granites are exposed (Adamia 1984; Gamkrelidze 1986) similar to those in the Eastern Pontides (Delaloye & Bingöl 2000). The western continuation of the suture marks the Permian Pulus subduction-accretion complex exposed in the Eastern Pontides (Topuz *et al.* 2004).

Detrital zircons from Jurassic sandstones in the Caucasus (Figure 16F) and the Shemshak Formation of the Alborz Mountains (Figure 16E) yield Palaeozoic and early Mesozoic ages.

East of Caucasus, the Carboniferous magmatic arc can be traced through a number of strike-slip stacked fragments (Natal'in & Şengör 2005) to the Gissar Range, Southern Tien Shan, where Viséan–Serpukhovian arc volcanic rocks and related granites are known (Baymukhamedov 1984; Zonenshain *et al.* 1990). It is overlain by continental dacite, rhyolite, andesite, and coarse-grained clastic rocks containing late Permian plant remnants. Geochemical features of Carboniferous and Permian rocks indicate a subduction-related tectonic setting (Schwab *et al.* 2004). In the Northern Pamirs (e.g., Schwab *et al.* 2004), thick (7 km) Lower Carboniferous andesite, basalts, tuffs, limestones and clastic rocks indicate a magmatic arc constructed on top of the older accretionary wedge. The Middle–Upper Carboniferous consists of unconformably lying flysch and intermediate and felsic volcanic rocks, indicating the continuity of the arc magmatism that was interrupted by intra-arc deformations. The Gissar and North Pamir Carboniferous arcs, as well as their early Palaeozoic basements, continue eastwards into the Western Kunlun. There, the Carboniferous magmatism includes mafic to felsic volcanic rocks occurring among siliciclastic rocks, flysch, and limestones (Pan 1996). These rocks are also well known beyond in the Eastern Kunlun (Schwab *et al.* 2004; Xiao *et al.* 2005).

Permo-Triassic History

The late Palaeozoic–Triassic history of the Strandja Massif is recorded by intrusions of the Kirklareli-type granites and the accumulation of the Koruköy and Triassic metasedimentary complexes. The granites yield well-defined Pb–Pb zircon evaporation ages of 271 and 257 Ma (A.I. Okay *et al.* 2001; Sunal *et al.* 2006). Using the same method a less reliable age of 309 ± 24 Ma has been obtained from the Üsküp metagranite (Figure 2). The mylonitic granite gneisses preserving relicts of the Kirklareli-type granites yield 279 and 295 Ma Rb–Sr ages. The calc-alkaline nature, negative Nb anomaly, mafic schlieren and dykes indicating magma mixing, as well as the absence of inherited zircons suggest a magmatic arc origin for the granites. Being somehow younger they lie on the eastern continuation of the subduction-related granitic belt (310–285 Ma) outlined in Bulgaria (Carrigan *et al.* 2006). Our data support earlier ideas about the Permian tectonic setting (Şengör & Yılmaz 1981; Robertson & Dixon, 1984; Şengör 1984; Şengör *et al.* 1984; Chatalov 1990, 1991; T. Ustaömer & Robertson 1993; Ricou 1994; Stampfli *et al.* 2001a, b).

Şengör (1984) and Chatalov (1991) inferred the same tectonic setting for Triassic times (the Strandzha type of the Triassic of Chatalov 1991) but originally assumed a Devonian–Triassic age of a ‘diabase-phyllitoid complex’ had been later revised to Devonian–late Carboniferous (Nikolov *et al.* 1999; Petrunova *et al.* 2010). Nevertheless, Gerdjikov (2005) assigned it to the Upper Permian–Upper Triassic volcano-sedimentary rocks (location 10 in Figure 1) including MORB-type basalt and rhyolites. Triassic rhyolite and andesite, as well as andesitic basaltic dykes, are known in the Sakar Unit (Chatalov 1990, 1991; Nikolov *et al.* 1999; Gerdjikov 2005). A single body of highly altered metavolcanics is exposed within the Triassic metasedimentary rocks in our study area and the frequent greenish colour of the Triassic metasandstone caused by chlorite and epidote may suggest a tuffaceous nature of the primary rocks. A.I. Okay *et al.* (2001) reported a Triassic age (228 ± 11 Ma) from granitic leucosome in migmatites but discounted it because of presumed Pb loss during the late Mesozoic metamorphism. We think that this age can also be accepted as evidence of Triassic magmatic events because Pb loss cannot affect the $^{207}\text{Pb}/^{206}\text{Pb}$ ratio. These data show that

the Permian magmatic activity continued until the Triassic but was less intense.

Being widespread in the Strandja Massif and its Bulgarian continuation, Permo–Triassic magmatic rocks have a limited distribution in the east. Cataclastically deformed granites, yielding a SHRIMP U–Pb zircon age of 249.4 ± 1.5 Ma (Permian/Triassic boundary), have been recently recognized in the eastern part of the Strandja Massif (location 11 in Figure 1; Yılmaz-Şahin *et al.* 2010). In the İstanbul Zone (location 12 in Figure 1), Kay & Lys (1980) reported that the Triassic mafic lavas are overlain by sandstones and limestones containing late Olenekian–early Anisian foraminifera. The high-K peralkaline granites of the Gebze pluton (location 13 in Figure 1) exposed in the same zone yield a 253.7 ± 1.75 Ma SHRIMP U–Pb age and a 255 ± 5 Ma Rb–Sr age (Yılmaz-Şahin *et al.* 2010). Farther east in the same zone, P.A. Ustaömer *et al.* (2005) reported a 262 ± 19 Ma Pb–Pb age of metagranites but they did not provide information on their chemistry. Considering these ages and the position of igneous rocks in the continuation of the Permian–Triassic magmatic belt in Strandja-Bulgaria, we infer a similar subduction-related nature of this magmatism. We are aware of alternative interpretations of its tectonic setting but think that they have their own problems. For instance, A.I. Okay *et al.* (2006) used the Triassic basaltic magmatism as evidence for the opening of the Intra-Pontide Ocean. Both sides of this inferred ocean are well exposed in the modern structures of the region, but dyke swarms typical of continental breakup (e.g., Kearey *et al.* 2009) are absent.

As in the Devonian and Carboniferous, the early Permian Söğüt granodiorites (209 Ma Ar–Ar and 272 Ma K–Ar ages) form a tectonic inclusion (location 14 in Figure 1) in the Triassic subduction-accretion complex of the Sakarya Zone (A.I. Okay *et al.* 2002). Eclogites (205–210 Ma Ar–Ar age) are exposed about 10 km to the south as a sliver within the south-vergent thrusts. We support the A.I. Okay *et al.* (2002) interpretation of Sakarya accretionary prism formation at the southern margin of Laurasia because of the northward subduction, but consider the Söğüt granodiorites to be a piece of magmatic arc paired with the Sakarya accretionary prism. Older parts of this accretionary prism could be tectonically eroded (cf. von Huene & Scholl 1991) or removed

by arc-shaving strike-slip faults (Natal'in & Şengör 2005). We also infer that the Söğüt granodiorites are part of the Permian–Triassic arc, which is identified in the Strandja Massif and Balkan Zone. Thrust vergence in the Sakarya Zone, the sharpness of the southern boundary of the Kırklareli-type granites in the Strandja Massif (magmatic front!), and the data from Carrigan *et al.* (2005) on the geodynamic setting of the early Permian granites in the Balkan Zone indicate the southern polarity of this arc. A tectonic sliver of ribbon metacherts and metagabbro, the ophiolitic(?) Kuzulu Complex (Figure 3), occurring among metaconglomerate and metasandstones (Koruköy Complex) suggests strong distortion of original relationships within the Permian–Triassic arc, probably because of arc-parallel tectonic transport.

All fragments of the late Palaeozoic–early Mesozoic Silk Road arc have the same polarity (Natal'in & Şengör 2005). In the Greater Caucasus, late Palaeozoic, especially Lower Permian rocks contain andesitic to felsic lavas. Granitic rocks yield ages as young as 280 Ma (Potapenko *et al.* 1999; Somin 2007). Zircons from Bajocian sandstones of the Greater Caucasus show a peak between 300 and 200 Ma (Figure 16F). Triassic subduction-related magmatic rocks are known in the Greater Caucasus but are mainly developed north of it beneath the Jurassic to Recent Scythian Platform cover (Natal'in & Şengör 2005 and references therein). Tikhomirov *et al.* (2004) established two periods of volcanic activity – Early–Middle Triassic and Late Triassic. Both are characterized by calc-alkaline lavas and extrusions. Sedimentary records of Early to Middle Triassic rocks indicate extension and subsidence that can be caused by rifting, backarc basin opening, or transtensional strike-slip motions. During the Late Triassic, eruptions were subaerial, mainly explosive, and chiefly rhyolitic-dacitic in composition with minor basalt and andesite. These features indicate an importance of crustal partial melting that is typical for Andean-type magmatic arcs. Tikhomirov *et al.* (2004) did not specify the polarity of the subduction zone but noted that it must be far to the south. The Silk Road arc model (Natal'in & Şengör 2005) implying strike-slip duplication of arc fragments solves this problem because the weakest zones used by strike-slip faults are located along the arc axis making the arc massif wider. In the framework of this model the Dizi

Series, containing Triassic clastics, can be considered as a preserved fragment of the accretionary prism. If so, the Triassic arc should have a southern polarity.

From the Greater Caucasus this arc continues to Turan, Iran and the Northern Pamirs. North of the Palaeo-Tethyan suture in Iran, the geological record of the late Palaeozoic–Triassic as well as older magmatism is very incomplete, while detrital zircons provide ages reflecting continuous activity from 500 to 200 Ma (Figure 16E).

During the Triassic the main strike-slip motions along the Silk Road arc occurred. These motions can explain the weak intensity of the Triassic arc magmatism in the Balkan, Strandja, İstanbul, and Sakarya zones because, during strike-slip displacements the subduction of the oceanic slab to the magma generation zone only occurs locally, thus creating time gaps in the magmatic records.

Conclusions

- (1) The Palaeozoic basement of the Strandja Massif contains metasedimentary rocks, but mainly metagranites and granite gneisses. The metasedimentary rocks have a uniform composition – biotite, biotite-muscovite, and muscovite schists and gneisses and subordinate amphibolites. Detrital zircon studies have revealed Ordovician, Early Silurian and late Carboniferous depositional ages of these rocks. Metagranites and granite gneisses intrude the metasediments. They are divided into three magmatic complexes: the biotite-hornblende granite gneisses, biotite-muscovite granite gneisses, and leucocratic granite gneisses. Isotopic dating using the single zircon evaporation method and conventional U-Pb technique have shown that magmatic ages of these rocks cluster around 308–315 Ma. After metamorphism and deformation, the Carboniferous granite gneisses and their country rocks were cut by K-feldspar metagranites varying in age from 309 ± 24 to 257 ± 6.2 Ma. Two tectonostratigraphic units were formed after the late Palaeozoic metamorphism and deformation. The fault-bounded Koruköy Complex contains clasts of metamorphic rocks and is cut by pegmatite veins of the K-feldspar metagranites,

- which allow us to assign it to the Permo–Triassic. The second unit, the Kuzulu Complex, occurs as a fault-bound lens comprising metamorphosed mafic rocks associated with metacherts and metapelites. It may be ophiolitic.
- (2) The thick pile of Triassic metasedimentary rocks constitutes the metasedimentary cover of the Strandja Massif (A.I. Okay *et al.* 2001). These rocks were affected only by the Late Jurassic–Early Cretaceous deformations that impose an upper limit on their age. Clasts of granite gneisses and metasedimentary rocks metamorphosed in the late Palaeozoic (after 308–315 Ma) impose a lower limit on the deposition of these rocks. The only fossils found in the upper part of the structural column are Early–Middle Triassic in age. This unit contains a highly significant small tectonic lens of pillow lava. The Triassic succession reveals obvious orogenic features because of its great thickness and rock deposition from high-energy currents. The presence of black shales at the top of the succession may indicate that it embraces all the Triassic series and part of the Jurassic because in neighbouring regions of Bulgaria the black shales are Jurassic in age.
- (3) The nappe of unmetamorphosed limestone and dolomite overlies all the above-mentioned units. The nappe surface is made of carbonate mylonites, which crosscut the structural frame of the underlying rocks on a regional scale. Kinematic indicators suggest the carbonate nappe arrived from the south. We infer a Jurassic age for the carbonate and the nappe emplacement occurred during the latest stage of the Late Jurassic–Early Cretaceous deformations.
- (4) Available geochemical features of the Carboniferous and Permian magmatic rocks indicate a subduction-related tectonic setting. Correlation with neighbouring regions of Bulgaria supports this conclusion.
- (5) We challenge the idea that the Strandja Massif, together with the İstanbul and Zonguldak zones in the east and the Balkan Zone in the west, represents a segment of the Variscan belt in Europe and shares all aspects of its Precambrian–Palaeozoic history. The Strandja Massif shows remarkable similarity with the late Palaeozoic–early Mesozoic Silk Road arc evolving on the southern margin of Eurasia, due to the northward subduction of Palaeo-Tethys (Natal'in & Şengör 2005; Natal'in *et al.* 2005a; Natal'in 2006). The fragments of this arc that are exposed in Caucasus, South Tien Shan, Pamir and Kunlun show the inheritance of magmatic arc activity at least since the early Palaeozoic. The Precambrian history, as recorded by stratigraphic and magmatic successions as well as from detrital and inherited zircon ages, of the Strandja Massif, İstanbul, and Zonguldak zones has many common features with the Baltica-Timanide collage, including its fragments distributed in Central Asia. Using various sets of data and correlation with surrounding tectonic units, we conclude that Strandja Massif is a fragment of the long-lived, Ordovician–Triassic magmatic arc, which evolved on the northern side of Palaeo-Tethys and thus has an Asiatic origin.

Acknowledgements

This study was supported by TÜBİTAK (The Scientific and Technological Research Council of Turkey, Project no. YDABCAG 101Y010 and 110Y177) and İstanbul Technical University Research Fund, Project no. 32766 and 23128. We sincerely thank Aral Okay who suggested this study, constantly helped during its progress and was insistent on finishing this part of the work. Criticism from Celal A.M. Şengör helped us to refine the arguments. Mark Somin generously shared data and his knowledge on the geology of Caucasus. We are grateful to the anonymous reviewers and Erdin Bozkurt who critically read the manuscript and made numerous suggestions for its improvement.

References

- ADAMIA, S.A. 1984. Pre-Alpine basement of Caucasus: its composition, structure and evolution. *In: Pre-Alpine Basement of Caucasus – Its Composition, Structure and Evolution*. Metsniereba, Tbilisi, 3–104 [In Russian].
- ADAMIA, S.A., CHKHOTUA, T., KEKELIA, M., LORDKIPANIDZE, M., SHAVISHVILI, I. & ZAKARIADZE, G. 1981. Tectonics of the Caucasus and adjoining regions: implications for the evolution of the Tethys ocean. *Journal of Structural Geology* 3, 437–447.

- ALAVI, M. 1991. Sedimentary and structural characteristics of the Paleo-Tethys remnants in northeastern Iran. *Geological Society of America Bulletin* **103**, 983–992.
- ALLEN, M.B., MORTON, A.C., FANNING, C.M., ISMAIL-ZADEH, A.J. & KROONENBERG, S.B. 2006. Zircon age constraints on sediment provenance in the Caspian region. *Journal of the Geological Society, London* **163**, 647–655.
- ANDRUSCHUK, V.L., DUBINSKY, A.Y. & KHAIN, V.E. 1968. *Geology of the USSR, Volume IX. North Caucasus. Book 1. Geological Description*. Nedra, Moscow [in Russian].
- AYDIN, Y. 1982. *Geology of the Yıldız (Istranca) Mountains*. PhD Thesis, İstanbul Technical University, İstanbul [in Turkish with English abstract].
- AYHAN, A., DİNÇER, A. & TUĞRUL, Y. 1972. *Istranca Masifi'nin 'Yıldız Dağları' Jeolojisi [Geology of Strandja Massif in Yıldız Mountains]*. Mineral Research and Exploration Institute (MTA) of Turkey Report no. 5130 [in Turkish, unpublished].
- BAYMUKHAMEDOV, K.N. 1984. *Map of the Magmatic Complexes of the Uzbek SSR*. Fan, Tashkent [in Russian].
- BECK, M.E. 1991. Coastwise transport reconsidered: lateral displacements in oblique subduction zones, and tectonic consequences. *Physics of the Earth and Planetary Interiors* **68**, 1–8.
- BELOV, A.A. 1981. *Tectonic Evolution of the Alpine Foldbelt in the Paleozoic*. Nauka, Moscow [in Russian].
- BISKE, Y.S. 1996. *Paleozoic Structure and History of the South Tien Shan*. St. Peterburg University, St. Peterburg [in Russian].
- BOGDANOVA, S.V., BINGEN, B., GORBATSHEV, R., KHERASKOVA, T.N., KOZLOV, V.I., PUCHKOV, V.N. & VOLOZH, Y.A. 2008. The East European Craton (Baltica) before and during the assembly of Rodinia. *Precambrian Research* **160**, 23–45.
- BONCHEVA, I., LAKOVA, I., SACHANSKI, V. & KOENIGSHOF, P. 2010. Devonian stratigraphy, correlations and basin development in the Balkan Terrane, western Bulgaria. *Gondwana Research* **17**, 573–582.
- BOZKURT, E., WINCHESTER, J.A., YİĞİTBAŞ, E. & OTTLEY, C.J. 2008. Proterozoic ophiolites and mafic-ultramafic complexes marginal to the İstanbul Block: an exotic terrane of Avalonian affinity in NW Turkey. *Tectonophysics* **461**, 240–251.
- BROOKFIELD, M.E. 2000. Geological development and Phanerozoic crustal accretion in the western segment of the southern Tien Shan (Kyrgyzstan, Uzbekistan and Tajikistan). *Tectonophysics* **328**, 1–14.
- ÇAĞLAYAN, M.A. & YURTSEVER, A. 1998. *1:100,000 Ölçekli, Türkiye Jeoloji Haritaları, no. 20, 21, 22, 23, Burgaz-A3, Edirne-B2 ve B3, Burgaz-A4 ve Kırklareli-B4; Kırklareli-B5 ve B6; Kırklareli-C6 Paftaları [Geological Map of Turkey at 1: 100,000 Scale, no. 20, 21, 22, 23, Burgaz-A3, Edirne-B2 ve B3, Burgaz-A4 ve Kırklareli-B4; Kırklareli-B5 ve B6; Kırklareli-C6 Sheets]*. Mineral Research and Exploration Institute (MTA) of Turkey Publications [in Turkish with English abstract].
- CARRIGAN, C.W., MUKASA, S.B., HAYDOUTOV, I. & KOLCHEVA, K. 2005. Age of Variscan magmatism from the Balkan sector of the orogen, central Bulgaria. *Lithos* **82**, 125–147.
- CARRIGAN, C.W., MUKASA, S.B., HAYDOUTOV, I. & KOLCHEVA, K. 2006. Neoproterozoic magmatism and Carboniferous high-grade metamorphism in the Sredna Gora Zone, Bulgaria: an extension of the Gondwana-derived Avalonian-Cadomian belt? *Precambrian Research* **147**, 404–416.
- CEMBRANO, J., SCHERMER, E., LAVENU, A. & SANHUEZA, A. 2000. Contrasting nature of deformation along an intra-arc shear zone, the Liquice-Ofqui fault zone, southern Chilean Andes. *Tectonophysics* **319**, 129–149.
- CHATALOV, G.A. 1988. Recent developments in the geology of the Strandzha Zone in Bulgaria. *Bulletin of the İstanbul Technical University* **41**, 433–466.
- CHATALOV, G.A. 1990. *Geology of the Strandzha Zone in Bulgaria*. Publishing House of the Bulgarian Academy of Sciences, Sofia [in Bulgarian with English abstract].
- CHATALOV, G.A. 1991. Triassic in Bulgaria – a review. *Bulletin of the Technical University of İstanbul* **44**, 103–135.
- CHEN, F., SIEBEL, W., SATIR, M., TERZIOĞLU, M.N. & SAK, K. 2002. Geochronology of the Karadere basement (NW Turkey) and implications for the geological evolution of the İstanbul zone. *International Journal of Earth Sciences* **91**, 469–481.
- CHEN, F., TODT, W. & HANN, H. P. 2003. Zircon and garnet geochronology of eclogites from the Moldanubian Zone of the Black Forest, Germany. *The Journal of Geology* **111**, 207–222.
- COCKS, L.R.M. & TORSVIK, T.H. 2005. Baltica from the late Precambrian to mid-Palaeozoic times: the gain and loss of a terrane's identity. *Earth-Science Reviews* **72**, 39–66.
- CONDIE, K.C. 1989. *Plate Tectonics & Crustal Evolution*. Pergamon Press, Oxford.
- COŞKUN, B. 1997. Oil and gas fields-transfer zone relationships, Thrace Basin, NW Turkey. *Marine and Petroleum Geology* **14**, 401–416.
- DEAN, W.T., MONOD, O., RICKARDS, R.B., DEMİR, O. & BULTYNCK, P. 2000. Lower Palaeozoic stratigraphy and palaeontology, Karadere-Zirze area, Pontus Mountains, Northern Turkey. *Geological Magazine* **137**, 555–582.
- DELALOYE, M. & BİNGÖL, E. 2000. Granitoids from Western and Northwestern Anatolia: geochemistry and modeling of geodynamic evolution. *International Geology Review* **42**, 241–268.
- DELONG, S.E., SCHWARZ, W.M. & ANDERSON, R.N. 1979. Thermal effects of ridge subduction. *Earth and Planetary Science Letters* **44**, 239–246.
- ERNST, W.G. 2010. Subduction-zone metamorphism, calc-alkaline magmatism, and convergent-margin crustal evolution. *Gondwana Research* **18**, 8–16.
- FORTEY, R.A. & COCKS, L.R.M. 2003. Palaeontological evidence bearing on global Ordovician–Silurian continental reconstructions. *Earth-Science Reviews* **61**, 245–307.
- GAGGERO, L., BUZZI, L., HAYDOUTOV, I. & CORTESOGNO, L. 2009. Eclogite relics in the Variscan orogenic belt of Bulgaria (SE Europe). *International Journal of Earth Sciences* **98**, 1853–1877.

- GAMKRELIDZE, I.P. 1986. Geodynamic evolution of the Caucasus and adjacent areas in Alpine time. *Tectonophysics* **127**, 261–277.
- GAMKRELIDZE, I.P. 1991. Tectonic nappes and horizontal layering of the Earth's crust in the Mediterranean belt (Carpathians, Balkanides and Caucasus). *Tectonophysics* **196**, 385–396.
- GAMKRELIDZE, I.P., DUDAURI, O., NADARESHILLI, G., SKHIRTLADZE, N., TUTBERIDZE, B. & SHENGLIA, L. 2002. Geodynamic typification of Precambrian–Phanerozoic magmatism of Georgia. In: TOPCHISHVILI, M.B. (eds), *Geodynamic Classification of Precambrian–Phanerozoic Magmatism of Georgia*. Georgian Academy of Sciences, Tbilisi, 105–126.
- GEE, D.G., BOGOLEPOVA, O.K. & LORENZ, H. 2006. The Timanide, Caledonide and Uralide orogens in the Eurasian high Arctic, and relationships to the palaeo-continent Laurentia, Baltica and Siberia. In: GEE, D.G. & STEPHENSON, R.A. (eds), *European Lithosphere Dynamics*. Geological Society, London, Memoirs **32**, 507–520.
- GEORGIEV, G., DABOVSKI, C. & STANISHEVA-VASSILEVA, G. 2001. East Srednogorie-Balkan Rift Zone. In: ZIEGLER, P.A., CAVAZZA, W., ROBERTSON, A.H.F. & CRASQUIN-SOLEAU, S. (eds), *East Srednogorie-Balkan Rift Zone*. Memoires du Museum National d'Histoire Naturelle **186**, 259–293.
- GERASIMOV, V.Y., PISMENNYI, A.N. & ENNA, N.L. 2010. Zircons study of the crystalline basement of Greater Caucasus. *Magmatism and Metamorphism in Earth History, Ekaterinburg, Abstracts*, p. 43.
- GERDJIKOV, I. 2005. Alpine metamorphism and granitoid magmatism in the Strandja Zone: new data from the Sakar Unit, SE Bulgaria. *Turkish Journal of Earth Sciences* **14**, 167–183.
- GOLONKA, J. 2000. *Cambrian–Neogene Plate Tectonic Maps*. Wydawnictwo Uniwersytetu Jagiellońskiego.
- GOLONKA, J. 2004. Plate tectonic evolution of the southern margin of Eurasia in the Mesozoic and Cenozoic. *Tectonophysics* **381**, 235–273.
- GÖRÜR, N., MONOD, O., OKAY, A.I., ŞENGÖR, A.M.C., TÜYSÜZ, O., YİĞİTBAŞ, E., SAKINÇ, M. & AKKÖK, R. 1997. Palaeogeographic and tectonic position of the Carboniferous rocks of the western Pontides (Turkey) in the frame of the Variscan belt. *Bulletin de la Société Géologique de France* **168**, 197–205.
- HAGDORN, H. & GÖNCÜOĞLU, M.C. 2007. Early–Middle Triassic echinoderm remains from the Istranca Massif, Turkey. *Neues Jahrbuch für Geologie und Paläontologie Abhandlungen* **246**, 235–245.
- HAYDOUTOV, I. 1989. Precambrian ophiolites, Cambrian island arc, and Variscan suture in the South Carpathian-Balkan region. *Geology* **17**, 905–908.
- HAYDOUTOV, I. & YANEV, S. 1997. The Protomoesian microcontinent of the Balkan Peninsula – a peri-Gondwanaland piece. *Tectonophysics* **272**, 303–313.
- HIMMERKUS, F., REISCHMANN, T. & KOSTOPOULOS, D. 2006. Late Proterozoic and Silurian basement units within the Serbo-Macedonian Massif, northern Greece: the significance of terrane accretion in the Hellenides. In: ROBERTSON, A.H.F. & MOUNTRAKIS, D. (eds), *Tectonic Development of the Eastern Mediterranean Region*. Geological Society, London, Special Publications **260**, 35–50.
- HORTON, B.K., HASSANZADEH, J., STOCKLI, D.F., AXEN, G.J., GILLIS, R. J., GUEST, B., AMINI, A., FAKHARI, M.D., ZAMANZADEH, S.M. & GROVE, M. 2008. Detrital zircon provenance of Neoproterozoic to Cenozoic deposits in Iran: implications for chronostratigraphy and collisional tectonics. *Tectonophysics* **451**, 97–122.
- HSÜ, K.J., NACHEV, I.K. & VUCHEV, V.T. 1977. Geologic evolution of Bulgaria in light of plate tectonics. *Tectonophysics* **40**, 245–256.
- ISOZAKI, Y., MARUYAMA, S. & FURUOKA, F. 1990. Accreted oceanic materials in Japan. *Tectonophysics* **181**, 179–205.
- IRVINE, T.N. & BARAGAR, W.R.A. 1971. A guide to the chemical classification of the common volcanic rocks. *Canadian Journal of Earth Sciences* **8**, 523–548.
- JARRARD, R.D. 1986. Relations among subduction parameters. *Reviews of Geophysics* **24**, 217–284.
- JIANG, Y.-H., JIANG, S.-Y., LING, H.-F., ZHOU, X.-R., RUI, X.-J. & YANG, W.-Z. 2002. Petrology and geochemistry of shoshonitic plutons from the western Kunlun orogenic belt, Xinjiang, northwestern China: implications for granitoid geneses. *Lithos* **63**, 165–187.
- KALVODA, J. & BÁBEK, O. 2010. The margins of Laurussia in Central and Southeast Europe and Southwest Asia. *Gondwana Research* **17**, 526–545.
- KALVODA, J., LEICHMANN, J. & BABEK, O. 2002. Brunovistulian terrane (Central Europe) and İstanbul Zone (NW Turkey): late Proterozoic and Paleozoic tectonostratigraphic development and paleogeography. *Geologica Carpathica* **53**, 81–154.
- KAY, O. & LYS, M. 1980. İstanbul Boğazı'nın batı yakasında (Kilyos) yeni bir Triyas bulgusu [A new Triassic findings in the western side (Kilyos) of İstanbul Strait] *Mineral Research and Exploration Institute (MTA) of Turkey Bulletin* **94**, 20–26 [in Turkish].
- KAZMIN, V.G. & TIKHONOVA, N.F. 2006. Evolution of Early Mesozoic back-arc basins in the Black Sea-Caucasus segment of a Tethyan active margin. In: ROBERTSON, A.H.F. & MOUNTRAKIS, D. (eds), *Tectonic Development of the Eastern Mediterranean Region*. Geological Society, London, Special Publications **260**, 179–200.
- KEAREY, P., KLEPEIS, K.A. & VINE, F.J. 2009. *Global Tectonics*. Wiley-Blackwell, Oxford.
- KHAIN, E.V. 1984. *Ophiolites and Hercynian Nappe Structure of the Peredivoi Range, Greater Caucasus*. Nauka, Moscow [in Russian].
- KOZLU, H., GÖNCÜOĞLU, Y., SARMIENTO, G.N. & GÖNCÜOĞLU, M.C. 2002. First finding of Late Silurian conodonts from the 'Orthoceras Limestones' Çamdağ area, NW Turkey: preliminary constraints for paleogeography. *Geologica Balcanica* **31**, 3–12.
- KOZUR, H. & GÖNCÜOĞLU, M.C. 2000. Mean features of the pre-Variscan development in Turkey. *Acta Universitatis Carolinae-Geologica* **42**, 459–464.

- KUZNETSOV, N.B., NATAPOV, L.M., BELOUSOVA, E.A., O'REILLY, S.Y. & GRIFFIN, W.L. 2010. Geochronological, geochemical and isotopic study of detrital zircon suites from late Neoproterozoic clastic strata along the NE margin of the East European Craton: implications for plate tectonic models. *Gondwana Research* **17**, 583–601.
- LE MAITRE, R.W. 1989. *A Classification of Igneous Rocks and Glossary of Terms*. Blackwell, Oxford.
- LILOV, P., MALIAKOV, Y. & BALOGH, K. 2004. K-Ar dating of metamorphic rocks from Strandja Massif, SE Bulgaria. *Geochemistry, Mineralogy and Petrology, Sofia* **41** 107–119.
- LUDWIG, K.R. 2003. *Isoplot 3.0, A Geochronological Toolkit for Microsoft Excel*. Berkeley Geochronology Center Special Publication no. 4.
- MACHEV, P., BORISOVA, B. & HECH, L. 2006. Metaeclogites from the Sredna Gora terrain – petrological features and P-T path of evolution. *Geosciences 2006, Abstracts*, 185–188.
- MANIAR, P.D. & PICOLLI, P.M. 1989. Tectonic discrimination of granitoids. *Bulletin of the American Geological Society* **101**, 635–643.
- MALINOV, O., VON QUARD, A., PEYTICHEVA, I., ALADJOV, T., ALADJOV, A., NAYDENOVA, S. & DJAMBAZOV, S. 2004. The Klissura granite in the western Balkan – questions and answers from new field and isotope studies. *Bulgarian Geological Society, Annual Scientific Conference 'Geology 2004' 16-17.12.2004, Abstracts*, p. 3.
- MATTE, P. 2001. The Variscan collage and orogeny (480–290 Ma) and the tectonic definition of the Armorica microplate: a review. *Terra Nova* **13**, 122–128.
- METELKIN, D.V., VERNIKOVSKY, V.A., KAZANSKY, A.Y., BOGOLEPOVA, O.K. & GUBANOV, A.P. 2005. Paleozoic history of the Kara microcontinent and its relation to Siberia and Baltica: Paleomagnetism, paleogeography and tectonics. *Tectonophysics* **398**, 225–243.
- MIYASHIRO, A. 1973. Paired and unpaired metamorphic belts. *Tectonophysics* **17**, 241–254.
- MURPHY, J.B., GUTIERREZ-ALONSO, G., NANCE, R.D., FERNANDEZ-SUAREZ, J., KEPPIE, J.D., QUESADA, C., STRACHAN, R.A. & DOSTAL, J. 2006. Origin of the Rheic Ocean: rifting along a Neoproterozoic suture? *Geology* **34**, 325–328.
- NATAL'IN, B.A. 2006. Paleozoic evolution of the northern margin of Paleo-Tethys. In: TOMURHUU, D., NATAL'IN, B., ARIUNCHIMEG, Y., KHISHIGSUREN, S. & ERDENESAIKHAN, G. (eds), *Paleozoic Evolution of the Northern Margin of Paleo-Tethys*. Institute of Geology and Mineral Recourses, Mongolian Academy of Sciences, Ulaanbaatar, 33–36.
- NATAL'IN, B.A. & ŞENGÖR, A.M.C. 2005. Late Palaeozoic to Triassic evolution of the Turan and Scythian platforms: the pre-history of the Palaeo-Tethyan closure. *Tectonophysics* **404**, 175–202.
- NATAL'IN, B.A., SUNAL, G. & TORAMAN, E. 2005a. The Strandja arc: anatomy of collision after long-lived arc parallel tectonic transport. In: SKLYAROV, E.V. (eds), *The Strandja Arc: Anatomy of Collision After Long-lived Arc Parallel Tectonic Transport*. IEC SB RAS, Irkutsk, 240–245.
- NATAL'IN, B.A., SUNAL, G. & TORAMAN, E. 2005b. *Structural and Metamorphic Evolution of the Strandja Massif*. The Scientific and Technological Research Council of Turkey, Project no. **101Y010**, Ankara-Turkey [in Turkish with English abstract, unpublished].
- NATAL'IN, B.A., SUNAL, G. & TORAMAN, E. 2009. Tectonics of the Strandja Massif: example of the collision after long-lived arc-parallel tectonic transport. *2nd International Symposium on the Geology of the Black Sea Region, Abstracts*, 134–136.
- NEMCHIN, A.A. & PIDGEON, R.T. 1997. Evolution of the Darling Range Batholith, Yilgarn Craton, Western Australia: a SHRIMP zircon study. *Journal of Petrology* **38**, 625–649.
- NIKISHIN, A.M., ZIEGLER, P.A., PANOV, D.I., NAZARREVIKH, B.P., BRUNET, M.-F., STEPHENSON, R.A., BOLOTOV, S.N., KOROTAEV, M.V. & TIKHOMIROV, P.L. 2001. Mesozoic and Cenozoic evolution of the Scythian Platform-Black Sea-Caucasus domain. In: ZIEGLER, P.A., CAVAZZA, W., ROBERTSON, A.H.F. & CRASQUIN-SOLEAU, S. (eds), *Mesozoic and Cenozoic Evolution of the Scythian Platform-Black Sea-Caucasus Domain*. Memoires du Museum National d'Histoire Naturelle **186**, 295–346.
- NIKOLOV, G., ANTOVA, N. & RANKOVA, T. 1999. Revising of the lithostratigraphic subdivision of the Strandzha allochthon (SE Bulgaria). *Second Balkan Geophysical Congress and Exhibition, 5-9 July, 1999, İstanbul, Turkey, Abstracts*, p. 298–299.
- NORTH AMERICAN COMMISSION ON STRATIGRAPHIC NOMENCLATURE, 2005. North American stratigraphic code. *The American Association of Petroleum Geologists Bulletin* **89**, 1547–1591.
- O'CONNOR, J.T. 1965. *A Classification for Quartz-rich Igneous Rocks Based on Feldspar Ratio*. US Geological Survey, Professional Papers B525, 79–84.
- OCZLON, M.S. 2006. *Terrane Map of Europe (1st Edition)*. Gaea Heidelbergensis **15**.
- OKAY, A.I., BOZKURT, E., SATIR, M., YIĞITBAŞ, E., CROWLEY, Q.G. & SHANG, C.K. 2008. Defining the southern margin of Avalonia in the Pontides: geochronological data from the Late Proterozoic and Ordovician granitoids from NW Turkey. *Tectonophysics* **461**, 252–264.
- OKAY, A.I., MONOD, O. & MONIE, P. 2002. Triassic blueschists and eclogites from northwest Turkey: vestiges of the Paleo-Tethyan subduction. *Lithos* **64**, 155–178.
- OKAY, A.I., SATIR, M., MALUSKI, H., SIYAKO, M., MONIE, P., METZGER, R. & AKYÜZ, S. 1996. Paleo- and Neo-Tethyan events in northwestern Turkey: geologic and geochronologic constraints. In: YIN, A. & HARRISON, M. (eds), *Paleo- and Neo-Tethyan Events in Northwestern Turkey: Geologic and Geochronologic Constraints*. Cambridge University Press, Cambridge, 420–441.
- OKAY, A.I., SATIR, M. & SIEBEL, W. 2006. Pre-Alpide Palaeozoic and Mesozoic orogenic events in the Eastern Mediterranean region. In: GEE, D.G. & STEPHENSON, R.A. (eds), *European Lithosphere Dynamics*. Geological Society, London, Memoirs **32**, 389–405.

- OKAY, A.I., SATIR, M., TÜYSÜZ, O., AKYÜZ, S. & CHEN, F. 2001. The tectonics of the Strandja Massif: late-Variscan and mid-Mesozoic deformation and metamorphism in the northern Aegean. *International Journal of Earth Sciences* **90**, 217–233.
- OKAY, A.I., ŞENGÖR, A.M.C. & GÖRÜR, N. 1994. Kinematic history of the opening of the Black Sea and its effect on the surrounding regions. *Geology* **22**, 267–270.
- OKAY, A.I. & TÜYSÜZ, O. 1999. Tethyan sutures of northern Turkey. In: DURAND, B., JOLIVET, L., HORVATH, F. & SERANNE, M. (eds), *Tethyan Sutures of Northern Turkey*. Geological Society, London, Special Publications **156**, 475–515.
- OKAY, N., ZACK, T., OKAY, A.I. & BARTH, M. 2011. Sinistral transport along the Trans-European Suture Zone: detrital zircon-rutile geochronology and sandstone petrography from the Carboniferous flysch of the Pontides. *Geological Magazine* **148**, 380–403.
- OLOVYANISHNIKOV, V.G. 1998. *Upper Precambrian of Timan and Kanin Peninsula*. Komi Science Centre, RAS, Ural Division, Syktyvkar [in Russian].
- PAN, Y. 1996. *Geological Evolution of the Karakorum and Kunlun Mountains*. Seismological Press, Beijing.
- PASSCHIER, C.W. & TROUW, R.A.J. 2005. *Microtectonics*. Springer.
- PATERSON, S.R., PIGNOTTA, G.S. & VERNON, R.H. 2004. The significance of microgranitoid enclave shapes and orientations. *Journal of Structural Geology* **26**, 1465–1481.
- PEASE, V. & SCOTT, R.A. 2009. Crustal affinities in the Arctic Uralides, northern Russia: significance of detrital zircon ages from Neoproterozoic and Palaeozoic sediments in Novaya Zemlya and Taimyr. *Journal of the Geological Society, London* **166**, 517–527.
- PERİNÇEK, D. 1991. Possible strand of the North Anatolian Fault in the Thrace Basin, Turkey - an interpretation. *American Association of Petroleum Geologists Bulletin* **75**, 241–257.
- PETRUNOVA, L., DIMITROVA, T., DIMITROV, I. & MALYAKOV, Y. 2010. New palynological finds from Southeast Strandzha Mountain, Bulgaria. *Bulgarian Geological Society, National Conference with International Participation 'GEOSCIENCES 2010', Abstracts*, 82–83.
- PEYTCHIEVA, I., VON QUADT, A., MALINOV, O., TACHEVA, E. & NEDIALKOV, R. 2006. Petrochan and Klissura plutons in Western Balkan: relationships, in situ and single grain U-Pb zircon/ monazite dating and isotope tracing. *Bulgarian Geological Society, National Conference, Geosciences 2006, Proceedings*, 221–224.
- POTAPENKO, Y.Y. 2004. *Geology of Karachay-Cherkessia*. Karachaevsk-Cherkesk University, Karachaevsk [in Russian].
- POTAPENKO, Y.Y., SNEZHKO, V.A., SOMIN, M.L. & USIK, V.I. 1999. Hercynian granitoids, structure, and evolution of the Greater Caucasus. In: *Hercynian Granitoids, Structure, and Evolution of the Greater Caucasus*. Georgian Academy of Sciences, Tbilisi, 148–167 [in Russian].
- PUCHKOV, V.N. 2009. The evolution of the Uralian orogen. In: MURPHY, J.B., KEPPIE, J.D. & HYNES, A.J. (eds), *Ancient Orogens and Modern Analogues*. Geological Society, London, Special Publications **327**, 161–195.
- RICOU, L.E. 1994. Tethys reconstructed: plates, continental fragments and their boundaries since 260 Ma from Central America to south-eastern Asia. *Geodinamica Acta* **7**, 169–218.
- RICOU, L.-E., BURG, J.-P., GODFRIAUX, I. & IVANOV, Z. 1998. Rhodope and Vardar: the metamorphic and the olistostromic paired belts related to the Cretaceous subduction under Europe. *Geodinamica Acta* **11**, 285–309.
- RINO, S., KON, Y., SATO, W., MARUYAMA, S., SANTOSH, M. & ZHAO, D. 2008. The Grenvillian and Pan-African orogens: world's largest orogenies through geologic time, and their implications on the origin of superplumes. *Gondwana Research* **14**, 51–72.
- ROBERTS, D. & OLOVYANISHNIKOV, V. 2004. Structural and tectonic development of the Timanide orogen. In: GEE, D.G. & PEASE, V. (eds), 2004. *The Neoproterozoic Timanide Orogen of Eastern Baltica*. Geological Society, London, Memoirs **30**, 47–57.
- ROBERTSON, A.H.F. & DIXON, J.E. 1984. Introduction: aspects of the geological evolution of the Eastern Mediterranean. In: DIXON, J.E. & ROBERTSON, A.H.F. (eds), *Geological Evolution of the Eastern Mediterranean*. Geological Society, London, Special Publications **17**, 1–74.
- ROLLINSON, H.R. 1994. *Using Geochemical Data: Evaluation, Presentation, Interpretation*. Longman Scientific & Technical, Singapore.
- RUBAN, D.A. 2007. Major Paleozoic–Mesozoic unconformities in the Greater Caucasus and their tectonic re-interpretation: a synthesis. *GeoActa* **6**, 91–102.
- SACHANSKI, V., GÖNCÜOĞLU, M.C., GEDİK, İ. & OKUYUCU, C. 2007. The Silurian of the Çatak and Karadere areas of the Zonguldak Terrane, NW Anatolia. *Geologica Balcanica* **36**, 103–110.
- SACHANSKI, V., GÖNCÜOĞLU, M.C. & GEDİK, İ. 2010. Late Telychian (early Silurian) graptolitic shales and the maximum Silurian highstand in the NW Anatolian Palaeozoic terranes. *Palaeogeography, Palaeoclimatology, Palaeoecology* **291**, 419–428.
- SAFONOVA, I., MARUYAMA, S., HIRATA, T., KON, Y. & RINO, S. 2010. LA ICP MS U-Pb ages of detrital zircons from Russia largest rivers: implications for major granitoid events in Eurasia and global episodes of supercontinent formation. *Journal of Geodynamics* **50**, 134–153.
- SALVADOR, A. 1994. *International Stratigraphic Guide – A Guide to Stratigraphic Classification, Terminology, and Procedure, 2nd Edition*. The Geological Society of America, Boulder, Colorado.
- SAKINÇ, M., YALTRAK, C. & OKTAY, F.Y. 1999. Palaeogeographical evolution of the Thrace Neogene Basin and the Tethys-Paratethys relations at northwestern Turkey (Thrace). *Palaeogeography, Palaeoclimatology, Palaeoecology* **153**, 17–40.
- SAPUNOV, I.G. & METODIEV, L.S. 2007. Main features of the Jurassic in Bulgaria. *Comptes rendus de l'Académie bulgare des Sciences* **60**, 169–178.

- SCHWAB, M., RATSCHBACHER, L., SIEBEL, W., MCWILLIAMS, M., MINAEV, V., LUTKOV, V., CHEN, F., STANEK, K., NELSON, B., FRISCH, W. & WOODEN, J. L. 2004. Assembly of the Pamirs: age and origin of magmatic belts from the southern Tien Shan to the southern Pamirs and their relation to Tibet. *Tectonics* **23**, TC4002, doi:10.1029/2003TC001583.
- ŞENGÖR, A.M.C. 1984. *The Cimmeride Orogenic System and the Tectonics of Eurasia*. The Geological Society of America, Special Paper **195**.
- ŞENGÖR, A.M.C., ÇİN, A., ROWLEY, D.B. & SHANGYOU, N. 1991. Magmatic evolution of the Tethysides: a guide to reconstruction of collage history. *Palaeogeography, Palaeoclimatology, Palaeoecology* **87**, 411–440.
- ŞENGÖR, A.M.C. & NATAL'IN, B.A. 1996. Palaeotectonics of Asia: fragments of a synthesis. In: YIN, A. & HARRISON, M. (eds), *Palaeotectonics of Asia: Fragments of a Synthesis*. Rubey Colloquium, Cambridge University Press, Cambridge, 486–640.
- ŞENGÖR, A.M.C. & OKUROĞULLARI, A.H. 1991. The role of accretionary wedges in the growth of continents: Asiatic examples from Argan to plate tectonics. *Eclogae Geologicae Helveticae* **84**, 535–597.
- ŞENGÖR, A.M.C. & YILMAZ, Y. 1981. Tethyan evolution of Turkey: a plate tectonic approach. *Tectonophysics* **75**, 181–190.
- ŞENGÖR, A.M.C., YILMAZ, Y. & SUNGURLU, O. 1984. Tectonics of the Mediterranean Cimmerides: nature and evolution of the western termination of Palaeo-Tethys. In: DIXON, J.E. & ROBERTSON, A.H.F. (eds), *Geological Evolution of the Eastern Mediterranean*. Geological Society, London, Special Publications **17**, 77–112.
- SHAND, S. J. 1927. *Eruptive Rocks*. D. Van Nostrand Company, New York.
- SOMIN, M.L. 2007. *Structure and Geodynamic Settings of the Formation of Metamorphic Complexes in Greater Caucasus and Cuba*. Thesis, Geological Institute RAS, Moscow [in Russian].
- STAMPFLI, G.M. 2000. Tethyan oceans. In: BOZKURT, E., WINCHESTER, J.A. & PIPER, J.D.A. (eds), *Tectonics and Magmatism in Turkey and Surrounding Area*. Geological Society, London, Special Publications **173**, 1–23.
- STAMPFLI, G.A., MOSAR, J., FAVRE, P., PILLEVUIT, A. & VANNAY, J.-C. 2001a. Permo–Mesozoic evolution of the western Tethys realm: the Neo-Tethys East Mediterranean Basin connection. In: ZIEGLER, P. A., CAVAZZA, W., ROBERTSON, A. H. F. & CRASQUIN-SOLEAU, S. (eds), *Permo–Mesozoic Evolution of the Western Tethys Realm: the Neo-Tethys East Mediterranean Basin Connection*. Mémoires du Muséum National D'Histoire Naturelle **186**, 51–108.
- STAMPFLI, G.M. & BOREL, G.D. 2002. A plate tectonic model for the Paleozoic and Mesozoic constrained by dynamic plate boundaries and restored synthetic oceanic isochrons. *Earth and Planetary Science Letters* **196**, 17–33.
- STAMPFLI, G.M. & BOREL, G.D. 2004. The TRANSMED transects in space and time: constraints on the paleotectonic evolution of the Mediterranean domain. In: CAVAZZA, W., ROURE, F., STAMPFLI, G.M. & ZIEGLER, P.A. (eds), *The TRANSMED Transects in Space and Time: Constraints on the Paleotectonic Evolution of the Mediterranean Domain*. Springer, Berlin Heidelberg, 53–80.
- STAMPFLI, G.M., RAUMER, J.F.V. & BOREL, G.D. 2002. Paleozoic evolution of pre-Variscan terranes: from Gondwana to the Variscan collision. In: MARTÍNEZ CATALÁN, J.R., HATCHER, R.D., JR., ARENAS, R. & DÍAZ GARCÍA, F. (eds), *Paleozoic Evolution of Pre-Variscan Terranes: From Gondwana to the Variscan Collision*. Geological Society of America, Special Paper **364**, Boulder, Colorado, 263–279.
- STAMPFLI, G.M., BOREL, G.D., CAVAZZA, W., MOSAR, J. & ZIEGLER, P.A. 2001b. Palaeotectonic and palaeogeographic evolution of the western Tethys and Peritethyan domain (IGCP Project 369). *Episodes* **24**, 221–228.
- SUN, S.S. & McDONOUGH, W.F. 1989. Chemical and isotopic systematics of oceanic basalts: implication for mantle composition and processes. In: SAUNDERS, A.D. & NORRY, M.J. (eds), *Chemical and Isotopic Systematics of Oceanic Basalts: Implication for Mantle Composition and Processes*. Geological Society, London, Special Publications **42**, 313–345.
- SUNAL, G., NATAL'IN, B.A., SATIR, M. & TORAMAN, E. 2006. Paleozoic magmatic events in the Strandja Massif, NW Turkey. *Geodinamica Acta* **19**, 283–300.
- SUNAL, G., SATIR, M., NATAL'IN, B.A. & TORAMAN, E. 2008. Paleotectonic position of the Strandja Massif and surrounding continental blocks based on zircon Pb-Pb Age studies. *International Geology Review* **50**, 519–545.
- SUNAL, G., SATIR, M., NATAL'IN, B.A., TOPUZ, G. & VONDERSCHMIDT, O. 2011. Metamorphism and diachronous cooling in a contractional orogen: the Strandja Massif, NW Turkey. *Geological Magazine* **148**, 580–596.
- TCHOUMATCHENCO, P., YANEVA, M., BUDUROV, K., IVANOVA, D., KOLEVA-REKALOVA, E., PETRUNOVA, L. & ZAGORCEV, I. 2004. Late Cimmerian tectonics of the Triassic and Jurassic rocks in Louda Kamchia, East Stara Planina Mts. (Bulgaria). *Bulgarian Geological Society, Annual Scientific Conference 'Geology 2004' Abstracts*, p. 3.
- TIKHOMIROV, P.L., CHALOT-PRAT, F. & NAZAREVICH, B.P. 2004. Triassic volcanism in the Eastern Fore-Caucasus: evolution and geodynamic interpretation. *Tectonophysics* **381**, 119–142.
- TOPUZ, G., ALTHERR, R., SATIR, M. & SCHWARZ, W.H. 2004. Low-grade metamorphic rocks from the Pulur complex, NE Turkey: implications for the pre-Liassic evolution of the Eastern Pontides. *International Journal of Earth Sciences* **93**, 72–91.
- TULYAGANOV, K.T. 1972. *Geology of the USSR, Volume XXIII, Uzbek SSR, Book 1. Geological Description*. Nedra, Moscow [in Russian].

- TURGUT, S. & ESELLER, G. 2000. Sequence stratigraphy, tectonics and depositional history in eastern Thrace Basin, NW Turkey. *Marine and Petroleum Geology* **17**, 61–100.
- TÜRKECAN, A. & YURTSEVER, A. 2002. *Geological Map of Turkey*. Mineral Research and Exploration Institute (MTA) of Turkey Publication.
- USTAÖMER, P.A. 1999. Pre-Early Ordovician Cadomian arc-type granitoids, the Bolu Massif, West Pontides, northern Turkey: geochemical evidence. *International Journal of Earth Sciences* **88**, 2–12.
- USTAÖMER, P.A., MUNDIL, R. & RENNE, P. R. 2005. U/Pb and Pb/Pb zircon ages for arc-related intrusions of the Bolu Massif (W Pontides, NW Turkey): evidence for Late Precambrian (Cadomian) age. *Terra Nova* **17**, 215–223.
- USTAÖMER, P.A., USTAÖMER, T., COLLINS, A.S. & ROBERTSON, A.H.F. 2009. Cadomian (Ediacaran–Cambrian) arc magmatism in the Bitlis Massif, SE Turkey: magmatism along the developing northern margin of Gondwana. *Tectonophysics* **473**, 99–112.
- USTAÖMER, T. & ROBERTSON, A.H.F. 1993. Late Palaeozoic–Early Mesozoic marginal basins along the active southern continental margin of Eurasia: evidence from the Central Pontides (Turkey) and adjacent regions. *Geological Journal* **28**, 219–238.
- USTAÖMER, T. & ROBERTSON, A.H.F. 1997. Tectonic-sedimentary evolution of the North-Tethyan active margin in the Central Pontides of Northern Turkey. In: ROBINSON, A.G. (ed), *Regional and Petroleum Geology of the Black Sea Region*. AAPG Memoir **68**, 245–290.
- VERNIKOVSKY, V.A., KAZANSKY, A.Y., MATUSHKIN, N.Y., METELKIN, D.V. & SOVETOV, J.K. 2009. The geodynamic evolution of the folded framing and the western margin of the Siberian craton in the Neoproterozoic: geological, structural, sedimentological, geochronological, and paleomagnetic data. *Russian Geology and Geophysics* **50**, 380–393.
- VERNON, R.H. 2004. *A Practical Guide to Rock Microstructures*. Cambridge University Press.
- VOLKOVA, N.I. & BUDANOV, V.I. 1999. Geochemical discrimination of metabasalt rocks of the Fan-Karatagin transitional blueschist/greenschist belt, South Tianshan, Tajikistan: seamount volcanism and accretionary tectonics. *Lithos* **47**, 201–216.
- VON HUENE, R. & SCHOLL, D.W. 1991. Observation at convergent margins concerning sediment subduction, subduction erosion, and the growth of continental crust. *Reviews of Geophysics* **29**, 279–316.
- VON QUADT, A., MORITZ, R., PEYTCHEVA, I. & HEINRICH, C.A. 2005. Geochronology and geodynamics of Late Cretaceous magmatism and Cu-Au mineralization in the Panagyurishte region of the Apuseni-Banat-Timok-Srednogie belt, Bulgaria. *Ore Geology Reviews* **27**, 95–126.
- VON RAUMER, J.F., STAMPFLI, G., BOREL, G. & BUSSY, F. 2002. Organization of pre-Variscan basement areas at the north-Gondwanan margin. *International Journal of Earth Sciences* **91**, 35–52.
- WIEBE, R.A. & COLLINS, W.J. 1998. Depositional features and stratigraphic sections in granitic plutons: implications for the emplacement and crystallization of granitic magma. *Journal of Structural Geology* **20**, 1273–1289.
- WINCHESTER, J.A., PHARAOH, T.C., VERNIERS, J., IOANE, D. & SEGHEDI, A. 2006. Palaeozoic accretion of Gondwana-derived terranes to the East European Craton: recognition of detached terrane fragments dispersed after collision with promontories. *Geological Society, London, Memoirs* **32**, 323–332.
- XIAO, W.J., WINDLEY, B.F., LIU, D.Y., JIAN, P., LIU, C.Z., YUAN, C. & SUN, M. 2005. Accretionary tectonics of the western Kunlun Orogen, China: a Paleozoic–Early Mesozoic, long-lived active continental margin with implications for the growth of southern Eurasia. *The Journal of Geology* **113**, 687–705.
- YALÇIN, M.N. & YILMAZ, İ. 2010. Devonian in Turkey – a review. *Geologica Carpathica* **61**, 235–253.
- YANEV, S. 2000. Palaeozoic terranes of the Balkan Peninsula in the framework of Pangea assembly. *Palaeogeography, Palaeoclimatology, Palaeoecology* **161**, 151–177.
- YANEV, S., GÖNCÜOĞLU, M.C., GEDİK, İ., LAKOVA, I., BONCHEVA, I., SACHANSKI, V., OKUYUCU, C., ÖZGÜL, N., TIMUR, E., MALIAKOV, Y. & SAYDAM, G. 2006. Stratigraphy, correlations and palaeogeography of Palaeozoic terranes of Bulgaria and NW Turkey: a review of recent data. In: ROBERTSON, A.H. F. & MOUNTRAKIS, D. (eds), *Stratigraphy, Correlations and Palaeogeography of Palaeozoic Terranes of Bulgaria and NW Turkey: A Review of Recent Data*. Geological Society, London, Special Publications **260**, 51–67.
- YANEV, S., LAKOVA, I., BONCHEVA, I. & SACHANSKI, V. 2005. The Moesian and Balkan terranes in Bulgaria: Palaeozoic basin development, palaeogeography and tectonic evolution. *Geologica Belgica* **8**, 185–192.
- YİĞİTBAŞ, E., KERRICH, R., YILMAZ, Y., ELMAS, A. & XIE, Q. 2004. Characteristics and geochemistry of Precambrian ophiolites and related volcanics from the İstanbul-Zonguldak Unit, Northwestern Anatolia, Turkey: following the missing chain of the Precambrian South European suture zone to the east. *Precambrian Research* **132**, 179–206.
- YILMAZ-ŞAHİN, S., AYSAL, N. & GÜNGÖR, Y. 2010. Petrogenesis and SHRIMP zircon U-Pb dating of some granitoids within the Western Pontides, Southeastern Balkans, NW Turkey. In: *Abstracts, XIX Congress of Carpathian-Balkan Geological Association, Geologica Balcanica, 23–26 September 2010*, p. 419.
- YILMAZ, Y., TÜYSÜZ, O., YİĞİTBAŞ, E., GENÇ, S.C. & ŞENGÖR, A.M.C. 1997. Geology and tectonic evolution of the Pontides. In: ROBINSON, A.G. (eds), *Geology and Tectonic Evolution of the Pontides*. AAPG Memoir **68**, 183–226.
- ZONENSHAIN, L.P., KUZMIN, M.I. & NATAPOV, L.M. 1990. *Geology of the USSR: A Plate Tectonic Synthesis*.